LBL-25240

Lawrence Berkeley Laboratory
UNIVERSITY OF CALIFORNIA

Materials & Chemical
Sciences Division

Tris[bis(trimethylsilyl)amido]uranium: Compounds with Tri-, Tetra-, and Penta-valent Uranium

J.L. Stewart
(Ph.D. Thesis)

April 1988

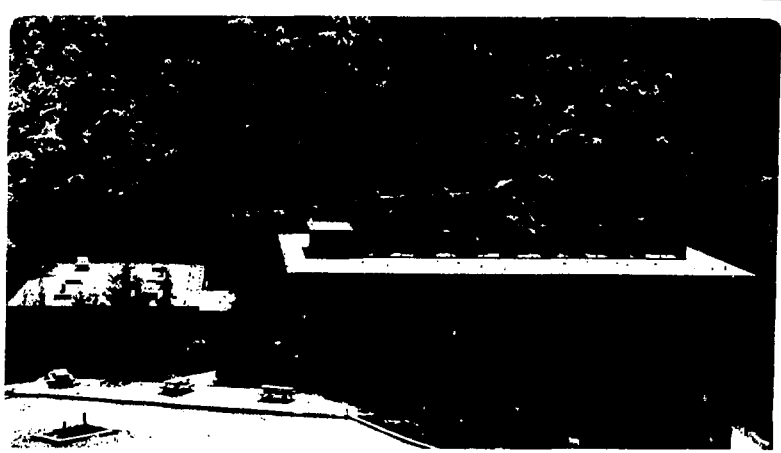

Prepared for the U.S. Department of Energy under Contract Number DE-AC03-76SF00098.

LBL--25240

DE88 010356

Tris[bis(trimethylsilyl)amido]uranium: Compounds with Tri-, Tetra-, and Penta-valent Uranium

Joanne Lee Stewart
(Ph.D. Thesis)

April 1988

Lawrence Berkeley Laboratory
1 Cyclotron Road
Berkeley, CA 94720
and
University of California, Berkeley
Berkeley, CA 94720

Supported by the U.S. Department of Energy under Contract Number DE-AC03-76SF00098.

Tris[bis(trimethylsilyl)amido]uranium: Compounds with Tri-, Tetra-, and Penta-valent Uranium

Joanne Lee Stewart

Abstract

The trivalent uranium compound, tris(bis(trimethylsilyl)amido)-uranium, serves as a precursor to new tri-, tetra-, and penta-valent uranium species. The geometry about the uranium atom in the three-coordinate bis(trimethylsilyl)amide compound is pyramidal. Lewis-base coordination compounds of $U[N(SiMe_3)_2]_3$ with a one-to-one ratio of Lewis base to uranium were isolated with pyridine, 4-dimethylamino-pyridine, 2,6-Me_2-C_6H_3NC, and triphenylphosphineoxide. Two-to-one coordination compounds were obtained with t-butylnitrile and t-butylisocyanide. Compounds with more sterically demanding bases could not be isolated, presumably due to the steric requirements of the bulky bis(trimethylsilyl)amide ligands.

Tris[bis(trimethylsilyl)amido]uranium reduces AgF and $(C_6H_5)_3CN_3$ to form $FU[N(SiMe_3)_2]_3$ and $N_3U[N(SiMe_3)_2]_3$, respectively. The reaction of $U[N(SiMe_3)_2]_3$ with either trimethylaluminum or methyllithium produces $MeU[N(SiMe_3)_2]_3$, *via* a redox/ligand redistribution process.

Reactions of $U[N(SiMe_3)_2]_3$ with organoazides, RN_3 (R = t-butyl, p-tolyl), yield the pentavalent compounds $U[N(SiMe_3)_2]_3(NR)$. The reaction of $U[N(SiMe_3)_2]_3$ and $U[N(SiMe_3)_2]_3[N(p\text{-tolyl})]$ leads to formation of the metallocycle, $[(Me_3Si)_2N]_2\overline{UCH_2(Me)_2SiNSiMe_3}$, and

$U[N(SiMe_3)_2]_3[NH(p\text{-tolyl})]$, which is isostructural with pentavalent $U[N(SiMe_3)_2]_3[N(p\text{-tolyl})]$. The expected decrease in U-$N(SiMe_3)_2$ bond length with increase in oxidation state is not observed; apparently interligand repulsions limit the approach of the bulky ligands to the metal.

The reaction of $ClU[N(SiMe_3)_2]_3$ and $Li[NH(p\text{-tolyl})]$ yields the uranium(IV) dimer, $U_2[N(SiMe_3)_2]_4[\mu\text{-}N(p\text{-tolyl})]_2$. The reaction of $U[N(SiMe_3)_2]_3$ with 2,4,6-trimethylaniline produces the uranium(III) dimer $U_2[N(SiMe_3)_2]_4[\mu\text{-}N(H)(2,4,6\text{-}Me_3C_6H_2)]_2$. Analogous substitution products could not be obtained with aniline or p-toluidine; the dimer appears isolable by virtue of its low hydrocarbon solubility and the unique steric properties of the ligands employed.

The ligands $t\text{-}Bu_3CO^-$ (tritox), $t\text{-}Bu_2CHO^-$ (ditox), and $t\text{-}Bu_3SiO^-$ (silox) are used to synthesize new tetravalent, mononuclear uranium compounds. The reaction of $ClU(tritox)_3$ with alkyllithium reagents leads to isolation of $RU(tritox)_3$, R = Me, Et, n-Bu, Me_3CCH_2, Me_3SiCH_2, and benzyl. The reaction of $U(ditox)_4$ with MeLi affords the addition product $U(ditox)_4(Me)Li$, whose crystal structure is described. The preparation of the silox compounds $U(silox)_3Cl_2Li$ and $U(silox)_4$ is reported.

Acknowledgements

The inspiration for this work came from my research director, Dick Andersen, who almost five years ago took an odd bunch of people who wanted to call themselves chemists and by example, instilled in us a joy and enthusiasm for making molecules. Dick, may your chemistry, and your group members, continue to excite and baffle you.

Many heartfelt thanks go to the rest of the "odd bunch" mentioned above, who are now my good friends: Nicole Rutherford, Carol Burns, Dave Berg, and Steve Stults. My roommate, Nicki, is the only person who went through as many labmates as I did...is it something we said? Thanks also to the rest of the Andersen group, both the campus contingent and the hilloids, for their help over the years.

X-ray crystallography was one of the more exciting and frustrating skills I attempted to learn. I'd like to thank Dr. Fred Hollander, an outstanding scientist, for both the exciting and the frustrating. Dr. Allan Zalkin collected the largest data set I've ever seen, and I thank him for tackling a tough structure.

Other friends have certainly contributed to my attempts to seek sanity in an insane place. Many thanks go to Felicia Etzkorn, Bill Ham, Karl Hagen, Ken Lewis, and Gary Hughes for sharing some wonderful times.

Without the love and support of my family, I never would have had the courage to be here. Try to teach them to be independent and look what happens. And to Will, who stood by me through all the laughter and the tears, thank you.

Table of Contents

INTRODUCTION

The use of sterically-demanding ligands to stablize the formation of low-valent, monomeric metal compounds has developed into a general synthetic theme in inorganic chemistry.[1] One example of such a ligand that has been used in the synthesis of compounds containing a wide variety of metals is the bis(trimethylsilyl)amide ligand, $(Me_3Si)_2N^-$.[2] Sodium or lithium salts of the ligand are easily prepared from the parent amine, $(Me_3Si)_2NH$, and sodium amide or n-butyllithium, respectively.[3] Many (bis(trimethylsilyl)amido)metal compounds have been synthesized by the metathetical reaction of a metal halide species with sodium of lithium bis(trimethylsilyl)amide (Eq. 1). The metal may be a main group element,[4] a d-transition metal,[5] or an f-transition metal.[6]

$$MX_n + m\ NaN(SiMe_3)_2 \text{ ----> } M[N(SiMe_3)_2]_mX_{n-m} + m\ NaX \qquad (1)$$

Bis(trimethylsilyl)amide complexes of the first-row transition metals, Cr through Cu, were synthesized in 1963 and 1964 by Bürger and Wannagat.[5] Since then, numerous other examples have been developed. The syntheses and chemical properties of (bis(trimethylsilyl)amido)-metal complexes were reviewed by Harris and Lappert in 1976.[7]

Tris(bis(trimethylsilyl)amido)metal(III) species comprise a special class of these compounds. These three-coordinate molecules are known for the Group 13(3B) metals, Al, Ga, In, and Tl;[4d] the d-transition metals, Ti, V, Cr, and Fe;[5] and most of the trivalent lanthanide series, Ce through Lu, including lanthanide-like Sc, Y, and La.[6] The geometry about the metal may be either planar or pyramidal. Examples of each configuration have been observed in both the solid

state[8] and gas phase.[9] In the planar compounds, the metal atom lies in the plane of the three amido-nitrogen atoms. The $MNSi_2$ group also forms a plane, and the dihedral angle between the two planes is generally near 50°. Thus, the ligands surround the metal in a "propeller" fashion. The structure of the pyramidal species is very similar. The ligand positions remain relatively unchanged, however, in the solid state, the metal atom is disordered above and below the plane of the amido-nitrogens. This phenomenon will be discussed in more detail in Section 1.1.

There have been few reports on the reactivity of the trivalent bis(trimethylsilyl)amide compounds. This may be due to the fact that the bulky ligands so surround the metal atom, that reactivity at the metal center is precluded. Some examples of Lewis base adducts of the tris(bis(trimethylsilyl)amido)lanthanide compounds with very non-sterically demanding Lewis bases include trimethylphosphineoxide,[10] triphenyl-phosphineoxide,[11] t-butylnitrile,[12] and t-butylisocyanide.[12] The four-coordinate adducts demonstrate that it is possible for some of the tris(bis(trimethylsilyl)amido)metal compounds to increase their coordination number, albeit in a limited manner.

The bis(trimethylsilyl)amide ligand has also been used in the synthesis of new actinide (5f) compounds.[13] The synthetic chemistry of the actinide elements has focused on the metals thorium and uranium, due to difficulties caused by the availability and radioactivity of the rest of the actinide series. The chemistry of thorium is limited in scope because it has only one stable oxidation state, +4. Uranium, on the other hand, has four stable oxidation states, +3 through +6. The aqueous reduction potentials (in volts) are:[14]

$$UO_2^{2+}(aq) \xrightarrow{0.06} UO_2^{+}(aq) \xrightarrow{0.58} U^{4+}(aq) \xrightarrow{-0.63} U^{3+}(aq).$$

According to the aqueous reduction potentials, the +4 oxidation state of uranium is the thermodynamically favored state. There are numerous examples of compounds containing uranium in the tetravalent state.[15-17] The tetravalent cation is slowly oxided by air to the uranyl ion, UO_2^{2+}. The uranyl ion is the stable species in sea water, and its chemistry has also been investigated extensively.[17] There are fewer examples of well-characterized compounds containing uranium in the +3 or +5 oxidation state.[17]

The instability of uranium(III) compounds toward oxidation and ligand redistribution reactions, has hindered the development of trivalent reagents of uranium. The synthesis of organometallic compounds in the trivalent oxidation state has been limited mostly to compounds of the type Cp'_3U, where Cp' represents the cylopentadienyl or substituted cyclopentadienyl ligand.[18] The trivalent cyclopentadienyl compounds are exceedingly versatile reagents, and have been used to synthesize a large number of new uranium compounds.[18,19] Some examples of reactions the cyclopentadienyl compounds may undergo are: (1) addition of a Lewis base (Eq.2),[18a] (2) one-electron oxidation to a uranium(IV) compound (Eq. 3),[18b] and (3) two-electron oxidation to a uranium(V) compound (Eq. 4).[18c]

$$(C_5H_5)_3U + thf \longrightarrow (C_5H_5)_3U(thf) \qquad (2)$$

$$2\ (MeC_5H_4)_3U(thf) + Ph_3PS \longrightarrow [(MeC_5H_4)_3U]_2(\mu\text{-}S) + Ph_3P + 2\ thf \qquad (3)$$

$$(MeC_5H_4)_3U(thf) + PhN_3 \text{ -----> } Cp_3U(NPh) + N_2 + thf \qquad (4)$$

In 1979, the bis(trimethylsilyl)amide ligand was used in the preparation of a new, trivalent reagent, $U[N(SiMe_3)_2]_3$.[12] The deep purple-red crystalline compound is soluble in common hydrocarbon solvents, volatile, and very sensitive to oxidation. The investigation of the reactivity of this molecule is the main subject of this thesis. The reactions of the trivalent cyclopentadienyl reagents (Eqs. 5-7) serve as a partial outline for the reactions of $U[N(SiMe_3)_2]_3$ that will be described. Compared to the cyclopentadienyl compounds, tris(bis-(trimethylsilyl)amido)uranium exhibited both similarities and differences in its reactivity. As this is only the second type of trivalent uranium compound that has been examined in this manner, an understanding of the complex interplay of steric and electronic factors that contribute to the ability to isolate new uranium compounds is just beginning to develop.

Prior to this study, many reactions of the tetravalent compound, $ClU[N(SiMe_3)_2]_3$, had been investigated.[13] As this work is quite relevent to the present studies, it will be reviewed briefly.

Tetravalent clorotris(bis(trimethylsilyl)amido)uranium was synthesized by the reaction of UCl_4 with three molar equivalents of $NaN(SiMe_3)_2$ in diethyl ether solution.[13] The reaction of $ClU[N(SiMe_3)_2]_3$ and MeLi led to formation of a uranium-carbon bond (Eq.2).[13]

$$ClU[N(SiMe_3)_2]_3 + MeLi \text{ ---> } MeU[N(SiMe_3)_2]_3 + LiCl \qquad (5)$$

Pyrolysis of the uranium-methyl compound results in isolation of a

four-membered metallocycle, $[(Me_3Si)_2N]_2\overline{UCH_2(Me)_2SiNSiMe_3}$, formed by γ-hydride elimination (Eq. 6).[20b]

$$MeU[N(SiMe_3)_2]_3 \xrightarrow{\text{neat; 150-160°; 1 atm}} [(Me_3Si)_2N]_2\overline{UCH_2(Me)_2SiNSiMe_3} + MeH \quad (6)$$

Another synthetic route to the metallocycle is shown in Eq. 4.[20e]

$$UCl_4 + 4\ Na[N(SiMe_3)_2] \xrightarrow{\text{toluene; reflux}} [(Me_3Si)_2N]_2\overline{UCH_2(Me)_2SiNSiMe_3} + 4\ NaCl + (Me_3Si)_2NH \quad (7)$$

If the reaction in Eq. 7 was carried out in tetrahydrofuran instead of toluene and not heated as extensively, conversion to a uranium-hydride species, $HU[N(SiMe_3)_2]_3$, was observed.[21] The crystal structure of the hydride was obtained[21] and will be compared to the structure of tris(bistrimethylsilyl)amido)uranium(III) in Section 1.1.

While the study of the bis(trimethylsilyl)amide compounds of uranium is the major focus of this work, attempts were also made to extend these synthetic schemes to uranium compounds of the bulky alkoxides and siloxide, $(t\text{-}Bu)_3CO^-$, $(t\text{-}Bu)_2CHO^-$, and $(t\text{-}Bu)_3SiO^-$. Although no new stable uranium(III) reagents were obtained, a variety of new tetravalent compounds were isolated and characterized. Ligand redistribution reactions appeared to play a major role in these studies, as attempts at the synthesis of uranium(III) compounds always resulted in mixtures of products from which only uranium(IV) species could be isolated.

REFERENCES

1. The following references provide an introduction to just a few of the ligand systems that have been developed. They are listed by ligand type. Alkyls: (a) Davidson, P.J.; Lappert, M.F.; Pearce, R. Acc. Chem. Res. 1974, 7, 209-217. (b) Barker, G.K.; Lappert, M.F. J. Organomet. Chem. 1974, 76, C45-C46. C_5Me_5: (c) Manriquez, J.M.; Bercaw, J.E. J. Amer. Chem. Soc. 1974, 96, 6229. (d) Watson, P.L. J. Amer. Chem. Soc. 1983, 105, 6491-6493. (e) Burns, C.J.; Andersen, R.A. J. Amer. Chem. Soc. 1987, 109, 941-942. Amides: (f) Bradley, D.C.; Chisholm, M.H. Acc. Chem. Res. 1976, 9, 273-280. (g) Murray, B.D.; Power, P.P. Inorg. Chem. 1984, 23, 4584-4588. (h) Planalp, R.P.; Andersen, R.A. J. Amer. Chem. Soc. 1983, 105, 7774-7775. Alkoxides: (i) Lubben, T.V.; Wolczanski, P.T.; Van Duyne, G.D. Organometallics, 1984, 3, 977-983. (j) Latesky, S.L.; Keddington, J.; McMullen, A.K.; Rothwell, I.P. Inorg. Chem. 1985, 24, 995-1001.

2. Lappert, M.F.; Power, P.P.; Sanger, A.R.; Srivastava, R.C. "Metal and Metalloide Amides"; Ellis Horwood: Chichester, England, 1980.

3. (a) Amonoo-Neizer, E.H.; Shaw, R.A.; Skovlin, D.O.; Smith, B.C. Inorg. Synth. 1966, 8, 20-22. (b) Kruger, C.R.; Niederprüm Inorg. Synth. 1966, 8, 15-17.

4. Group 1(1A): (a) Bürger, H.; Seyffert, H. Ang. Chem. Int. Ed. Engl. 1964, 3, 646. Group 2(2A): (b) Bürger, H.; Forker, C.; Goubeau, J. Monatsh. Chem. 1965, 96, 597-601. (c) Wannagat, U.;Autzen, H.; Kuckertz, H.; Wismar, H.J. Z. Anorg. Chem. 1972, 394, 254-262. Group 13(3B): (d) Bürger, H; Cichon, J.; Goetze, U.; Wannagat, U.; Wismar, H.J. J. Organomet. Chem. 1971, 33, 1-12. Group 14(4B): (e) Scherer, O.J. Organomet. Chem. Rev. 1968, 3A, 281. (f) Harris, D.H.; Lappert, M.F. J. Chem. Soc., Chem. Comm. 1974, 895-896. Group 15(5B): (g) Scherer, O.J. Ang. Chem. Int. Ed. Engl. 1969, 8, 861-876.

5. (a) Bürger, H.; Wannagat, U. Monatsh. Chem. 1963, 94, 1007-1012. (b) Bürger, H.; Wannagat, U. Monatsh. Chem. 1964, 95, 1099-1102. (c) Bürger, H.; Smrekar, O.; Wannagat, U. Monatsh. Chem. 1964, 95, 292. (d) Schmidbauer, H.; Shiotani, A. J. Amer. Chem. Soc. 1970, 92, 7003.

6. (a) Bradley, D.C.; Ghotra, J.S.; Hart, F.A. J. Chem. Soc., Dalton Trans. 1973, 1021-1023. (b) Andersen, R.A.; Templeton, D.H.; Zalkin, A. Inorg. Chem. 1978, 17, 2317-2319.

7. Harris, D.H.; Lappert, M.F. J. Organomet. Chem. Library 1976, 2, 13-102.

8. Eller, P.G.; Bradley, D.C. Hursthouse, M.B.; Meek, D.W. Coord. Chem. Rev. 1977, 24, 1-95.

9. (a) Fjeldberg, T.; Andersen, R.A. J. Mol. Struc. 1985, 128, 49-57. (b) Fjeldberg, T.; Andersen, R.A. J. Mol. Struc. 1985, 129, 93-105.

10. Bradley, D.C.; Gao, Y.C. Polyhedron 1982, 1, 307.

11. (a) Bradley, D.C.; Ghotra, J.S.; Hart, F.A.; Hursthouse, M.B.; Raithby, P.R. J. Chem. Soc., Dalton Trans. 1977, 1166-1172.

12. Andersen, R.A. Inorg. Chem. 1979, 18, 1507-1509.

13. Turner, H.W.; Andersen, R.A.; Zalkin, A.; Templeton, D.H. Inorg. Chem. 1979, 18, 1221-1224.

14. Johnson, D.A. "Some Thermodynamic Aspects of Inorganic Chemistry", 2nd ed.; Cambridge University: Cambridge, 1982; Chapter 6.

15. Takats, J. In "Fundamental and Technological Aspects of Organo-f-Element Chemistry"; Marks, T.J.; Fragala, I.L., Eds.; NATO ASI Series C155; D.Reidel: New York, 1985; pp 159-193.

16. Marks, T.J.; Ernst, R.D. In "Comprehensive Organometallic Chemistry"; Wilkinson, G; Stone, F.G.A.; Abel, E.W., Eds.; Pergamon: Oxford, England, 1982; Chapter 21.

17. Weigel, F. In "The Chemistry of the Actinide Elements", 2nd ed.; Katz, J.J.; Morss, L.R.; Seaborg, G.T., Eds.; Chapman and Hall: London, England, 1986; Chapter 5.

18. (a) Kanellakopulos, B.; Fischer, E.O.; Dornberger, E.; Baumgartner, F. J. Organomet. Chem. 1970, 24, 507-514. (b) Brennan, J.G.; Andersen, R.A.; Zalkin, A. Inorg. Chem. 1986, 25, 1761-1765. (c) Brennan, J.G.; Andersen, R.A. J. Amer. Chem. Soc. 1985, 107, 514-517.

19. Brennan, J.G., Ph.D. Thesis, University of California, Berkeley, 1986.

20. (a) Turner, H.W.; Simpson, S.J.; Andersen, R.A. J. Amer. Chem. Soc. 1979, 101, 2782. (b) Simpson, S.J.; Turner, H.W.; Andersen, R.A. J. Amer. Chem. Soc. 1979, 101, 7728-7729. (c) Simpson, S.J.; Andersen, R.A. J. Amer. Chem. Soc. 1981, 103, 4063-4066. (d) Simpson, S.J.; Turner, H.W.; Andersen, R.A. Inorg. Chem. 1981, 20, 2991-2995. (e) Dormand, A.; El Bouadili, A.; Aaliti, A.; Moise, C. J. Organomet. Chem. 1985, 285, C1-C5.

21. Andersen, R.A.; Zalkin, A.; Templeton, D.H. Inorg. Chem. 1981, 20, 622-623.

CHAPTER ONE

The Chemistry of [Bis(trimethylsilyl)amido]uranium Compounds

Section 1.1. Lewis base coordination compounds of $U[N(SiMe_3)_2]_3$. The Starting Point: $U[N(SiMe_3)_2]_3$

Stable, well-characterized compounds containing uranium in its trivalent oxidation state are rare. Compounds of this type could potentially serve as precursors to new uranium(III) species, *via* substitution reactions, or to new uranium(IV) and (V) compounds, through oxidative routes.

The study of metal complexes of the bis(trimethylsilyl)amido ligand has resulted in the synthesis of a large number of trivalent, homoleptic tris(bis(trimethylsilyl)amido)metal(III) compounds, $M[N(SiMe_3)_2]_3$. These species are known for main group metals (Al, Ga, In, and Tl),[1] 3d transition metals (Ti, V, Cr, and Fe),[2] and for most of the lanthanide(4f) metals, including lanthanide-like Sc, Y, and La.[3] The compounds that have been characterized in the solid state all crystallize in the space group $P\bar{3}1c$ and fall into two structural classes. In the first class (M = Ti, V, Cr, Fe, Al, Ga, In, and Tl),[4] the metal atom is found in the plane formed by the three amido-nitrogen atoms. In the second class (M = Sc, Nd, Eu, and Yb),[4a,5] the metal atom is disordered above and below the plane of the nitrogens. The first group exhibits trigonal-planar geometry about the metal atom, and the second group exhibits trigonal-pyramidal geometry.

The uranium analogue of the above compounds was successfully synthesized in 1979.[6] The geometry about the metal in this three-

coordinate compound was of interest, as low-coordinate uranium compounds are very unusual. The metal generally exhibits coordination numbers of nine, ten, or higher.[6] It has been observed that the $\nu_{as}(NSi_2)$ stretching frequencies for the planar bis(trimethylsilyl)-amide compounds are found in the range of 899-913 cm^{-1}, whereas the frequencies for the pyramidal compounds are found at 950-995 cm^{-1}.[4a] The stretching frequency for the uranium compound is found at 990 cm^{-1},[7] suggesting a pyramidal structure.

Crystals suitable for X-ray studies were obtained by cooling a saturated cyclohexane solution slowly to -15°C. Earlier attempts at growing crystals from either hexane or pentane also produced long purple needles, however, the crystals from these solvents never proved suitable for X-ray studies. The crystal structure of the uranium compound showed it to be isostructural with other known pyramidal compounds. As with the other pyramidal compounds, the uranium atom is disordered above and below the plane of the three nitrogen atoms. The distance from the plane to the metal atom is 0.456(1) Å. An ORTEP drawing of the molecule with only one of the metal sites occupied is shown is Figure 1-1. Relevant bond lengths and angles are listed in Tables 1-1 and 1-2.

The U-N bond length is approximately what one would predict from a simple ionic bonding model. The sum of the ionic radius for three coordinate, trivalent uranium, 0.87 Å,[8] and the effective ionic radius of the silylamide ligand, 1.47(3) Å, derived by Eigenbrot and Raymond from the structural data for all the known tris(bis(trimethylsilyl)-amido)metal compounds,[9] predicts a bond length of 2.34(3) Å. This is close to the observed U-N bond length of 2.320(4) Å.

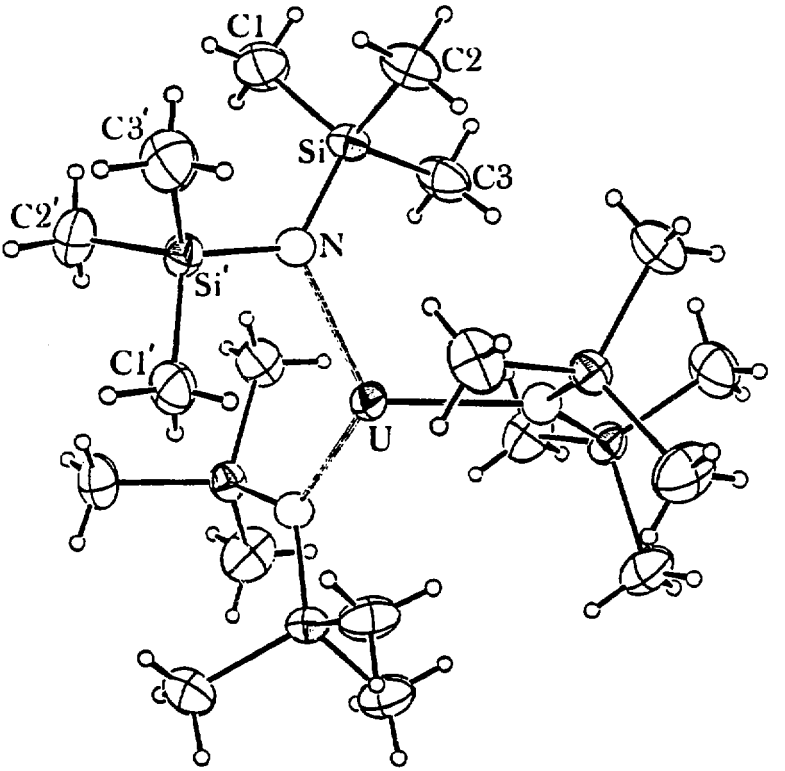

Figure 1-1. ORTEP diagram of $U[N(SiMe_3)_2]_3$.

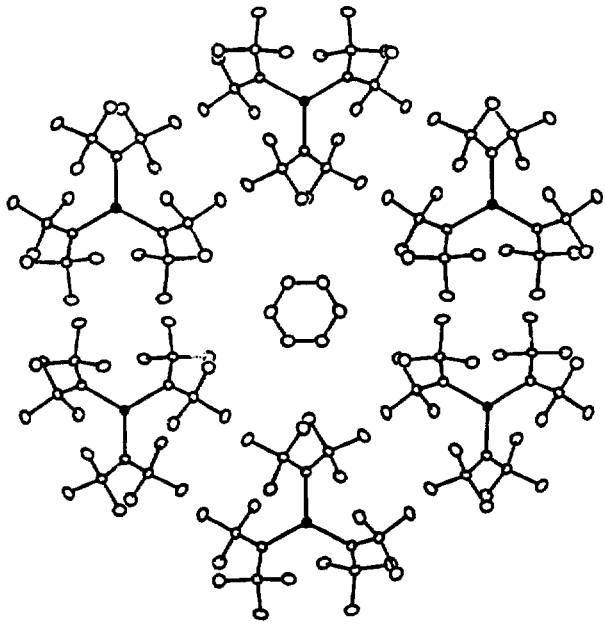

Figure 1-2. Packing diagram of $U[N(SiMe_3)_2]_3$ showing the channel containing the cyclohexane molecule.

Table 1-1. Bond lengths (Å) for $U[N(SiMe_3)_2]_3$.

U-N	2.320(4)	Si-C1	1.873(5)
		Si-C2	1.875(4)
N-Si	1.713(1)	Si-C3	1.869(4)
C4-C4'	1.54(3)		
C4'-C4"	1.48(3)		

Table 1-2. Intramolecular angles (°) for $U[N(SiMe_3)_2]_3$.

N-U-N	116.24(7)	C1-Si-C2	107.3(2)
Si-N-Si'	125.8(2)	C1-Si-C3	107.9(2)
		C2-Si-C3	107.5(2)
U-N-Si	124.5(2)		
U-N-Si	108.31(6)	C4-C4'-C4"	118.2(1)
N-Si-C1	113.7(2)		
N-Si-C2	107.7(2)		
N-Si-C3	112.5(1)		

The tris(bis(trimethylsilyl)amido)uranium molecules pack such that a channel is formed along the z-axis. Slightly disordered cyclohexane molecules are located in the channel, with approximately one cyclohexane molecule per three "layers" of uranium molecules. A packing diagram is shown in Figure 1-2. The orientation of the cyclohexane ring is perpendicular to the crystallographic z-axis. The carbon atom of the cyclohexane, C4, (all other carbon atoms in the cyclohexane are generated by symmetry operations) was refined anisotropically at 1/3 occupancy. It exhibits a large thermal parameter in the z direction (B(3,3) = 19(1)), suggesting disorder in this direction. Indeed, the bond lengths and angles for the cyclohexane ring, listed in the above tables, also show the molecule to be either disordered or severely distorted.

Three possible explanations for the observed geometry in the tris(bis(trimethylsilyl)amido)metal compounds include: (1) metal-

nitrogen π-bonding, (2) crystal packing forces, or (3) the polarized-ion model. Each will be discussed relative to physical studies that have been carried out on this class of molecules.

Originally it was proposed that the main group metal compounds have a strong pπ-pπ component in the M-N bond (dπ-pπ for the transition metals). This interaction favors the planar arrangement for the best orbital overlap.[4a] The bonding in the lanthanide and actinide compounds was said to be more ionic, consequently removing any strong stereochemical requirements. This explanation was addressed in a photoelectron spectroscopy study by Green and co-workers, in which the He-I and He-II spectra of a large number of bis(trimethylsilyl)amide compounds were examined.[10] Assuming a planar geometry for the $MNSi_2$ fragment, the lone pairs on the amido-nitrogens break into two sets, σ and π. Under three-fold symmetry, both sets of lone pairs transform as a + e, thus there is the possibility of four ionization bands due to the nitrogen lone pairs. However, in Green's analysis, there is no energy separation observed between the a and e bands of the lone pairs, i.e., only one band is observed for each of the σ and π type lone pairs. This phenomenon can be explained by a lack of significant lone pair interaction with the metal, or in other words, minimal M-N π-bonding.

Eigenbrot and Raymond also addressed the question of M-N π-bonding in their analysis of all the structurally characterized tris(bis-(trimethylsilyl)amido)metal compounds.[9] They refute earlier claims[4a] that the M-N bond lengths in the transition metal compounds are shorter than would be predicted from the sum of the ionic radii. Eigenbrot and Raymond's analysis of the metal-nitrogen bond lengths shows no

shortening in the transition metal compounds relative to the lanthanide compounds. They suggest a second explanation for the observed geometries about the metal, crystal packing forces. The bis(trimethylsilyl)amide ligands adopt their most stable D_3 symmetry, forming a "pocket" in which the metals with larger ionic radius do not fit. This is supported by the fact that the ligands pack in a similar manner in both the planar and pyramidal structures, and only the metal atom position changes to determine planar versus pyramidal geometry.

The explanation of crystal packing forces was used earlier to explain the pyramidal geometry of the Sc, Eu, and Yb compounds.[4a] Evidence comes from the infrared spectrum of the Sc compound.[4a] The planar compounds exhibit one band in the infrared near 380 cm^{-1}, assigned to the MN_3 antisymmetric stretching vibrations. In the solid, the scandium compound exhibits two resonances in this area, at 385 and 370 cm^{-1}, as would be predicted for pyramidal geometry. These two bands collapse into one band in solution. Gas-phase electron diffraction (GED) data on the Sc compound also support a nearly planar structure, $\angle NScN = 119.1(1.5)°$.[11]

In contrast to the scandium compound, GED results on the Ce, Pr, and La compounds show them to retain their pyramidal configuration in the gas phase,[12] with NMN angles of 112(3)°, 113(3)°, and 110(3)°, respectively. Fjeldberg and Andersen[12] suggest two important factors affecting the geometry: 1) non-bonded carbon-carbon interligand repulsions and 2) charge-induced dipole interactions. Large polarizable cations, such as the lanthanide and actinide ions, may favor non-planar geometry, which is observed for the Ce, Pr, and La compounds. However, for the smaller scandium cation, repulsive

interactions between methyl groups of the ligands prevent a non-planar geometry. Table 1-3 summarizes the GED results for the Sc, Ce, Pr, and La compounds, along with their ionic radii (for coordination number = 3).[8]

Table 1-3. Gas-phase electron diffraction of $M[N(SiMe_3)_2]_3$ compounds.[12]

M^{+3}	Ionic radius (Å)	M-N (Å)	∠NMN (°)	Shortest inter-ligand C-C distance (Å)
Sc	0.53	2.02(3)	119.5(1.5)	3.20(10)
Ce	0.85	2.33(4)	112(3)	3.30(25)
Pr	0.83	2.31(4)	113(3)	3.60(16)
La	0.87	2.36(3)	110(3)	-----

Lewis base coordination compounds of $U[N(SiMe_3)_2]_3$

The tris(cyclopentadienyl) compounds of the lanthanide and actinide elements form isolable Lewis base adducts with a wide variety of Lewis bases. Complexes have been made with ligands containing many different donor atoms, including nitrogen, oxygen, phosphorus, and sulfur.[13] The coordination chemistry of tris(bis(trimethylsilyl)-amido)metal compounds, on the other hand, is rather meager. Examples in the literature include only $M[N(SiMe_3)_2]_3(OPR_3)$ (M=La, Pr, Eu, Gd, In and R=Me; or M=La, Eu, Lu and R=Ph),[14] $Nd[N(SiMe_3)_2]_3(NCBu^t)$,[7] and $Nd[N(SiMe_3)_2]_3(CNBu^t)$.[7] The reason for the lack of coordination chemistry is most likely due to the extreme steric congestion caused by the bulky bis(trimethylsilyl)amide ligands. The coordination compounds that have been described all have the bulk of the coordinating ligand well away from the metal center.

Reactions of Lewis bases with tris(bis(trimethylsilyl)amido)-uranium follow the same trend. Coordination compounds may be isolated only when the donor ligand is not very sterically demanding. Compounds with a Lewis base to uranium rato of one-to-one may be obtained with pyridine, 4-dimethylaminopyridine, 2,6-dimethylphenylisocyanide, and triphenyl-phosphineoxide. Two-to-one coordination compounds may be obtained with t-butylnitrile and t-butylisocyanide.

When $U[N(SiMe_3)_2]_3$ was allowed to react with one molar equivalent of pyridine in pentane solution, the red-purple color of the solution changed to blue-purple. Filtration of the solution, followed by concentration and cooling produced dark purple block-like crystals. The infrared spectrum of the compound showed an absorption at 1599 cm^{-1}, corresponding to the ring stretches of a coordinated pyridine molecule. The ^1H NMR spectrum showed the resonance due to the trimethylsilyl groups to be shifted from -11.38 ppm in the base-free compound to -7.90 ppm.

The reaction of $U[N(SiMe_3)_2]_3$ with the substituted pyridine, 4-dimethylaminopyridine, proceeded in a similar manner. The pyridine ring breathing mode in the infrared spectrum is shifted to 1629 cm^{-1}, from its position in the free ligand at 1600 cm^{-1}. The chemical shift of the trimethylsilyl protons is at -5.64 ppm. Resonances due to the ligand are also assignable and the integration indicated a one-to-one ligand to metal ratio.

The reaction of $U[N(SiMe_3)_2]_3$ with 2,6-dimethylphenylisocyanide in pentane solution led to a dramatic color change from purple-red to deep blue-green. A blue-green compound was crystallized by cooling the solution to -15°C. All the resonances of the expected one-to-one

coordination compound were located in the ^{1}H NMR spectrum, and the integration confirmed the one-to-one stoichiometry. The C-N stretching frequency shifts to slightly higher energy upon coordination, from a value of 2115 cm^{-1} in the free ligand to 2200 cm^{-1} for the coordinated ligand. This increase suggests the bond is primarily σ-donor in nature, with little to no π-backbonding conponent, which would be expected to lower the frequency upon coordination.

The success of the reactions of the tris(bis(trimethylsilylamido)-lanthanide compounds and trialkylphosphineoxide species suggested these ligands as obvious candidates for the uranium amide. Dark purple crystals were isolated from the reaction of $U[N(SiMe_3)_2]_3$ with triphenylphosphineoxide in pentane solution, though the crystals turned brown on the surface and crumbled after drying at reduced pressure. Crystals obtained from toluene solution were somewhat more robust, however, toluene was always present in the ^{1}H NMR spectrum in variable amounts. Prolonged drying of the product removed all of the toluene, but again the crystals discolored and crumbled. The infrared spectrum indicated the presence of the coordinated ligand and elemental analyses supported a one-to-one stoichiometry.

In order to better understand the extent of steric crowding in the tris(bis(trimethylsilyl)amido)uranium coordination compounds, the X-ray crystal structure of the triphenylphosphineoxide coordination compound was obtained. The crystals were grown from a saturated toluene solution cooled slowly to -25°C. They were isolated by filtration, dried at reduced pressure for less than one minute, and immediately loaded in quartz capillaries. An ORTEP drawing is shown in Figure 1-3. Some bond lengths and angles are given in Tables 1-4 and 1-5.

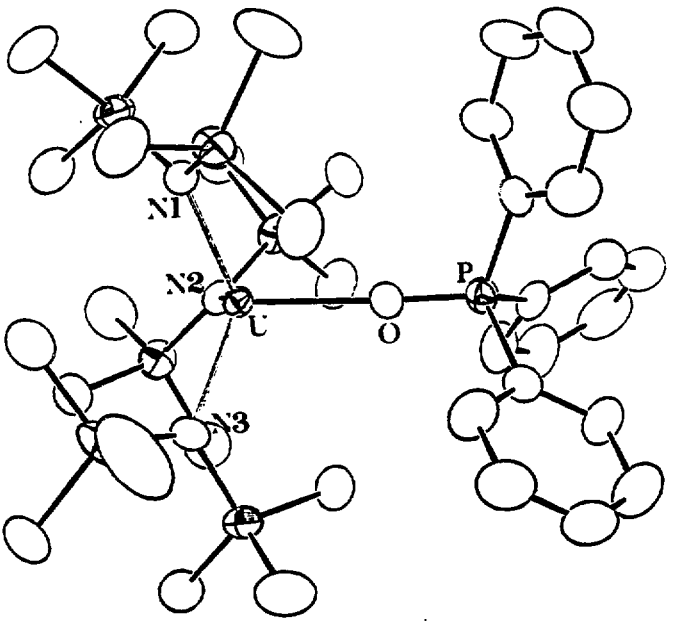

Figure 1-3. ORTEP diagram of $U[N(SiMe_3)_2]_3(OPPh_3)$.

Table 1-4. Bond lengths (Å) for $U[N(SiMe_3)_2]_3(OPPh_3)$.

U-O	2.382(2)	N1-Si11	1.724(4)
U-N1	2.367(3)	N1-Si12	1.720(4)
U-N2	2.343(4)	N2-Si21	1.726(4)
U-N3	2.362(4)	N2-Si22	1.720(4)
		N3-Si31	1.713(4)
O-P	1.512(2)	N3-Si32	1.720(3)
P-C1	1.790(5)		
P-C7	1.786(5)		
P-C13	1.787(4)		

Table 1-5. Intramolecular Angles (°) for $U[N(SiMe_3)_2]_3(OPPh_3)$.

U-O-P	176.5(2)	U-N1-Si11	124.3(2)
		U-N1-Si12	116.9(2)
N1-U-N2	109.8(1)	U-N2-Si21	122.9(2)
N1-U-N3	115.6(1)	U-N2-Si22	117.6(2)
N2-U-N3	110.7(1)	U-N3-Si31	117.7(2)
		U-N3-Si32	122.2(2)
O-U-N1	107.9(1)		
O-U-N2	107.0(1)	O-P-C1	111.4(2)
O-U-N3	105.3(1)	O-P-C7	111.8(2)
		O-P-C13	111.5(2)
Si11-N1-Si12	118.8(2)		
Si21-N2-Si22	119.4(2)		
Si31-N3-Si32	120.2(3)		

The compound is isostructural with the analogous lanthanum species, $La[N(SiMe_3)_2]_3(OPPh_3)$.[14b] The geometry about uranium is pseudotetrahedral. The U-N bond lengths of 2.343(4), 2.362(4), and 2.367(3) Å, are slightly longer than the U-N bond in $U[N(SiMe_3)_2]_3$, 2.320(3) Å, as would be expected for a higher coordinate compound. The U-O distance, 2.382(2) Å, is essentially the same as that found in the similar U(III) compound, $(MeC_5H_4)_3U(OPPh_3)$, U-O = 2.389(6) Å. The fact that this distance does not change on going from a 4-coordinate to a 10-coordinate compound suggests that interligand repulsions may play a role in determining the U-O bond length. The U-O-P angle is nearly linear (176.5(2)°) as it is in the isostructural lanthanum compound (174.6(9)°).[14b]

After refinement of all non-hydrogen atoms with anisotropic thermal parameters, several large peaks (>2 $e^{-1}/Å^3$) were located near the inversion center at (1/2, 1/2, 0). The map of electron density in this region indicated the presence of a severely disordered toluene molecule. The toluene was modeled by placing three carbon atoms at the positions of the three largest peaks in the difference Fourier map and allowing their positions and occupancies to refine.

Although the coordination sphere about $U[N(SiMe_3)_2]_3$ appears to be very sterically congested, it was possible to form two-to-one coordination compounds with the ligands t-butylnitrile and t-butylisocyanide. These reactions were the most difficult to reproduce, possibly due to decomposition caused by adventitious oxygen. The nitrile and isocyanide compounds could only be obtained if the glassware used in the reaction was carefully flame-dried, while a dynamic vacuum was applied. Recrystallization of reaction products was never successful.

Addition of one or two molar equivalents of t-butylnitrile to a pentane solution of the uranium compound produced an immediate color change to deep blue. The coordination compound crystallized as large blue plates that turned to a blue flaky powder when isolated, probably due to loss of occluded solvent. The integration of the ^1H NMR spectrum gave a t-BuCN to $U[N(SiMe_3)_2]_3$ ratio of two-to-one.

When one or two molar equivalents of t-butylisocyanide was added to a pentane solution of $U[N(SiMe_3)_2]_3$, a similar blue compound was isolated. However, there appeared to be a few needle-shaped crystals mixed in with the blue plates. The ^1H NMR spectrum suggests the needles may be a one-to-one adduct, as the spectrum integrates to

slightly less than two t-BuNC ligands to one molecule of $U[N(SiMe_3)_2]_3$. The C-N stretching frequencies of the t-butylnitrile and t-butylisocyanide ligands increase slightly upon coordination. These frequencies, as well as the location of the ^1H NMR resonance for the Me_3Si groups, are listed in Table 1-6.

Table 1-6. Stretching frequencies (cm^{-1}) and ^1H NMR shifts (ppm) for t-butylnitrile and t-butylisocyanide adducts of $U[N(SiMe_3)_2]_3$.

	ν_{CN} (free)	ν_{CN}(coord.)	$\delta(Me_3Si)$
t-BuCN	2238	2253	-2.75
t-BuNC	2175	2248	-4.75
$(2,6\text{-}Me_2C_6H_3)NC$	2115	2200	-5.39

The structures of the two-to-one adducts are believed to be trigonal bipyramidal. There are a several structurally characterized compounds of the type $Cp_3M(NCR)_2$ (M = early lanthanide metal) that exhibit trigonal bipyramidal geometry.[15]

Reactions of tris(bis(trimethylsilyl)amido)uranium with a variety of other Lewis bases were carried out. No isolable coordination compounds were obtained with trimethylamine, trimethylphosphine, trimethylphosphite, tetrahydrofuran, and carbon monoxide. When methylisocyanide was added to one molar equivalent of $U[N(SiMe_3)_2]_3$, in pentane solution, the color changed immediately from purple-red to blue, then after one minute a brown precipitate formed. The precipitate may have been a uranium(IV) cyanide compound, formed by the reduction of methylisocyanide, however, the brown solid was not further characterized. The reaction with benzonitrile did appear to produce a

U-CN containing product, which will be discussed in greater detail in the Section 1.2.

The product from the reaction of $U[N(SiMe_3)_2]_3$ with ammonia was somewhat unexpected, as the ammonia coordination compound of tris(methylcyclopentadienyl)uranium, $(MeC_5H_4)U(NH_3)$, is a very stable, crystalline species.[16] When $U[N(SiMe_3)_2]_3$ was allowed to react with a hexane solution saturated with ammonia, a grey precipitate formed immediately. When isolated, the precipitate proved to be an an exceedingly pyrophoric, free-flowing grey powder. The elemental analysis showed the presence of some carbon (5.2%), nitrogen (7.2%), and hydrogen (1.5%), from which no reasonable empirical formula may be derived. The grey powder is insoluble in hydrocarbon solvents, tetrahydrofuran, methylene chloride and acetonitrile. Possibly, substitution of the bis(trimethylsilyl)amido ligands by ammonia, followed by condensation, may have led to the formation of a polymeric product (Eq. 1-1). However, simple acid-base considerations would not predict the initial substitution, as $HN(SiMe_3)_2$ is deprotonated by $NaNH_2$ to form $NaN(SiMe_3)_2$ and ammonia.[17]

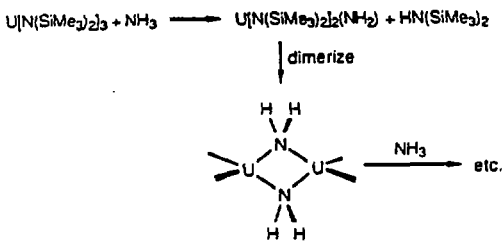

(1-1)

In conclusion, the coordination chemistry of $U[N(SiMe_3)_2]_3$ is very different from that of the cyclopentadienyl system. The coordination compounds that may be isolated are not very stable, and difficulties were encountered in the reproducibility of the reactions. In some cases, it appears that the difficulty is due to the steric requirements of the bulky bis(trimethylsilyl)amide ligands. In other cases, complications arose due to unexpected redox chemistry or reactivity of the bis(trimethylsilyl)amide ligands.

Section 1.2. One-electron redox/redistribution reactions.

One-electron redox reactions

An interesting aspect of the chemistry of uranium is the wide range of stable oxidation states the metal exhibits (+3 through +6). The only other f-elements with as many stable oxidation states are the unstable synthetic elements, neptunium, plutonium, and americium. In light of this, a U(III) compound could potentially act as a one, two, or even three electron reducing agent. In this section, one electron redox reactions will be discussed. The products fall into two different classes. The first set of reactions involves formation of new U(IV) compounds, from the reaction of $U[N(SiMe_3)_2]_3$ with reducible substrates. These reactions were found to be particularly useful in the synthesis of uranium(IV) species that could not be made by simple metathesis reactions with uranium(IV) precursors. The second set of reactions also start with $U[N(SiMe_3)_2]_3$, but involve substrates not normally considered to be reducible. The reactions appear to combine the stability of uranium's +4 oxidation state, relative to the +3 state, with the extreme lability of its ligands, to form stable uranium(IV) species *via* disproportionation reactions.

Studies of tris(cyclopentadienyl)uranium flouride have shown it to be different from its chloride, bromide, and iodide analogues.[19] The uranium flouride compound appears to auto-associate in benzene solution, and magnetic measurements on solid samples suggest there may be magnetic interaction between metal centers.[19] Tris(cyclopentadienyl)uranium flouride displaces the tetrahydrofuran from $Cp_3U(thf)$, to form a mixed-valence adduct.[20] The methylcyclo-

pentadienyl analogue of the adduct has also been made.[13a] Unfortunately, the high insolubility of these interesting mixed-valence compounds has hindered their purification, and further studies on the compounds have not been reported. It was of interest to see whether the flouride, $FU[N(SiMe_3)_2]_3$, could be made, and if it would exhibit any of the same unusual phenomena.

Silver(I) salts, AgX, are a reducible source of X^- anions, where X^- may be halide, azide, cyanide, or a variety of other anions. When $U[N(SiMe_3)_2]_3$ was stirred with a pentane suspension of AgF, the dark purple solution lightened slowly to a pink-yellow color. During the reaction, a silvery-black precipitate of Ag metal was formed. Filtering the reaction mixture and then cooling the filtrate slowly (-78°), produced pale pink crystals. The reaction was very clean and the product was obtained as crystals in good yield. The infrared spectrum of the pink crystals showed a new, strong absorption in the region of metal-flouride stretches (509 cm^{-1}).[21] The U-F stretch in $(MeC_5H_4)_3UF$ occurs at 467 cm^{-1}.[13a] A molecular ion for $FU[N(SiMe_3)_2]_3$ was observed in the mass spectrum.

The ^1H NMR spectrum of an equimolar mixture of $FU[N(SiMe_3)_2]_3$ and $U[N(SiMe_3)_2]_3$, indicated no adduct formation. Resonances for each of the compounds were observed, unchanged from their positions in the pure compounds. Magnetic measurements on $FU[N(SiMe_3)_2]_3$ did not indicate any unusual behavior. A plot of $1/\chi_M$ vs. T is shown in Figure 3-2. Its qualitative appearance, and the calculated magnetic moment of the compound, are similar to other $X\text{-}U[N(SiMe_3)_2]_3$ compounds that have been measured. Evidently, the bulky bis(trimethylsilyl)amide ligand, which limited the chemistry of $U[N(SiMe_3)_2]_3$ with Lewis bases, also hinders

the reactivity of the uranium flouride.

The triphenylmethyl, or trityl compounds, Ph_3C-X, are another class of readily reducible substrates. The relatively stable trityl radical, $Ph_3C^{\bullet}$, may be isolated as the dimerized "bitrityl" compound which has the structure,

as determined by ^1H and ^{13}C NMR spectroscopy.[22]

When a hexane solution of $U[N(SiMe_3)_2]_3$ was added to one molar equivalent of trityl azide, the color of the solution changed from deep purple to pale yellow. A mixture of brown and white solids were crystallized from the reaction mixture (-15°C). Physical separation of the two solids, followed by recrystallization from hexane, yielded two pure products. The white solid was shown to be bitrityl by ^1H NMR spectroscopy.[22] The brown solid recrystallized as gold-colored crystals, which had new, strong stretches in the infrared spectrum at 2120, 2106, and 2082 cm^{-1}, indicative of an azide compound.[21] The mass spectrum contained a molecular ion for $N_3U[N(SiMe_3)_2]_3$.

Normal mode analyses of metal azides show the absorptions near 2000 cm^{-1} to be due to the $\nu_{as}(N_3)$ mode.[23] The observation of more than one band in this region is attributed to the reduced symmetry of the compound, caused by a nonlinear M-N-N angle.[23] A weak band is expected for the symmetric N_3 stretch, near 1300 cm^{-1}.[23] In the uranium compound, this band may be obscured by Nujol absorptions. There is a weak absorption at 595 cm^{-1}, attributed to the N_3 bend.[23]

Reactions with other organic azides, in which the organic group does not form a stable alkyl radical, did not yield the uranium azide

compound. These reactions will be discussed in Section 1.3.

As mentioned at the end of Section 1.1, the reaction of $U[N(SiMe_3)_2]_3$ with benzonitrile (PhCN), did not result in isolation of the simple coordinated nitrile species. Instead, the color of the reaction mixture, which was initially blue when the benzonitrile was added, slowly turned brown. Fine, brown needles were crystallized from the reaction mixture (-25°C). The infrared spectrum of the product had a strong absorption in the region of metal-cyanide stretches (2063 cm^{-1}) and a weaker stretch indicative of coordinated benzonitrile (2252 cm^{-1}).[21] The product is proposed to be $(NC)U[N(SiMe_3)_2]_3(NCPh)$. This formulation is supported by the mass spectrum, in which the highest peak corresponds to loss of HCN from the proposed product. Attempts to isolate the uranium-cyanide compound, free of coordinated benzonitrile, both by controlling the stoichiometry of the reaction carefully to 1:1, and by sublimation of the product, were not successful.

The electrochemical reduction of benzonitrile in 75% dioxan shows two waves at -2.26 and -2.37 V, relative to S.C.E.[24] The ability of $U[N(SiMe_3)_2]_3$ to reduce benzonitrile is consistent with the observations made below, involving R_3PE compounds (E = O, S, Se, Te). Electrochemical reduction of some substituted benzonitriles, in neutral solution, has been shown to lead to formation of CN^- and an alkyl radical.[24,25]

Bridging Chalcogenides

Reactions of $(MeC_5H_4)_3U(thf)$ and $(C_5Me_5)_2Yb(OEt_2)$ with R_3PE compounds (E = S, Se, or Te) have identified the trialkylphosphine-chalcogenides as another class of reducible substrates. The products

obtained were the bridging compounds, $(MeC_5H_4)_3U\text{-}E\text{-}U(MeC_5H_4)_3$[26] and $(Me_5C_5)_2Yb\text{-}E\text{-}Yb(Me_5C_5)_2$.[27] It was of interest to investigate whether the analogous uranium bis(trimethylsilyl)amide compounds could be made.

When a dark purple, pentane solution of $U[N(SiMe_3)_2]_3$ was added to one molar equivalent of Ph_3PS, the solution turned bright gold and triphenylphosphine precipitated. An orange-gold crystalline solid was isolated after filtering and cooling the reaction mixture (-78°C). The compound appeared to crystallize with occluded solvent, as the gold crystals turned opaque after they were isolated. A new absorption was observed in the infrared spectrum at 322 cm^{-1}, which has been assigned to the U-S-U asymmetric stretch. This may be compared to the values of 358 and 379 cm^{-1} observed for the cyclopentadienyl Yb and U compounds, respectively, that are described above.

Reactions of tris(bis(trimethylsilyl)amido)uranium with Ph_3PSe or $n\text{-}Bu_3PTe$ gave the analogous bridging Se and Te compounds. The color of the selenium compound is darker orange than that of the sulfur one, and the tellurium compound is red. Both reactions proceeded rapidly at room temperature. Like the sulfur compound, the selenium dimer crystals turned opaque after they were isolated, whereas the tellurium compound remained crystalline. The asymmetric U-E-U stretches for the Se and Te compounds appear to be below the detection limits of the spectrometer. Some comparative information on the bis(trimethylsilyl)amide and methylcyclopentadienyl uranium compounds is given in Table 1-7.

Table 1-7. Physical data for $(UL_3)_2(\mu\text{-}E)$.

	L = $N(SiMe_3)_2$			L = (MeC_5H_4)[26]		
E	color	m.p.(°C)	νUXU(cm^{-1})	color	m.p.(°C)	νUXU(cm^{-1})
S	gold	145	322	red	275	358
Se	orange	145	<250	red	240	216
Te	red	158	<250	green	200	<200

The bis(trimethylsilyl)amide species do not follow the same trends in melting points and solubilities that the cyclopentadienyl compounds do. The trends of decreasing melting point and increasing hydrocarbon solubility, proceeding down the chalcogenide group, is also observed in the ytterbium compounds. One explanation for the observed trends is that steric repulsions of the two $(MeC_5H_4)_3U$ units force the U-S-U angle to be nearly linear for the sulfur compound (as is confirmed by its crystal structure, $\angle USU = 164.9(5)°$)[26], whereas the longer U-Se and U-Te bonds move the uranium units further apart, allowing the U-E-U angle to bend. The identical melting point and solubility behavior of the sulfur and selenium bis(trimethylsilyl)amide compounds suggest they may be isostructural. If, as the lack of coordination chemistry implies, the bis(trimethylsilyl)amide ligand is effectively bigger than the methylcyclopentadienyl ligand, then both the sulfur and selenium compounds may be forced by steric repulsions to have near linear U-E-U geometries, whereas, the Te compound may be able to bend.

The X-ray structure of the bridging telluride was determined by Dr. A. Zalkin. The trimethylsilyl groups on one half of the molecule (specifically on N1, N2, and N3) are disordered in the following manner. The plane defined by the $UNSi_2$ portion of the bis(trimethyl-

sily)amide ligand is tilted with respect to the axis defined by the U-Te bond. This gives the $[(Me_3Si)_2N]_3U$ unit a "handedness". The two positions for each of the trimethylsilyl groups in the disordered portion of the molecule may be thought of as the two isomers of the $[(Me_3Si)_2N]_3U$ unit. This means that in the crystal lattice, half of the dinuclear species have $[(Me_3Si)_2N]_3U$ units with the same handedness, and half with the opposite. An ORTEP of each molecule, looking down the U1-Te-U2 axis is shown in Figure 1-4. A packing diagram shows no obvious reason for this disorder or for why the disorder is observed on only one of the uranium atoms in the molecule. Some bond lengths and angles are given in Tables 1-8 and 1-9. An ORTEP drawing of the molecule, including only one set of the disordered sites, is shown in Figure 1-5.

Table 1-8. Bond lengths (Å) in $([(Me_3Si)_2N]_3U)_2(\mu\text{-Te})$.[a]

U1-N1	2.22(2)	U2-N4	2.25(2)
U1-N2	2.25(1)	U2-N5	2.22(1)
U1-N3	2.27(1)	U2-N6	2.26(1)
U1-Te	3.01(1)	U2-Te	3.03(1)
U...U	6.05(1)		

[a]Preliminary results.

Table 1-9. Intramolecular angles (°) in $([(Me_3Si)_2N]_3U)_2(\mu\text{-Te})$.[a]

U1-Te-U1	177.5		
N1-U1-N2	113.86	N4-U2-N5	112.82
N1-U1-N3	109.27	N4-U2-N6	107.42
N2-U1-N3	110.99	N5-U2-N6	109.94
Te-U1-N1	106.39	Te-U2-N4	108.44
Te-U1-N2	108.62	Te-U2-N5	104.83
Te-U1-N3	107.41	Te-U2-N6	109.94

[a]Preliminary results, no esd's available.

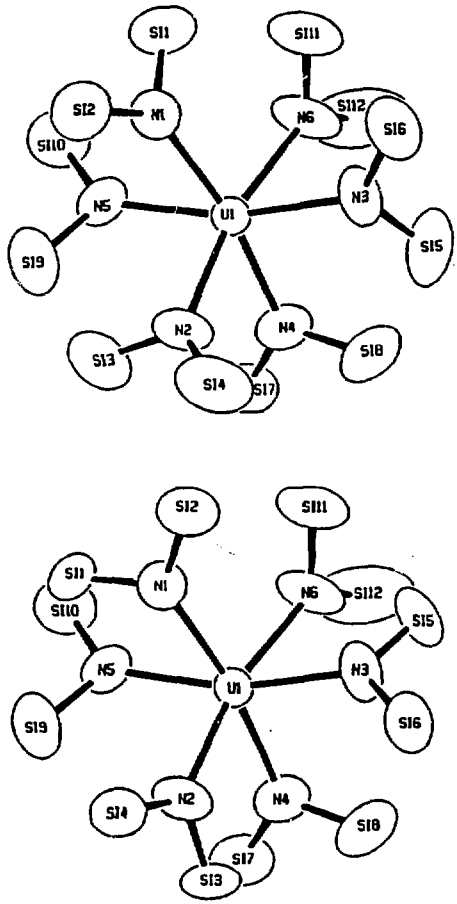

Figure 1-4. ORTEP diagrams of $([(Me_3Si)_2N]_3U)_2(\mu\text{-Te})$, looking down the U1-Te-U2 axis, showing the two disordered positions for the trimethylsilyl groups on U1 (carbon atoms omitted for clarity).

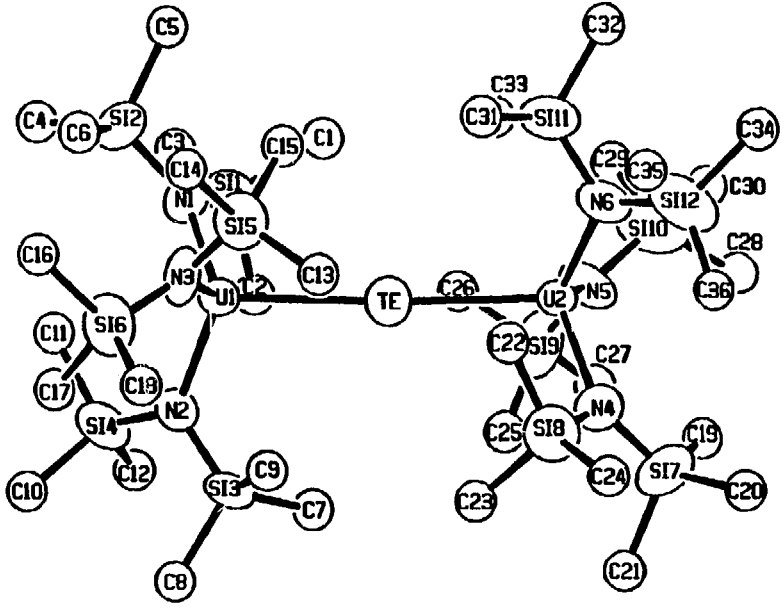

Figure 1-5. ORTEP diagram of $\{[(Me_3Si)_2N]_3U\}_2(\mu\text{-Te})$ (carbon atoms drawn with isotropic thermal parameter).

The U-Te-U angle is 177.45°, essentially linear. Electron donation from lone-pair orbitals on the tellurium to orbitals of appropriate symmetry on the uranium could cause the angle to be linear, however this interaction should shorten the U-Te bond, whereas the U-Te distances of 3.01(1) and 3.03 Å are essentially the sum of the ionic radii (Te^{2-} = 2.22 Å, U^{4+} = 0.83 Å).[8] As described above for the sulfur and selenium compounds, the angle about tellurium also may be determined by interligand repulsions between $[(Me_3Si)_2N]_3U$ units. There are a number of interligand contacts between the two units (carbon-carbon distances), of 3.6-3.8 Å.

As was noted earlier, the reaction of Ph_3PO with $U[N(SiMe_3)_2]_3$ did not result in formation of the bridging oxo compound, but gave the U(III) coordination compound described in Section 1.1. This is consistent with the trend in bond strengths and reduction potentials of the R_3PE species shown in Table 1-10.

Table 1-10. Reduction potentials[a] and E-O bond strengths in Ph_3PE compounds.

E	$-\xi_{1/2}$(V)[28]	E-O bond strength (kcal/mol)[29]
O	2.5	137
S	2.4	91
Se	2.1	--

[a]Measured at a dropping mercury electrode relative to S.C.E.

It should also be noted that in the electrochemical reduction of Ph_3PS and Ph_3PSe, formation of triphenylphosphine and S^{2-} or Se^{2-} was observed, whereas the analogous reactivity was not observed in the reduction of Ph_3PO.[28a]

Ligand redistribution reactions

The second set of reactions that will be described in this section also result in isolation of stable uranium(IV) products from uranium(III) starting materials. However, instead of simple one-electron redox reactions, the products appear to arise from a series of steps involving uranium's ability to redistribute its ligands in order to reach the more stable +4 oxidation state. The first example of this type of reaction came out of investigations into the reactivity of the lone pair electrons on the bis(trimethylsilyl)amido nitrogens. Boncella observed that the reaction of $\{Yb[N(SiMe_3)_2]_2\}_2$ with the Lewis acid, trimethylaluminum, led to isolation of a coordination compound, with trimethlyaluminum coordinated to the nitrogens of the amide ligands.[30] The reaction between $U[N(SiMe_3)_2]_3$ and trimethylaluminum proceeded in a very different manner. In hydrocarbon solvents, the purple-red solution of $U[N(SiMe_3)_2]_3$ turned black slowly, after addition of one to three equivalents of trimethylaluminum. After stirring the reaction mixture overnight, removal of the solvent left a black, oily solid. Several recrystallizations of the solid, from hexane, yielded gold-colored blocks. The ^1H NMR spectrum contained a large resonance for the silylamide protons at -1.76 ppm and a small resonance at -224 ppm. This spectrum, along with the infrared spectrum and melting point, showed the product to be the methyl compound, $MeU[N(SiMe_3)_2]_3$, which had been made earlier by the metathesis reaction between $ClU[N(SiMe_3)_2]_3$ and MeLi.[31]

The geometry about the uranium in $MeU[N(SiMe_3)_2]_3$ and $U[N(SiMe_3)_2]_3(OPPh_3)$ should be similar, so the crystal structure of the methyl compound should allow a good comparison of bond lengths and

angles in uranium(III) and (IV) compounds. The crystal structure was solved by Dr. F. J. Hollander. Bond lengths and angles are given in Tables 1-11 and 1-12. An ORTEP drawing of the methyl compound is shown in Figure 1-4.

Table 1-11. Bond lengths (Å) for $MeU[N(SiMe_3)_2]_3$.

U-N	2.252(4)	Si1-C11	1.867(6)
U-C1	2.397(13)	Si1-C12	1.857(6)
		Si1-C13	1.846(6)
N-Si1	1.752(5)	Si2-C21	1.861(7)
N-Si2	1.738(5)	Si2-C22	1.862(6)
		Si2-C23	1.846(6)

Table 1-12. Intramolecular angles (°) for $MeU[N(SiMe_3)_2]_3$.

C1-U-N	99.37(11)	U-N-Si1	121.5(2)
N-U-N	117.40(6)	U-N-Si2	118.5(2)
		Si1-N-Si2	120.1(2)
N-Si1-C11	109.1(3)	N-Si2-C21	109.3(4)
N-Si1-C12	114.5(2)	N-Si2-C22	113.1(2)
N-Si1-C13	112.1(3)	N-Si2-C23	112.6(3)
C11-Si1-C12	104.5(3)	C21-Si2-C22	106.3(4)
C11-Si1-C13	108.4(3)	C21-Si2-C23	109.7(4)
C12-Si1-C13	107.8(30	C22-Si2-C23	106.6(3)

The compound crystallizes in the acentric space group R3c, with the uranium on the crystallographic three-fold, defining the origin. The unique methyl group is also on the three-fold, 2.397(13) Å above the uranium. The U-N bond distance is 2.252(4) Å, which compares nicely to the U-N bond length of 2.24(1) Å in $HU[N(SiMe_3)_2]_3$.[32] It is 0.11 Å shorter than the average U-N bond length in the uranium(III) compound, $U[N(SiMe_3)_2]_3(OPPh_3)$, as would be expected for an increase in oxidation state. The N-U-N angle, 117.40(6)°, is larger than in

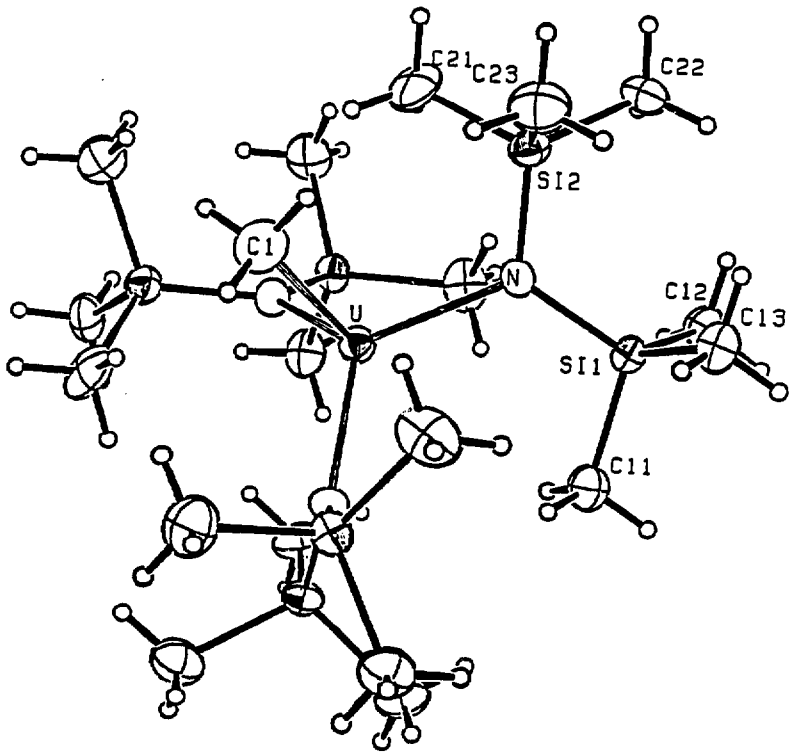

Figure 1-6. ORTEP diagram of $MeU[N(SiMe_3)_2]_3$.

$U[N(SiMe_3)_2]_3(OPPh_3)$, $(\angle N\text{-}U\text{-}N)_{ave.}$ = 112.1(1). The shorter U-N bond length in the uranium(IV) compound may cause interligand repulsions to push the ligands away from each other, increasing the N-U-N angle.

The reaction of the uranium(IV) alkyl compounds, Cp_3UR (R = Me, Pr^i, or Bu^n), with alkyl-lithium reagents, LiR', leads to the formation of very reactive uranium(III) alkyl anions, $Cp_3UR'^-$.[33] Another possible route to these types of compounds is the addition of an alkyl-lithium reagent to a uranium(III) starting material. It was of interest to *see* if the uranium(III) anion, $MeU[N(SiMe_3)_2]_3^-$, is obtainable in an analogous set of reactions.

Addition of one molar equivalent of MeLi to a pentane solution of $U[N(SiMe_3)_2]_3$ at -78°C led to immediate formation of a blue-black precipitate, presumably the addition species. However, as the solution was allowed to warm slowly to room temperature, the color of the mixture changed to pale gold and a tan precipitate formed. Filtration of the mixture, followed by concentration and cooling of the filtrate(-15°C), led to the isolation of $MeU[N(SiMe_3)_2]_3$, in less than 50% yield. The ^1H NMR spectrum, IR, and melting point all confirm the identity of the product. Equation 1-2 shows a possible route to the uranium(IV) product.

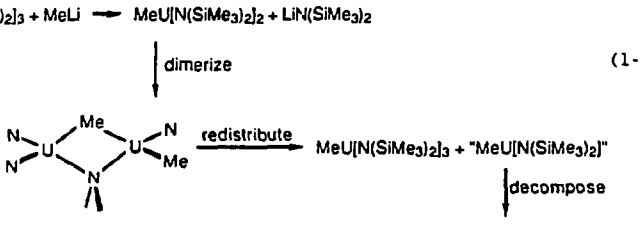

(1-2)

Both of the routes to $MeU[N(SiMe_3)_2]_3$ described above, appear to be driven by the thermodynamic stability of the uranium(IV) product formed. Although a variety of reaction pathways may be proposed, the key factor appears to be uranium's ability to move ligands around with minimal orbital restrictions. This can be a positive factor in developing a catalytic system, where ability to adopt different coordination numbers and stereochemistries is important.[34] However, it can make isolation of a specific uranium compound difficult. Kinetic barriers must be built in very precisely, through judicious choice of ligands, in order to be able to control and predict which products will be obtained.

Section 1.3. Two-electron redox reactions.

Uranium(V) imide compounds

The chemistry of the pentavalent oxidation state of uranium is relatively unexplored. The only stable, well characterized class of uranium(V) compounds are the alkoxides, $[U(OR)_5]_n$.[35] In fact, the U(IV)/U(IV) dimer, $KU_2(OBu^t)_9$, decomposes readily (in hexane solution, at 5°C) to a mixed-valence U(IV)/U(V) dimer.[36] A balanced reaction for the decomposition is shown in Eq. 1-3, although no products, other than the mixed-valence dimer, have been isolated, and yields of the dimer were not reported.

$$2\ KU_2(OBu^t)_9 \text{ ----> } U_2(OBu^t)_9 + \text{"}K_2U(OBu^t)_9\text{"} \qquad (1\text{-}3)$$

This suggests that for this compound, the tetravalent state may not be the most stable, as it is for the uranium ion in aqueous solution.[37] This stability of the pentavalent oxidation state is not observed in the halide compounds of uranium. The instabilty of UX_5 or UOX_3, relative to redistribition to U(IV) and (VI), makes the synthesis of compounds from these starting materials very difficult.[6] Therefore, oxidative or reductive pathways to kinetically stable U(V) compounds seem like possible synthetic routes. Indeed, Brennan reacted a uranium(III) cyclopentadienyl compound with an organoazide, RN_3 and obtained a uranium(V) compound (Eq. 1-4).[13a]

$$(MeC_5H_4)_3U(thf) + RN_3 \text{ ------> } (MeC_5H_4)_3U(NR) + N_2 + thf \qquad (1\text{-}4)$$

He also synthesized $U[N(SiMe_3)_2]_3(NSiMe_3)$ from $U[N(SiMe_3)_2]_3$ and trimethlsilylazide.[13a] There was interest in exploring the scope of this reaction with other organoazide species.

The reaction of $U[N(SiMe_3)_2]_3$ with p-tolylazide or t-butylazide, in pentane solution, resulted in gas evolution and isolation of the

black crystalline U(V) imido compounds, $U[N(SiMe_3)_2]_3[N(p\text{-tolyl})]$ and $U[N(SiMe_3)_2]_3(NBu^t)$. The resonances in the ^1H NMR spectrum of the compounds have large peak widths; the peak widths at half-maximum for the bis(trimethylsilyl)amide protons were 35 and 123 Hz, respectively, for the p-tolyl and t-butyl compounds. Broad peak widths were also observed in the ^1H NMR spectrum of the uranium(V)cyclopentadienylimide compounds ($\nu_{1/2}$ = 40-60 Hz).[13a] Although the imido compounds are stable at room temperature, gentle heating caused them to decompose to $[(Me_3Si)_2N]_2\overline{UCH_2(Me)_2SiNSiMe_3}$ and the primary amine, RNH_2.

Very few crystal structures of U(V) compounds have been determined. In order to investigate the geometry and bonding in the imido compounds, the structures of $U[N(SiMe_3)_2]_3(NSiMe_3)$, originally synthesized by Brennan,[13a] and $U[N(SiMe_3)_2]_3[N(p\text{-tolyl})]$ were obtained.

The p-tolyl compound crystallizes in the triclinic space group $P\bar{1}$. An ORTEP drawing of the molecule is shown in Figure 1-7 and bond lengths and angles are given in Tables 1-13 and 1-14.

Table 1-13. Bond lengths (Å) for $U[N(SiMe_3)_2]_3[N(p\text{-tolyl})]$.

U-N1	2.244(6)	N4-C1	1.397(9)
U-N2	2.229(5)		
U-N3	2.253(6)	C1-C2	1.40(1)
U-N4	1.940(6)	C1-C6	1.40(1)
		C2-C3	1.38(1)
N1-Si11	1.746(6)	C3-C4	1.39(1)
N1-Si12	1.744(6)	C4-C5	1.39(1)
N2-Si21	1.751(6)	C4-C7	1.51(1)
N2-Si22	1.738(6)	C5-C6	1.38(1)
N3-Si31	1.734(6)		
N3-Si32	1.743(6)		

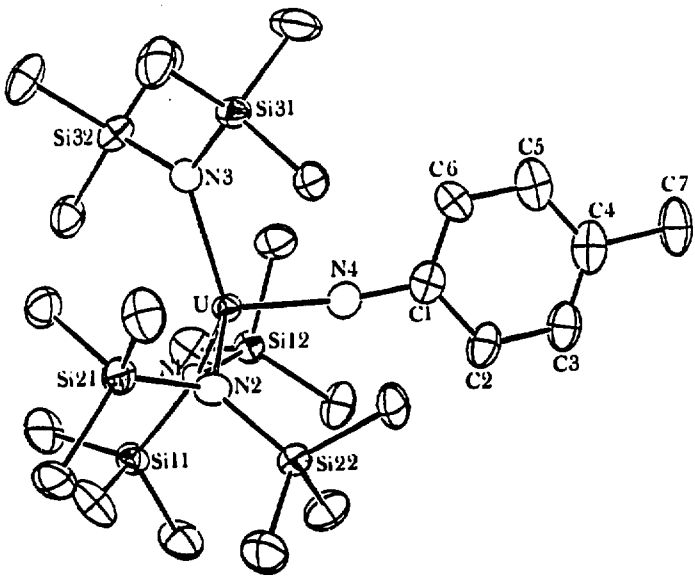

Figure 1-7. ORTEP diagram of $U[N(SiMe_3)_2]_3[N(p\text{-tolyl})]$.

Table 1-14. Intramolecular Angles (°) for $U[N(SiMe_3)_2]_3[N(p\text{-tolyl})]$.

N1-U-N2	109.5(2)	Si11-N1-Si12	118.9(3)
N1-U-N3	120.9(2)	Si21-N2-Si22	123.3(3)
N2-U-N3	115.1(2)	Si31-N3-Si32	120.4(3)
N1-U-N4	100.6(2)		
N2-U-N4	102.6(2)	U-N1-Si11	129.6(3)
N3-U-N4	105.1(2)	U-N1-Si12	111.4(3)
		U-N2-Si21	118.4(3)
U-N4-C1	171.4(5)	U-N2-Si22	118.1(2)
		U-N3-Si31	115.5(3)
Si11-N1-Si12	118.9(3)	U-N3-Si32	124.0(3)
Si21-N2-Si22	123.3(3)		
Si31-N3-Si32	120.4(3)	N4-C1-C2	121.3(7)
		N4-C1-C6	121.2(7)

The geometry about uranium is pseudo-tetrahedral, with large angles between the bis(trimethlylsilyl)amide ligands, presumably due to interligand steric repulsion. The amide nitrogens are N1, N2, and N3, and the average N-U-N angle is 115.2°. The U-N bond length for the imido-nitrogen is 1.940(6) Å, whereas the equivalent bond length in $(MeC_5H_4)_3U(NPh)$ is 2.019(6) Å.[38] The average U-N amide bond length is 2.242(6) Å, which is somewhat longer than expected, since bond lengths monatonically decrease with increasing oxidation state. Changes in the U-N bond length, relative to changes in oxidation state, will be discussed at the end of this section. The U-N-C angle for the imido-ligand is 171.4(5)°, similar to the 167.4(6)° angle observed in $(MeC_5H_4)_3U(NPh)$.[38] Linear, or near linear, angles for terminal imides, have been taken to reflect triple bond character in the M-N bond,[39] and the U-N(imide) bond length in this compound is significantly shorter than the U-N(amide) length. However, steric effects and crystal packing forces may also play a role in the observed ligand geometry.

The trimethylsilyl imide compound crystallizes in the same acentric space group as $MeU[N(SiMe_3)_2]_3$, R3c. Some bond lengths and

angles are listed in Tables 1-15 and 1-16. An ORTEP diagram of the molecule is shown in Figure 1-8.

Table 1-15. Bond lengths (Å) in $U[N(SiMe_3)_2]_3(NSiMe_3)$.

U-N1	1.906(9)	Si21-C211	1.871(6)
U-N2	2.247(4)	Si21-C212	1.872(6)
		Si21-C213	1.863(4)
N1-Si1	1.754(9)		
Si1-C1	1.859(7)	Si22-C221	1.897(5)
		Si22-C222	1.865(5)
N2-Si21	1.745(3)	Si22-C223	1.843(6)
N2-Si22	1.737(4)		

Table 1-16. Intramolecular angles (°) for $(Me_3SiN)U[N(SiMe_3)_2]_3$.

N1-U-N2	102.64(9)	U-N2-Si21	123.3(2)
N2-U-N2'	115.4(2)	U-N2-Si22	116.5(2)
N1-Si1-C1	111.1(2)		
		Si21-N2-Si22	119.9(2)
U-N1-Si1	180[a]		

[a]Angle is required to be linear by symmetry.

The uranium is found on the crystallographic three-fold axis and defines the origin. The imido nitrogen and silicon atoms are also located on the three-fold axis. The U-N-Si angle is required by symmetry to be linear. Both the amido and imido U-N bond lengths and N-U-N angles are very similar to those in the p-tolyl compound, as is shown in Table 1-17.

Table 1-17. Bond lengths (Å) and angles (°) in $U[N(SiMe_3)_2]_3(NR)$ compounds, R = p-tolyl or Me_3SiN

R	p-tolyl[a]	Me_3Si
U-N, imide	1.940(6)	1.906(9)
U-N, amide	2.242(6)	2.247(4)
N-U-N, imide	102.8(2)	102.6(1)
N-U-N, amide	115.2(2)	115.4(2)

[a]Average bond lengths and angles are reported for the p-tolyl compound.

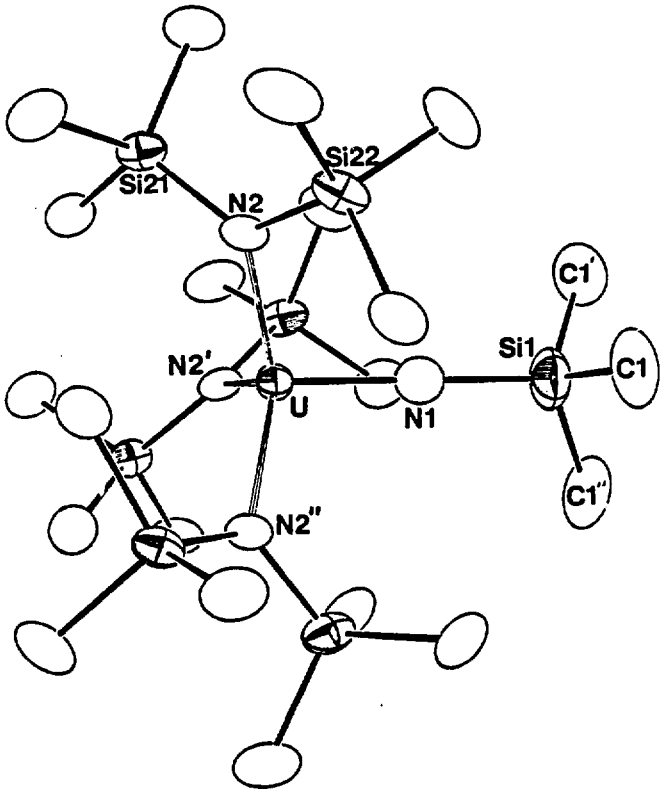

Figure 1-8. ORTEP diagram of $U[N(SiMe_3)_2]_3(NSiMe_3)$.

The crystal structure of this compound had been determined earlier,[40] and an anomolously long U-N(amide) bond length, 2.30(1) Å, was found. There are no obvious reasons why the bond length should vary greatly from the average U-N(amide) bond length in $U[N(SiMe_3)_2]_3[N(p\text{-tolyl})]$, U-N(ave.) = 2.242(6) Å. Although the differences are not enormous, the bond length in the trimethylsilyl-imide compound is not within 3σ of that in the p-tolylimide species. More disturbingly, the bond length is longer than the typical U-N(amide) bond lengths in the four-coordinate uranium(IV) compounds described in Section 1.2. This makes the U^{5+} cation appear larger than U^{4+}, when the opposite would be predicted. However, there were several factors that brought the anomolous bond length in question. The crystal data was collected at room temperature and the compound exhibited significant thermal motion. The carbon of the trimethylsilylimide group had the largest thermal parameter, with B_{eqv} = 12(2). No absorption correction had been applied to the data, although the compound had a large absorption coefficient, μ = 41.7 cm^{-1}. For these reasons, it was of interest to determine whether the bond length was anomolously long, or if it was a result of the problems listed above. A data set was collected on a new crystal at -115°C, an empirical absorption correction was applied to the data, and the structure was redetermined. There were no major changes in any of the atomic positions and the U-N(imide) bond length remained unchanged; it was 1.90(1) Å in the room temperature structure and it is now 1.906(9) Å. The thermal parameter of Cl has a more reasonable value, B_{eqv} = 5.8(2). Most importantly, the new U-N(amide) bond length is 2.247(4) Å, which fits in perfectly with the expected value. This points out

that care must be taken in over-interpreting crystal structure results and that bond length arguments, in particular, must be made conservatively, with an eye toward the quality of the structure in question.

Magnetic susceptibility studies

The magnetic behavior of the uranium(V) imide compounds was quite different, qualitatively, from that of the uranium(III) and (IV) bis(trimethylsilyl)amide compounds. Plots of $1/\chi_M$ vs. T and calculated magnetic moments are given in the Experimental Section for many of the compounds reported here. The measurements were more investigative in nature, than quantitative, due to the fact that there is no well-defined coupling scheme for the actinide ions.[41] The major terms in the Hamiltonian will be mentioned; however, without information from EPR and optical spectra, quantitative interpretation of the magnetism is not possible.[42]

The first term to consider in the Hamiltonian is the electrostatic Coulomb repulsion between pairs of electrons, or e^2/r term. This term is smaller for the large actinide ions than it is for smaller elements, and may be on the order of spin-orbit coupling. The second term is the spin-orbit coupling term, which becomes increasingly more important as Z, the atomic number, increases. Spin-orbit coupling is a magnetic interaction between an electron's spin, $m_s = \pm 1/2$, and the magnetic moment due to the orbital motion of an electron. The spin-orbit coupling for the actinide elements is on the order of 2000 cm^{-1}.[41] For the lanthanide ions, the interpretation may generally stop here, and magnetic behavior can be predicted using the Van Vleck equations for

free ions.[41] However, for the actinide ions, the electric field term, V, can not be ignored. The electric field, created by the ligands surrounding the ion, has been treated theoretically in a number of different manners.[42] As the identity of the ligands and the geometry about the metal changes, the effect of the ligand field changes; therefore, the electronic structure of each compound must be developed separately.

Plots of $1/\chi_M$ versus T, for $U[N(SiMe_3)_2]_3[N(p\text{-tolyl})]$ and $U[N(SiMe_3)_2]_3(NSiMe_3)$, are shown in Figures 3-5 and 3-6. A linear least squares fit to the 5 kG data gave magnetic moments of 1.49 B.M. (5-40 K) and 2.26 B.M. (140-240 K) for the p-tolyl compound, and 1.61 B.M. (5-40 K) and 2.04 (140-280 K) for the trimethylsilyl compound. The shape of the line and the very low moment are good evidence for the pentavalent oxidation state. The uranium(III) and (IV) bis(trimethylsilyl)amide compounds displayed a wide range of moments (2.90-3.41 B.M.), with no obvious distinction between the two oxidation states. The uranium(V) moment, on the other hand, has a significantly lower value. In this case, the magnetic behavior provides useful informaton about the oxidation state of uranium. Interestingly, the qualitative trend in magnetic moments observed for the bis(trimethylsilyl)amide compounds matches that predicted by the "free ion" moments, calculated from the Van Vleck equation (Table 1-18). The free ion values for uranium(III) and (IV) are very similar, whereas uranium(V) is significantly lower.

Table 1-18. Calculated magnetic moments for f^1, f^2, and f^3 configuration.

Oxidation State	Configuration	"free ion" moment
U(III)	f^3	3.62
U(IV)	f^2	3.58
U(V)	f^1	2.54

Conproportionation reactions.

In Section 1.2, redox routes to new uranium(IV) compounds were investigated. According to the aqueous redox potentials, the tetravalent oxidation state is thermodynamically favored relative to the trivalent state. This was used as a driving force to synthesize new uranium(IV) compounds from uranium(III) precursors. If the trend observed in the aqueous potentials holds true, the reaction of a U(III) compound with a U(V) compound could lead to U(IV) products, given a kinetically feasible pathway. This type of reaction was observed for the uranium cyclopentadienyl compounds as shown in Eq. 1-4.[13a]

$$(MeC_5H_4)_3U(thf) + (MeC_5H_4)_3U(NPh) \longrightarrow [(MeC_5H_4)_2U(\mu\text{-}NPh)]_2 + \text{other products} \qquad (1\text{-}4)$$

When a similar reaction was carried out with bis(trimethylsilyl)-amide compounds, different results were observed. The reaction of $U[N(SiMe_3)_2]_3$ and $U[N(SiMe_3)_2]_3[N(p\text{-tolyl})]$ led to formation of two gold-colored products that could be separated by fractional crystallization. The more soluble product is $[(Me_3Si)_2N]_2\overline{UCH_2(Me)_2SiNSiMe_3}$, as identified by comparison of its ^1H

NMR spectrum with the reported values.[43] The other product is somewhat less soluble than the metallocycle, and its ^{1}H NMR spectrum also indicated its identity. Aside from the resonances expected for the bis(trimethylsilyl)amide and p-tolyl ligands, there was one new resonance, far upfield, at -213 ppm. Resonances in this region have been observed before, for a hydrogen on an atom directly attached to uranium, as in $(MeC_5H_4)_3U(\underline{N}HPh)$.[13a] The second product in the "III + V" reaction is $U[N(SiMe_3)_2]_3[NH(p\text{-tolyl})]$ and the balanced reaction is shown in Equation 1-5.

$$U[N(SiMe_3)_2]_3 + U[N(SiMe_3)_2]_3[N(p\text{-tolyl})] \text{ ----> } [(Me_3Si)_2N]_2\overbrace{UCH_2(Me)_2SiNSiMe_3} + U[N(SiMe_3)_2]_3[NH(p\text{-tolyl})] \quad (1\text{-}5)$$

The structure of the new U(IV) compound was determined for comparison with its uranium(V) analogue, $U[N(SiMe_3)_2]_3[N(p\text{-tolyl})]$, in order to investigate the effect of change in oxidation state on bond lengths and ligand geometry. The two compounds are isostructural; cell constants for both compounds are listed in Table 1-18. Some bond lengths and angles for the uranium(IV) compound are listed in Tables 1-19 and 1-20. An ORTEP drawing of the molecule is shown in Figure 1-9.

Table 1-18. Unit cell dimensions for isostructural U(IV) and (IV) compounds, space group P1.

	$U[N(SiMe_3)_2]_3[NH(p\text{-tolyl})]$	$U[N(SiMe_3)_2]_3[N(p\text{-tolyl})]$
a, Å	11.506(2)	11.425(2)
b, Å	12.035(2)	11.978(2)
c, Å	13.987(3)	14.081(3)
α, deg	94.77(2)	94.69(2)
β, deg	90.09(1)	89.98(2)
γ, deg	91.13(2)	90.50(2)
Volume $Å^3$	1929(1)	1920(1)

Table 1-19. Bond lengths (Å) for $U[N(SiMe_3)_2]_3[NH(p\text{-tolyl})]$.

U-N1	2.250(2)	N4-C1	1.400(4)
U-N2	2.257(2)	N4-H	0.865(2)
U-N3	2.259(2)		
U-N4	2.209(2)	C1-C2	1.392(4)
		C1-C6	1.401(5)
N1-Si1	1.745(3)	C2-C3	1.371(5)
N1-Si2	1.746(2)	C3-C4	1.380(5)
N2-Si3	1.733(2)	C4-C5	1.381(6)
N2-Si4	1.750(2)	C4-C7	1.514(5)
N3-Si5	1.743(2)	C5-C6	1.384(5)
N3-Si6	1.733(2)		

Table 1-20. Intramolecular angles (°) for $U[N(SiMe_3)_2]_3[NH(p\text{-tolyl})]$.

N1-U-N2	122.27(8)	Si1-N1-Si2	117.9(1)
N1-U-N3	108.50(8)	Si3-N2-Si4	121.1(1)
N2-U-N3	117.98(8)	Si5-N3-Si6	122.4(1)
N1-U-N4	94.77(9)	U-N1-Si1	130.1(1)
N2-U-N4	110.59(9)	U-N1-Si2	111.9(1)
N3-U-N4	97.16(9)	U-N2-Si3	115.9(1)
		U-N2-Si4	122.9(1)
U-N4-C1	149.4(2)	U-N3-Si5	121.4(1)
U-N4-H	96.7(2)	U-N3-Si6	116.1(1)
Si1-N1-Si2	117.9(1)		
Si3-N2-Si4	121.1(1)		
Si5-N3-Si6	122.4(1)		

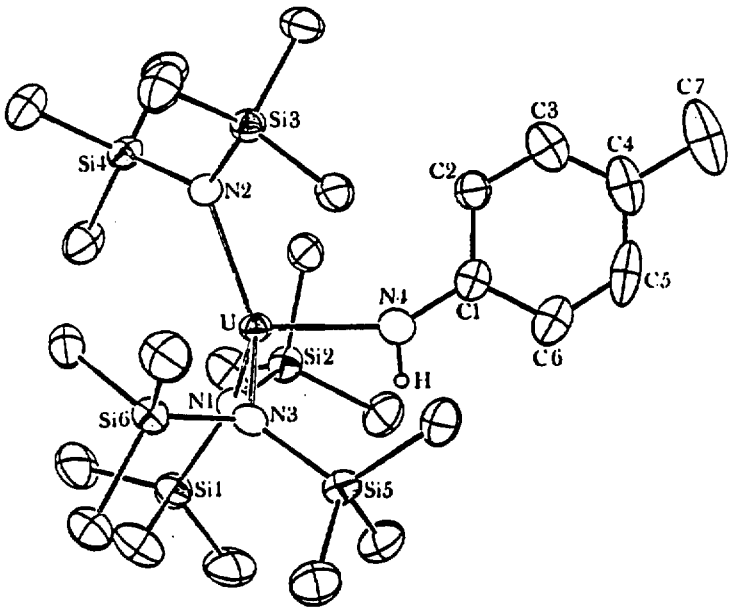

Figure 1-9. ORTEP diagram of $U[N(SiMe_3)_2]_3[NH(p\text{-tolyl})]$.

The structure is similar to that of $U[N(SiMe_3)_2]_3[N(p\text{-tolyl})]$, which has already been described. The U-N-C angle of the p-tolyl ligand is 149.4(2)°, compared to the nearly linear angle of 171.4(5)°, in the uranium(V) compound. Bond lengths and angles of the two compounds are compared in Table 1-21. The largest peak in the difference Fourier map, calculated after all the trimethylsilyl-hydrogen atoms were placed in their calculated positions, corresponded to the expected position of the unique amido-hydrogen. Unfortunately, attempts at refining the position of the hydrogen atom, with an anisotropic thermal parameter, were unsuccessful. The hydrogen was placed in its observed position, with the N-H bond length adjusted to 0.87 Å.

Table 1-21. Isostructural U(IV) and (V) compounds.

	$U[N(SiMe_3)_2]_3[NH(p\text{-tolyl})]$	$U[N(SiMe_3)_2]_3[N(p\text{-tolyl})]$
U-N, Å	2.209(2)	1.940(6)
∠UNC, deg	149.4(2)	171.4(5)
U-N (amide), Å	2.259(2)	2.253(6)
	2.257(2)	2.244(6)
	2.250(2)	2.229(5)

The reaction of $U[N(SiMe_3)_2]_3(NSiMe_3)$ and $U[N(SiMe_3)_2]_3$ did not result in isolation of a new amide species. As in the previous reaction, the metallocycle was formed, but the second product proved to be the methyl compound, $MeU[N(SiMe_3)_2]_3$. A possible reaction scheme is shown in Eq. 1-6.

$$(Me_3SiN)U[N(SiMe_3)_2]_3 + U[N(SiMe_3)_2]_3 \longrightarrow \quad (1\text{-}6)$$
$$MeU[N(SiMe_3)_2]_3 + [(Me_3Si)_2N]_2\overline{UCH_2(Me)_2SiNSiMe_3} + (Me_2SiNH)_n$$

Cyclic silazanes are very stable, particularly for n = 3 or 4.[44] The primary amine, Me_3SiNH_2, is unstable to condensation,[44] so the inability to isolate the corresponding uranium-trimethylsilylamide species is not entirely unanticipated.

The X-ray structures described up to this point, form the basis for a comparison of structurally similar uranium compounds, in three different oxidation states. There are very few examples of such comparisons for any metals, for two reasons. First, the wide variability of uranium's stable oxidation states is unusual for the lanthanide and actinide elements. Secondly, changes in oxidation state in the d-transition metals generally cause changes in geometry about the metal, due to the directionality requirements of the d-orbitals.

The changes in the U-N bond lengths in $U[N(SiMe_3)_2]_3(OPPh_3)$, $U[N(SiMe_3)_2]_3[NH(p\text{-tolyl})]$, and $U[N(SiMe_3)_2]_3[N(p\text{-tolyl})]$ will be compared. Of course, the uranium(III) p-toluidine coordination compound would have been the ideal one to complete the series, instead of the (triphenylphosphine)oxide compound. However, substituted anilines react in a different, and interesting, manner with tris(bis(trimethylsilyl)amido)uranium, as will be seen in the next section. Table 1-22 contains the U-N(ave.) bond lengths for the three compounds, and the Shannon-Prewitt ionic radii for uranium in the corresponding oxidation state.[8] The radii are adjusted to the four-coordination observed in the compounds.[45] The change in the U-N bond lengths of the uranium(III) and (IV) compounds, is predicted nearly exactly by the change in the ionic radii of the metal. However, the U-N bond length in the uranium(V) compound is nearly the same as in the

Cyclic silazanes are very stable, particularly for n = 3 or 4.[44] The primary amine, Me_3SiNH_2, is unstable to condensation,[44] so the inability to isolate the corresponding uranium-trimethylsilylamide species is not entirely unanticipated.

The X-ray structures described up to this point, form the basis for a comparison of structurally similar uranium compounds, in three different oxidation states. There are very few examples of such comparisons for any metals, for two reasons. First, the wide variability of uranium's stable oxidation states is unusual for the lanthanide and actinide elements. Secondly, changes in oxidation state in the d-transition metals generally cause changes in geometry about the metal, due to the directionality requirements of the d-orbitals.

The changes in the U-N bond lengths in $U[N(SiMe_3)_2]_3(OPPh_3)$, $U[N(SiMe_3)_2]_3[NH(p\text{-tolyl})]$, and $U[N(SiMe_3)_2]_3[N(p\text{-tolyl})]$ will be compared. Of course, the uranium(III) p-toluidine coordination compound would have been the ideal one to complete the series, instead of the (triphenylphosphine)oxide compound. However, substituted anilines react in a different, and interesting, manner with tris(bis(trimethylsilyl)amido)uranium, as will be seen in the next section. Table 1-22 contains the U-N(ave.) bond lengths for the three compounds, and the Shannon-Prewitt ionic radii for uranium in the corresponding oxidation state.[8] The radii are adjusted to the four-coordination observed in the compounds.[45] The change in the U-N bond lengths of the uranium(III) and (IV) compounds, is predicted nearly exactly by the change in the ionic radii of the metal. However, the U-N bond length in the uranium(V) compound is nearly the same as in the

isostructural uranium(IV) compound, showing little shrinkage. An analogous trend is observed in the U-C bond lengths in $(MeC_5H_4)_3UL$ compounds.[13a] The bulky bis(trimethylsilyl)amide ligands appear to have reached the limit of closest approach in compounds of this type. The bond lengths can no longer be predicted by a simple radii summation, ignoring the size of the ligands within the inner coordination sphere.

Table 1-22. Ionic radii of four-coordinate uranium in its tri-, tetra-, and penta-valent oxidation state; and the average U-N(bis(trimethylsilyl)amide) bond lengths in $U[N(SiMe_3)_2]_3(OPPh_3)$, $U[N(SiMe_3)_2]_3[NH(p\text{-tolyl})]$, and $U[N(SiMe_3)_2]_3[N(p\text{-tolyl})]$.

	U(III)	U(IV)	U(V)
Metal ionic radius, Å	0.95	0.83	0.74
U-N bond length (ave.), Å	2.36	2.26	2.24

Section 1.4. Uranium dimers.

Both of the compounds described in this section arose from attempts at finding another synthetic route to the uranium(IV) p-tolylamide compound, $U[N(SiMe_3)_2]_3[NH(p\text{-tolyl})]$. This compound was one of two uranium(IV) products obtained from the U(III) + U(V) reaction described in the previous section. The low yields, which resulted from the fractional crystallization required in the isolation of the compound, made finding a better synthetic route desirable. The first compound described in this section, $U_2[N(SiMe_3)_2]_4[\mu\text{-}N(p\text{-tolyl})]_2$, has several analogues in both uranium and Group 4 transition metal chemistry. The second compound, $U_2[N(SiMe_3)_2]_4[\mu\text{-}N(H)(2,4,6\text{-}Me_3C_6H_2)]_2$, does not appear to have a precedent in either early transition metal or f-metal chemistry. It nicely concludes the story of uranium bis(trimethylsilyl)amide chemistry, by exemplifying the point made in Section 1.2, viz., that kinetic barriers must be designed carefully to allow isolation of specific uranium compounds. This new, fairly unstable, compound appears to be on the borderline of kinetic stability, and its isolation depends to an extent on the unique steric properties of the bis(trimethylsilyl)amide ligand.

$U_2[N(SiMe_3)_2]_4[\mu\text{-}N(p\text{-tolyl})]_2$

A logical starting point for the synthesis of the p-tolylamido-uranium compound is the metathesis reaction of $ClU[N(SiMe_3)_2]_3$ and $Li[NH(p\text{-tolyl})]$. However, reaction of the uranium chloride with a suspension of $Li[NH(p\text{-tolyl})]$ in hexane solution, yielded a red solution, instead of the expected gold color of the amide compound. Filtration of the reaction mixture, followed by slow cooling of the

filtrate(-15°C), yielded large, dark-red crystals.

Space-group determination and density calculations suggested a compound with a ratio of bis(trimethylsilyl)amide ligand to p-tolyl-amide ligand of two-to-one instead of three-to-one. Elemental analysis and the integration of the ^1H NMR spectrum also supported this formulation, although no amido-hydrogen resonance was observed in the spectrum. In a strange twist of reactivity, the product appeared reminiscent of the bridging imido dimer, $U_2(MeC_5H_4)_4(\mu\text{-NPh})_2$, which Brennan obtained from the U(III) + U(V) reaction of $(MeC_5H_4)_3U(thf)$ and $(MeC_5H_4)_3U(NPh)$.[13a] In other words, it appeared that in trying to make the product obtained from the bis(trimethylsilyl)amide III + V reaction, an analogue of the product from the cyclopentadienyl III + V reaction was obtained instead. Subsequent solution of the crystal structure showed this formulation to be correct; the product is the bridging imido dimer, $U_2[N(SiMe_3)_2]_4[\mu\text{-N(p-tolyl)}]_2$. Some bond lengths and angles are given in Tables 1-23 and 1-24. An ORTEP diagram of the dimer is shown in Figure 1-10.

Table 1-23. Bond lengths (Å) for $U_2[N(SiMe_3)_2]_4[\mu\text{-N(p-tolyl)}]_2$.

U-N1	2.293(3)	C1-C2	1.389(5)
U-N2	2.274(2)	C1-C6	1.385(5)
U-N3	2.172(3)	C2-C3	1.388(4)
U-N3'	2.278(3)	C3-C4	1.370(5)
		C4-C5	1.379(5)
N3-C1	1.415(4)	C4-C7	1.515(4)
		C5-C6	1.389(5)
N1-Si11	1.721(3)		
N1-Si12	1.738(3)		
N2-Si21	1.715(3)		
N2-Si22	1.732(3)		

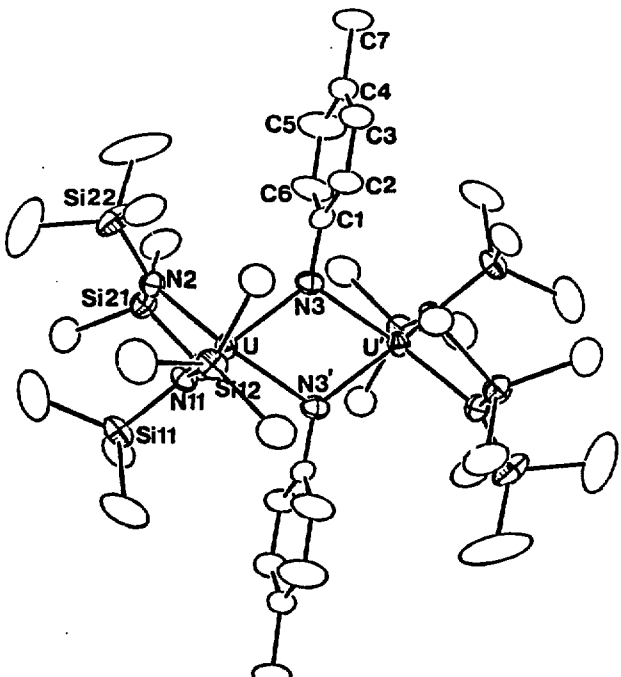

Figure 1-10. ORTEP diagram of $U_2[N(SiMe_3)_2]_4[\mu\text{-}N(p\text{-tolyl})]_2$.

Table 1-24. Intramolecular angles (°) for $U_2[N(SiMe_3)_2]_4[\mu\text{-}N(p\text{-tolyl})]_2$.

N1-U-N2	109.12(9)	Si11-N1-Si12	118.5(2)
N1-U-N3	114.83(9)	Si21-N2-Si22	123.6(2)
N1-U-N3	107.13(9)		
N2-U-N3	100.93(9)	U-N3-U'	105.8(1)
N2-U-N3	141.71(9)	U-N3-C1	138.2(2)
N3-U-N3'	74.2(1)	U'-N3-C1	113.9(2)
U-N1-Si11	109.9(1)	N3-C1-C2	122.6(3)
U-N1-Si12	131.3(1)	N3-C1-C6	121.1(3)
U-N2-Si21	113.2(1)		
U-N2-Si22	123.1(1)		

The X-ray structure shows the dimer to be bridged in a slightly asymmetric fashion by the imido nitrogens. The difference between the long and short U-N(imide) bond lengths is approximately 0.11 Å. Molecular orbital studies have beer carried out on bridging imido compounds to explain the observation of symmetric and asymmetric bridging modes.[46] The M-N(bridge) bonds in the tungsten and molybdenum compounds, $M_2(Me)_4(NBu^t)_2(\mu\text{-}NBu^t)_2$, exhibit a large asymmetry in the solid state; the difference between the M-N(bridge) bonds for the tungsten compound is 0.45 Å.[46] The other compounds in the molecular orbital study, $M_2(NMe_2)_4(\mu\text{-}NBu^t)_2$, M = Ti or Zr, are symmetrically bridged, within experimental error.[46] The geometry about the metal in the tungsten and molybdenum compounds is distorted trigonal bipyramidal, and the molecular orbital calculations suggested the asymmetry is due to a second-order Jahn-Teller distortion.[46] The geometry in the titanium and zirconium compounds is the same as in the uranium dimer, distorted tetrahedral, and they do not experience the distortion. Other examples of bridging imides in uranium chemistry include $U_2(MeC_5H_5)_4(\mu\text{-}NSiMe_3)_2$,[13a] which is bridged more symmetrically

than the bis(trimethylsilyl)amide dimer, and $U_2(MeC_5H_5)_4(\mu\text{-}NPh)_2$,[13a] which is slightly more asymmetric. The U-N(imide) bond lengths in the latter compound are 2.156(8) and 2.315(8) Å, however each phenyl group is "leaning" toward a uranium atom and there is a close interaction between the uranium and the ipso-carbon of the phenyl group (2.86(1) Å). This may contribute to the slightly greater distortion.

The bis(trimethylsilyl)amide dimer has a crystallographic center of inversion, which makes the U_2N_2 core planar. The U-N(silylamide) bond lengths are slightly longer than those in uranium(IV) compounds of the type $LU[N(SiMe_3)_2]_3$, however, they are still reasonable for uranium(IV).

The reaction is qualitatively similar to the formation of the $[(Me_3Si)_2N]_2\overline{UCH_2(Me)_2SiNSiMe_3}$. The reaction of $ClU[N(SiMe_3)_2]_3$ with one molar equivalent of $Na[N(SiMe_3)_2]$ produces the metallocycle and $(Me_3Si)_2NH$, instead of a fourth substitution.[43] To show this qualitative similarity, the balanced reactions are given in Equations 1-7 and 1-8.

$$Li[NH(p\text{-tolyl})] + ClU[N(SiMe_3)_2]_3 \text{ -----> } U_2[N(SiMe_3)_2]_4[\mu\text{-}N(p\text{-tolyl})]_2 + LiCl + HN(SiMe_3)_2 \quad (1\text{-}7)$$

$$LiN(SiMe_3)_2 + ClU[N(SiMe_3)_2]_3 \text{ -----> } [(Me_3Si)_2N]_2\overline{UCH_2(Me)_2SiNSiMe_3} + LiCl + HN(SiMe_3)_2 \quad (1\text{-}8)$$

Earlier, the point was made that redox reactions with uranium(III) precursors could be useful in making compounds that could not be made by metathetical reactions of uranium(IV) compounds. The inability to

isolate the desired amide compound in this metathetical reaction illustrates that statement.

$\underline{U_2[N(SiMe_3)_2]_4[\mu\text{-}N(H)(2,4,6\text{-}Me_3C_6H_2)]_2}$

There are two routes to the methylcyclopentadienyl analogue of the desired amide compound, tris(methylcyclopentadienyl)(p-tolylamido)-uranium(IV). Melting the uranium(III) p-toluidine coordination compound, $(MeC_5H_4)_3U[NH_2(p\text{-tolyl})]$, results in evolution of hydrogen and formation of the amide.[16] The second route was discovered while investigating the reactions of $(MeC_5H_4)_3U(thf)$ with organoazides. The synthesis of $(MeC_5H_4)_3U(NPh)$, from $(MeC_5H_4)_3U(thf)$ and phenylazide, was always plagued by the presence of some of the amide, $(MeC_5H_4)_3U(NHPh)$.[13a] It was found that contamination of the phenylazide, used in the reaction, with a small amount of aniline, $PhNH_2$, led to the formation of the uranium(IV) compound, by the series of reactions shown in Eqs. 1-9 through 1-11.[16]

$$(MeC_5H_4)_3U(thf) + PhN_3 \text{ --> } (MeC_5H_4)_3U(NPh) + N_2 + thf \qquad (1\text{-}9)$$

$$(MeC_5H_4)_3U(thf) + PhNH_2 \text{ --> } (MeC_5H_4)_3U(H_2NPh) + thf \qquad (1\text{-}10)$$

$$(MeC_5H_4)_3U(NPh) + (MeC_5H_4)_3U(H_2NPh) \text{ --> } 2\ (MeC_5H_4)_3U(NHPh) \qquad (1\text{-}11)$$

For the bis(trimethylsilyl)amide system, both of these synthetic routes to the amide would involve starting with the unknown uranium(III) coordination compound, $U[N(SiMe_3)_2]_3[NH_2(p\text{-tolyl})]$. The U(IV) p-tolylamide and the U(V) p-tolylimide have already been described. To complete the series, the p-toluidine coordination compound of $U[N(SiMe_3)_2]_3$ was needed.

The reaction of $U[N(SiMe_3)_2]_3$ with p-toluidine led to the formation of a brown, oily solid, that could not be purified by either

crystallization or sublimation, and was not further characterized. The reaction with unsubstituted aniline led to isolation of a tan-colored powder that was insoluble in hydrocarbon solvents. The powder was soluble in tetrahydrofuran, but in solution slowly deposited a black solid that would not redissolve.

It was hoped that further alkyl-substitution of the aniline ring would increase the stability of the desired product, since a bulkier ligand may block decomposition routes. The reaction of one molar equivalent of 2,4,6-trimethylaniline with $U[N(SiMe_3)_2]_3$ in pentane, led to the immediate precipitation of thin, turquoise plates. Unfortunately, the crystals were insoluble in hexane and toluene. They were soluble in tetrahydrofuran, but the product appeared to decompose slowly in solution and could not be recrystallized.

The infrared spectrum showed absorptions due to the bis(trimethylsilyl)amide ligand, and the p-tolyl group. However, no N-H stretches were observed, although they may be very weak and difficult to observe. Because the compound was not stable in solution, its composition in the solid state was determined by X-ray crystallography. Dark-blue crystals were obtained by slow diffusion of a pentane solution of 2,4,6-trimethylaniline with a pentane solution of $U[N(SiMe_3)_2]_3$. As with the above uranium(IV) dimer, the space-group determination of this species gave a unit cell too small for $U[N(SiMe_3)_2]_3(H_2NAr)$, whereas it was a perfect match for a compound with two bis(trimethylsilyl)amide ligands and one aniline-type ligand. The solution of the crystal structure showed this to be the case. Instead of simply coordinating, the 2,4,6-trimethylaniline substituted a bis(trimethylsilyl)amide ligand, and the resulting uranium(III) compound was isolated as a

dimer.

As with the compound, $U[N(SiMe_3)_2]_3[NH(p\text{-tolyl})]$, the unique amido-hydrogen atom was the largest peak in the difference Fourier map after all the other hydrogens were placed in their calculated positions. Attempts at refinement of the position of the amido-hydrogen were again unsuccessful, and it was placed in its observed position with the N-H bond length adjusted to 0.87 Å. Selected bond lengths and angles are listed in Tables 1-25 and 1-26. An ORTEP drawing of the molecule is shown in Figure 1-11. Table 1-27 shows a comparison of bond lengths and angles for the uranium(III) and uranium(IV) dimers.

Table 1-25. Bond lengths (Å) for $U_2[N(SiMe_3)_2]_4[\mu\text{-}N(H)(2,4,6\text{-}Me_3C_6H_2)]_2$.

U-N1	2.354(3)	C1-C2	1.414(5)
U-N2	2.324(3)	C1-C6	1.416(5)
U-N3	2.453(3)	C2-C2A	1.507(5)
U-N3'	2.646(3)	C2-C3	1.389(5)
		C3-C4	1.372(6)
N3-C1	1.427(4)	C4-C4A	1.515(6)
N3-H	0.872(3)	C4-C5	1.377(5)
		C5-C6	1.398(5)
N1-Si11	1.715(3)	C6-C6A	1.504(5)
N1-Si12	1.722(3)		
N2-Si21	1.715(3)		
N2-Si22	1.728(3)		

Table 1-26. Intramolecular Angles (°) for $U_2[N(SiMe_3)_2]_4[\mu\text{-}N(H)(2,4,6\text{-}Me_3C_6H_2)]_2$.

N1-U-N2	107.01(9)	Si11-N1-Si12	132.2(1)
N1-U-N3	112.90(9)	Si21-N2-Si22	121.4(2)
N1-U-N3'	124.61(8)		
N2-U-N3	103.52(9)	U-N3-U'	102.85(9)
N2-U-N3'	123.88(9)	U-N3-C1	135.8(2)
N3-U-N3'	77.15(9)	U-N3-H	103.0(2)
		U'-N3-C1	94.3(2)
U-N1-Si11	132.2(1)	U'-N3-H	105.4(2)
U-N1-Si12	108.0(1)	C1-N3-H	111.3(3)
U-N2-Si21	118.8(1)		
U-N2-Si22	119.8(1)	N3-C1-C2	122.4(3)
		N3-C1-C6	118.8(3)

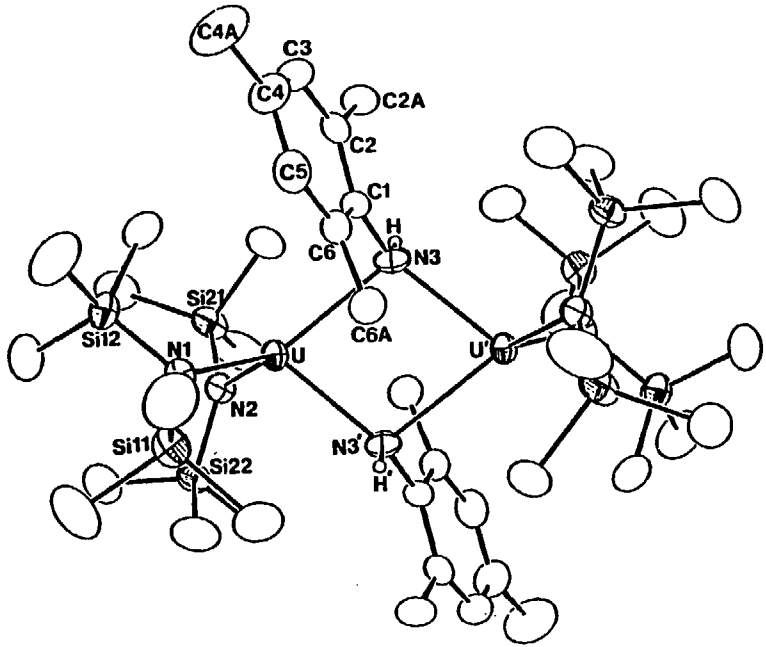

Figure 1-11. ORTEP diagram of $U_2[N(SiMe_3)_2]_4[\mu\text{-}N(H)(2,4,6\text{-}Me_3C_6H_2)]_2$.

Table 1-27. Comparison of bond lengths and angles in $U_2[N(SiMe_3)_2]_4[\mu\text{-}N(H)(2,4,6\text{-}Me_3C_6H_2)]_2$ and $U_2[N(SiMe_3)]_4[\mu\text{-}N(p\text{-}tolyl)]_2$.

	U(III)	U(IV)
U-N1, Å	2.354(3)	2.293(3)
U-N2, Å	2.324(3)	2.274(2)
U-N3 (short), Å	2.453(3)	2.172(3)
U-N3' (long), Å	2.646(3)	2.278(3)
N3-C1, Å	1.427(4)	1.415(4)
∠U-N3-U', deg	102.85(9)	105.82(10)
∠U-N3-C1, deg	94.3(2)	113.9(2)
∠U'-N3-C1, deg	135.8(2)	138.2(2)

The dimer is bridged asymmetrically by the arylamide ligands, with U-N(bridge) bond lengths of 2.453(3) and 2.646(3) Å. Structures of this type have not been investigated to the extent that the bridging imido compounds have been. There are few crystal structures of compounds with $R(H)N^-$ ligands, and even fewer of these contain the amide in a bridging position. A list of M-N(bridge) bond lengths for compounds of this type is given in Table 1.28. Both chemically and structurally, the compounds have very little in common, so comparisons of the bridging mode of the amide have little meaning. The uranium compound is the most asymmetric of the examples. The crystal structure shows that the U-N3-C1 angle is bent such that the aryl ring and one of its methyl substituents are brought close to a uranium atom. This interaction, which may contribute to the asymmetry of the bridge, is shown in Figure 1.10.

Table 1-28. M-N(bridge) bond lengths (Å) in the compounds $Fe_2(CO)_6(ONCMe_2)(\mu\text{-}NHPr^i)$,[47] $Au_2Me_4(\mu\text{-}NHMe)_2$,[48] $Ir_2(\mu\text{-}p\text{-}CH_3C_6H_4NCHN\text{-}p\text{-}C_6H_4CH_3)(\mu\text{-}NH\text{-}p\text{-}C_6H_4CH_3)(COD)_2$, (COD = C_8H_{14}),[49] $Li_2(\mu\text{-}NH(2,4,6\text{-}Bu^t_3C_6H_2)_2(OEt_2)_2$,[50] and $U_2[N(SiMe_3)_2]_4[\mu\text{-}N(H)(2,4,6\text{-}Me_3C_6H_2)]_2$.

M	M-N	M'-N	Δ[a]
Fe	1.959(4)	1.975(4)	0.016
Au	2.137(5)	2.140(5)	0.003
Ir	2.128(7)	2.140(6)	0.012
Li	1.987(5)	2.041(6)	0.054
U	2.453(3)	2.646(3)	0.193

[a] Δ = (M-N) - (M-N')

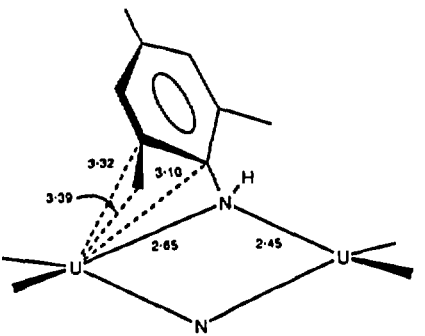

Figure 1-12. Close contacts (Å) in $U_2[N(SiMe_3)_2]_4[\mu\text{-}N(H)(2,4,6\text{-}Me_3C_6H_2)]_2$.

The bond lengths and angles of the bis(trimethylsilyl)amide ligands in the uranium(III) dimer are normal. The bond lengths are similar to

the other uranium(III) bis(trimethylsilyl)amide species described in this thesis.

The pKa values of the ligands involved in this reaction suggest that substitution should be the thermodynamically favored process. Values of 29.5[51] and 25.8[52] have been suggested for the pKa of $HN(SiMe_3)_2$, as determined by NMR studies. Substituted anilines have pKa values ranging from 18-25.[53] Using the relative acidities of the ligands involved to drive substitution reactions is a common route to metal-alkoxide compounds, from metal-amide species and alcohols (Eq. 1-12).[54]

$$M(NR_2)_n + n\ ROH \text{ ---> } M(OR)_n + n\ HNR_2 \qquad (1\text{-}12)$$

Surprisingly, prior to this, no characterizable substitution products had ever been obtained from reactions of $U[N(SiMe_3)_2]_3$ with a variety of protic sources, such as PhCCH, Me_5C_5H, $CpW(CO)_3H$, $Bu^t{}_3COH$, and $Bu^t{}_3SiOH$. The 2,4,6-trimethylaniline substitution product may only be isolable by virtue of its insolubility. Its instability in solution supports this suggestion.

REFERENCES

1. (a) Pump, J.; Rochow, E.G.; Wannagat, U. Ang. Chem. Int. Ed. Engl. 1963, 2, 264. (b) Bürger, H.; Chicon, J.; Goetze, U.; Wannagat, U.; Wismar, H.J. J. Organomet. Chem. 1971, 33, 1. (c) Krommes, P.; Lorberth, J. J. Organomet. Chem. 1977, 131, 415-422.

2. (a) Bürger, H.; Wannagat, U. Monatsh. Chem. 1963, 94, 1007-1012. (b) Bürger, H.; Wannagat, U. Monatsh. Chem. 1964, 95, 1099-1102. (c) Alyea, E.C.; Bradley, D.C.; Copperthwaite, R.G. J. Chem. Soc., Dalton Trans. 1972, 1580-1584.

3. Bradley, D.C.; Ghotra, J.S.; Hart, F.A. J. Chem. Soc., Dalton Trans. 1973, 1021-1023.

4. (a) Eller, P.G.; Bradley, D.C.; Hursthouse, M.B.; Meek, D.W. Coord. Chem. Rev. 1977, 24, 1-95. (b) Hursthouse, M.B.; Rodesiler, P.F. J. Chem. Soc., Dalton Trans. 1972, 2100-2102. (c) Sheldrick, G.M.; Sheldrick. W.S. J. Chem. Soc. (A) 1962, 2279-2282. (d) Allmann, R.; Henke, W.; Krommes, P.; Lorberth, J. J. Organomet. Chem. 1978, 162, 283-287.

5. (a) Ghotra, J.S.; Hursthouse, M.B.; Welch, A.J. J. Chem. Soc., Chem. Comm. 1973, 669-670. (b) Andersen, R.A.; Templeton, D.H.; Zalkin, A. Inorg. Chem. 1978, 17, 2317-2319.

6. Weigel, F. In "The Chemistry of the Actinide Elements", 2nd ed.; Katz, J.J.; Morss, L.R.; Seaborg, G.T., Eds.; Chapman and Hall: London, England, 1986; Chapter 5.

7. Andersen, R.A Inorg. Chem. 1979, 18, 1507-1509.

8. Shannon, R.D.; Prewitt, C.T. Acta Cryst. 1969, B25, 925-946.

9. Raymond, K.N.; Eigenbrot, C.W. Acc. Chem. Res. 1980, 13, 276-283.

10. Green, J.C.; Payne, M; Seddon, E.A.; Andersen, R.A. J. Chem. Soc., Dalton Trans. 1982, 887-892.

11. Fjeldberg, T; Andersen, R.A. J. Mol. Struc. 1985, 128, 49-57.

12. Fjeldberg, T; Andersen, R.A. J. Mol. Struc. 1985, 129, 93-105.

13. (a) Brennan, J.G., Ph.D Thesis, University of California, Berkeley, 1986. (b) Kanellakopulos, B.; Fischer, E.O.; Dornberger, E.; Baumgartner, F. J. Organomet. Chem. 1970, 24, 507. (c) Wasserman, H.J.; Zozulin, A.J.; Moody, D.C.; Ryan, R.R.; Salazar, K.V. J. Organomet. Chem. 1983, 254, 305. (d) Stults, S.D; Zalkin, A.; Acta Cryst. 1987, C43, 430-432. (e) Brennan, J.G.; Zalkin, A. Acta Cryst. 1985, C41, 1038. (f) Zalkin, A.; Brennan, J.G. Acta Cryst. 1985, C41, 1295.

14. (a) Bradley, D.C.; Gao, Y.C. Polyhedron 1982, 1,307. (b) Bradley, D.C.; Ghotra, J.S.; Hart, F.A.; Hursthouse. M.B.; Raithby, R. J. Chem. Soc., Dalton Trans. 1977, 1166-1172.

15. Xing-Fu, L.; Eggers, S.; Kopf, J.; Jahn, W.; Fischer, R.D.; Apostolidis, C.; Kanellakopulos, B.; Benetollo, F.; Polo, A.; Bombieri, G. Inorg. Chim. Acta 1985, 100, 183-199.

16. Rosen, R., University of California, Berkeley, personal communication.

17. Krüger, C.R.; Niederprüm Inorg. Synth. 1966, 8, 15-17.

18. Lowry, T.H.; Richardson, K.S. "Mechanism and Theory in Organic Chemistry", 2nd ed.; Harper and Row: New York, 1981.

19. (a) Fischer, R.K.; von Ammon, R.; Kanellakopulos, B. J. Organomet. Chem. 1970, 25, 123-137. (b) Ryan, R.R.; Penneman, R.A.; Kanellakopulos, B. J. Amer. Chem. Soc. 1975, 97, 4258-4260.

20. Kanellakopulos, B.; Dornberger, E.; von Ammom, R.; Fischer, R.D. Ang. Chem. 1970, 9, 957.

21. Nakamoto, K. "Infrared and Raman Spectra of Inorganic and Coordination Compounds" 4th ed.; Wiley-Interscience: New York, 1986.

22. (a) Lankamp, H.; Nauta, W.Th.; MacLean, C. Tet. Let. 1968, 249-254. (b) Staab, H.A.; Brettschneider, H.; Brunner, H. Chem. Ber. 1970, 103, 1101-1106. (c) For an interesting review on why it took nearly 70 years to determine the proper structure of bitrityl see: McBride, J.M. Tetrahedron 1974, 30, 2009-2022.

23. (a) Dori, Z.; Ziolo, R.F. Chem. Rev. 1973, 73, 247-254. (b) Beck, W.; Fehlhammer, W.P.; Pöllmann, P.; Schuierer, E.; Feldl, K. Chem. Ber. 1967, 100, 2335-2361.

24. Manousek, O.; Zuman, P. J. Chem. Soc., Chem. Comm. 1965, 158-159.

25. Rieger, P.H.; Bernal, I.; Reinmuth, W.H.; Fraenkel, G.K. J. Amer. Chem. Soc. 1963, 85, 683-693.

26. Brennan, J.G.; Andersen, R.A.; Zalkin, A. Inorg. Chem. 1986, 25, 1761-1765.

27. Berg, D.J.; Ph.D. Thesis, University of California, Berkeley, 1987.

28. (a) Matschiner, Von H.; Tzschach, A.; Steinert, A. Z. Anorg. Allg. Chem. 1970, 373, 237-244. (b) Santhanam, K.S.V.; Bard, A.J. J. Amer. Chem. Soc. 1968, 90, 1118-1122.

29. (a) Chernick, C.L.; Skinner, H.A. J. Chem. Soc. 1956, 1401. (b) Chernick, C.L.; Pedley, J.B.; Skinner, H.A. J. Chem. Soc. 1957,

1851.

30. Boncella, J.M.; Andersen, R.A. Organometallics 1985, 4, 205-206.

31. Turner, H.W.; Andersen, R.A.; Zalkin, A.; Templeton, D.H. Inorg. Chem. 1979, 18, 1221-1224.

32. Andersen, R.A.; Zalkin, A.; Templeton, D.H. Inorg. Chem. 1981, 20, 622-623.

33. (a) Arnaudet, L.; Folcher, G.; Marquet-Ellis, H.; Klähne, E.; Yünlü, K.; Fischer, R.D. Organometallics 1983, 2, 344-346. (b) Arnaudet, L.; Charpin, P; Folcher, G.; Lance, M.; Nierlich, M.; Vigner, K. Organometallics 1986, 5, 270-274.

34. Masters, C. "Homogeneous Transition-metal Catalysis - a gentle art"; Chapman and Hall: London, England, 1981.

35. (a) Jones, R.G.; Bindschadler, E.; Blume, D.; Karmas, G.; Martin, Jr., G.A.; Thirtle, J.R.; Gilman, H. J. Amer. Chem. Soc. 1956, 78, 6027-6029. (b) Bradley, D.C.; Chakravarti, B.N.; Chatterjee, A.K. J. Inorg. Nucl. Chem. 1957, 3, 367-369. (c) Bradley, D.C.; Chatterjee, A.K. J. Inorg. Nucl. Chem., 1957 4, 279-282.

36. Cotton, F.A.; Marler, D.O.; Schwotzer, W. Inorg. Chem. 1984, 23, 4211-4215.

37. Johnson, D.A. "Some Thermodynamic Aspects of Inorganic Chemistry" 2nd ed.; Cambridge University: Cambridge, England, 1982.

38. Brennan, J.G.; Andersen, R.A. J. Amer. Chem. Soc. 1985, 107, 514-517.

39. Nugent, W.A.; Haymore, B.L. Coord. Chem. Rev. 1980, 31, 123-175.

40. Zalkin, A.; Brennan, J.G.; Andersen, R.A., submitted for publication in Acta Cryst.

41. Siddall III, T.H. In "Theory and Applications of Molecular Paramagnetism"; Bouduraux E.A., Mulay, L.N., Eds.; Wiley Interscience: New York, 1974; pp 317-340.

42. Edelstein, N. In "Fundamental and Technological Aspects of Organo-f-Element Chemistry"; Marks, T.J.; Fragala, I.L., Eds.; NATO ASI Series C155; D. Reidel: New York, 1985.

43. Simpson, S.J.; Turner, H.W.; Andersen, R.A. Inorg. Chem. 1981, 20, 2992-2995.

44. Rochow, E.G. In "Comprehensive Inorganic Chemistry"; Bailar Jr., J.C.; Emeleus, H.J.; Nyholm, R.; Trotman-Dickenson, A.F., Eds.; Pergamon: Oxford, England, 1973; Vol. 1, Chapter 1.

45. Pauling, L. "The Nature of the Chemical Bond", 3rd ed.; Corr

University: Ithaca ,NY, 1960.

46. Thorn, D.L.; Nugent, W.A.; Harlow, R.L. J. Amer. Chem. Soc. 1981, 103, 357-363.

47. Aime, S.; Gervasio, G.; Milone, L.; Rossetti, R.; Stanghellini, P.L. J. Chem. Soc., Dalton Trans. 1978, 534-540.

48. Grässle, U.; Hiller, W.; Strähle, J. Z. Anorg. Allg. Chem. 1985, 529, 29-34.

49. Cotton, F.A.; Poli, R. Inorg. Chim. Acta 1986, 122, 243-248.

50. Cetinkaya, B.; Hitchcock, P.B.; Lappert, M.F.; Misra, M.C.; Thorne, A.J. J. Chem. Soc., Chem. Comm. 1984, 148-149.

51. Fraser, R.R.; Mansour, R.S. J. Org. Chem. 1984, 49, 3443-3444.

52. Fraser, R.R.; Mansour, R.S.; Savard, S. J. Org. Chem. 1985, 50, 3232-3234.

53. Dolman, D.; Stewart, R. Can. J. Chem. 1967, 45, 911-924.

54. Bradley, D.C.; Mehrotra, R.C.; Gaur, D.P. "Metal Alkoxides"; Academic: London, England, 1978.

CHAPTER TWO

Uranium(IV) Alkoxide and Siloxide Chemistry

Introduction

Many of the homoleptic uranium(IV), (V), and (VI) alkoxide compounds, $U(OR)_n$, were synthesized by Gilman and co-workers in 1956.[1] The compounds were generally purified by either vacuum distillation or crystallization from alcohol solvents. The degree of polymerization in a large number of the uranium(V) compounds was determined ebullioscopically in benzene by Bradley and co-workers.[2] The methoxide, $U(OMe)_5$, was determined to be a trimer in benzene, whereas compounds with larger R groups showed lesser degrees of association. Similar measurements could not be carried out on the uranium(IV) compounds due to their low solubility, and the compounds are believed to be polymeric.[2a] Little is known about their structure and reactivity.

The propensity of metal-(OR) compounds to bridge through the alkoxide-oxygen may be hindered by very bulky R groups. Bochmann and co-workers used the ligand ($t\text{-}Bu_2CHO^-$) (ditox) to synthesize a number of monomeric first-row transition metal compounds.[3] However, this ligand has also been shown to be very capable of bridging, as in the dimer $[Cr(\mu\text{-}OCHBu^t_2)(OCBu^t_3)]_2$.[4b] Power and co-workers have used the bulkier alkoxide, ($t\text{-}Bu_3CO^-$) (tritox), to synthesize a number of low-coordinate, first-row transition metal compounds, including some of the first examples of three-coordinate Co, Mn, and Cr compounds.[4]

In the last few years, many new mononuclear Group 4 and 5 metal-alkoxide compounds have been synthesized. Wolczanski and co-workers

have used the tritox ligand to make species such as $M(tritox)_2Cl_2$ (M = Ti, Zr).[5] Another class of alkoxide ligands that has been investigated is the 2,6-dialkylphenoxides.[6] These ligands are synthetically quite useful because the substituents in the 2 and 6 positions block polymerization and may be varied to change the steric properties of the ligand. The most frequent choice is the 2,6-di-t-butylphenoxo ligand (OAr'), and the compounds $M(OAr')_3Cl$ (M = Zr, Hf),[6a] and $Ta(OAr')_2Cl_3$[6b] have been synthesized.

Lappert and co-workers have also used the t-butyl substituted aryloxide ligand to synthesize some mononuclear uranium and thorium compounds.[7] They obtained the crystal structure of $U(NEt_2)(OAr')_3$. This is one of the few uranium(IV)-alkoxide compounds that has been structurally characterized. Some others include $U(OPh)_4(dmpe)_2$ (dmpe = $Me_2P(CH_2)_2PMe_2$),[8] $KU_2(OCMe_3)_9$,[9] and $[U(\eta\text{-}C_3H_5)_2(OPr^i)_2]_2$.[10]

$(t\text{-}Bu)_3CO^-$ (tritox) Chemistry

The successful synthesis of the unusual, low-coordinate transition metal alkoxide compounds, mentioned above, warranted investigation into the synthesis of uranium compounds containing alkoxides derived from the sterically bulky alcohols $(t\text{-}Bu)_3COH$ (tritoxH) and $(t\text{-}Bu)_2CHOH$ (ditoxH). These larger ligands should allow isolation of monomeric compounds with reasonable solubility properties. The bulky tritox ligand has been referred to as a "steric cyclopentadienyl equivalent"[5] and its cone angle (125°), as determined by space-filling models, approaches that of cyclopentadienyl (136°).[11] The t-butyl substituents on the ligand should hinder formation of alkoxide bridges.

The reaction of UCl_4 with three molar equivalents of Li(tritox) in

diethyl ether yielded the pink compound $ClU(tritox)_3$. The desired product could not be obtained when tetrahydrofuran was used instead of diethyl ether. Attempts to substitute the fourth chloride with another equivalent of tritox ligand were unsuccessful, probably due to steric crowding.

The compound $ClU(tritox)_3$ was reacted with a variety of alkyl-lithium reagents to make new uranium-alkyl compounds.

$$ClU(tritox)_3 + RLi \text{ ----> } RU(tritox)_3 + LiCl \qquad (2\text{-}1)$$

R = Me, Et, n-Bu, Me_3CCH_2, Me_3SiCH_2, benzyl

The new compounds are all easily crystallized from hydrocarbon solvents with the exception of the Me_3SiCH_2 compound, which is extremely soluble. The ^1H NMR shifts for the alkyl-species are given in Table 2-1.

Table 2-1. ^1H NMR shifts for $RU(tritox)_3$ compounds (C_6D_6, 20°C).

R	tritox	a	b	c	d
CH_3 a	6.73	-226			
CH_2CH_3 a b	6.51	-220	-33.42		
$CH_2CH_2CH_2CH_3$ a b c d	6.15	-220.4	-46.77 br(2H)	-30.19 m(2H)	-16.94 t(3H)
$CH_2C(CH_3)_3$ a b	5.85	-191.9	-27.95		
$CH_2Si(CH_3)_3$ a b	6.16	-209.9	-20.22		
CH_2-C$_6$H$_5$ a b c d	5.93	-212.2	-32.52 d(2H)	-2.20 t(2H)	-4.35 t(1H)

In all of the compounds, the tritox protons appear as a single resonance between 5.8 and 6.8 ppm. The protons on the carbon directly attached to uranium are found far up field, near -200 ppm. A similar

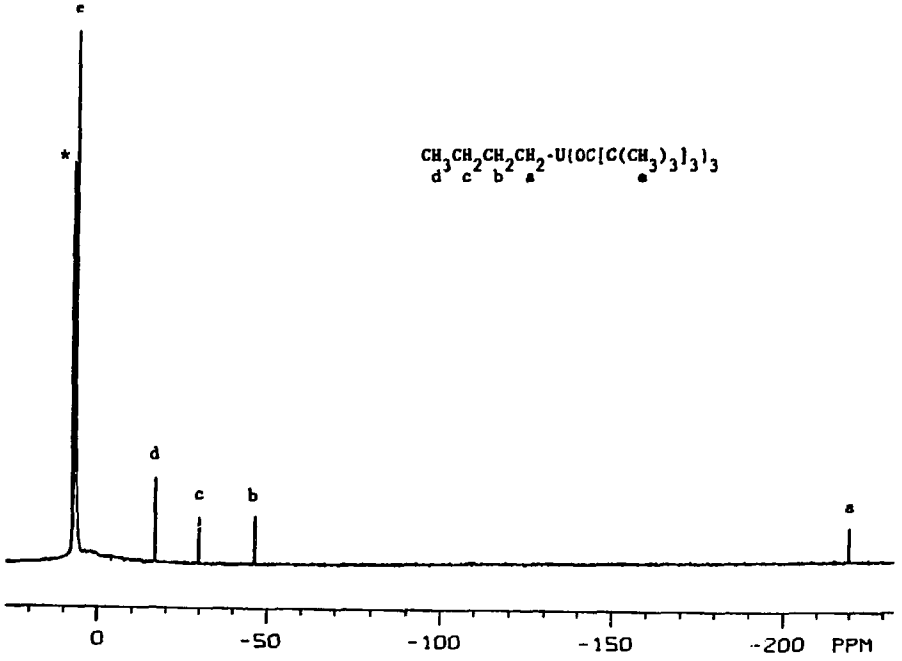

Figure 2-1. ^{1}H NMR of n-BuU(tritox)$_3$ ($^*C_6D_6$, 20°C).

shift is observed in the compound $MeU[N(SiMe_3)_2]_3$, in which the methylprotons are found at -224 ppm.[12] In the tritox-alkyl compounds, ligand protons located further away from the paramagnetic center are less drastically shifted. The spectrum of the n-Bu compound (Fig. 2-1) illustrates the chemical shifts observed in these compounds.

To investigate the solid state structure of these uranium-alkoxide compounds, the methyl compound was chosen for study. The amber-colored $MeU(tritox)_3$ crystallized in the monoclinic space group $P2_1/c$. An ORTEP drawing of the molecule is given in Figure 2-2. Relevant bond lengths and angles are given in Tables 2-2 and 2-3. The geometry about the metal is distorted-tetrahedral with large O-U-O angles, probably due to the steric requirements of the large tritox ligands. The geometry is very similar to that of the analogous silylamide compound, $MeU[N(SiMe_3)_2]_3$, in which the N-U-N angle is 117.40(6)° and the C-U-N angle is 99.4(1)°. The metal-carbon distances are also very similar, 2.397(13) Å for the silylamide compound versus 2.422(8)Å for the tritox compound. The U-O bond lengths are slightly shorter than those in the four-coordinate aryloxide $U(NEt_2)(OC_6H_2\text{-}2,6\text{-}Bu^t)_3$, $U\text{-}O_{ave}$ = 2.143(4) Å,[7] and the dimer $KU_2(OCMe_3)_9$, $U\text{-}O_{ave}$ = 2.12(2) Å,[9] in which uranium is six-coordinate. The U-O-C angles are large, which is often taken to imply a significant amount of metal-oxygen π-bonding; however, steric and ligand packing effects probably play a more influential role.

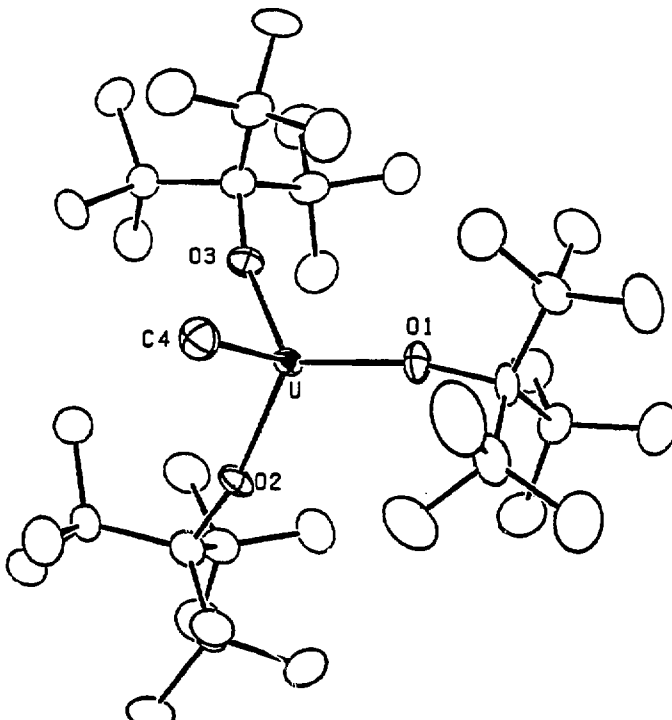

Figure 2-2. ORTEP Diagram of $MeU(critox)_3$.

Table 2-2. Bond lengths (Å) for $MeU(tritox)_3$.

U-O1	2.086(4)	C1-C11	1.612(8)
U-O2	2.092(4)	C1-C12	1.615(10)
U-O3	2.092(5)	C1-C13	1.616(10)
		C2-C21	1.608(9)
U-C4	2.422(8)	C2-C22	1.623(10)
		C2-C23	1.615(9)
O1-C1	1.456(7)	C3-C31	1.633(10)
O2-C2	1.433(7)	C3-C32	1.634(8)
O3-C3	1.455(8)	C3-C33	1.587(10)

Table 2-3. Intramolecular Angles (°) for $MeU(tritox)_3$.

U-O1-C1	166.9(4)	C4-U-O1	99.2(2)
U-O2-C2	165.5(4)	C4-U-O2	98.5(2)
U-O3-C3	162.8(3)	C4-U-O3	100.7(2)
O1-U-O2	116.5(2)		
O1-U-O3	121.0(2)		
O2-U-O3	114.5(2)		

The investigation of the reactivity of the alkyl compounds proved dissappointing. When dissolved in hexane or toluene and pressurized with CO, a red-orange product was formed. For the Me and Et cases, the product was very slightly soluble in toluene but could not be crystallized. The Me_3CCH_2 and Me_3SiCH_2 reactions with CO produced red oils. The elemental analyses suggested addition of approximately one or two equivalents of CO to the starting alkyl species, but the compounds were never obtained completely pure.

The reactions with H_2 or D_2 led to formation of a small amount of pink powder that was insoluble in all common solvents. The infrared spectrum of the pink powder did not contain any bands that were assignable to U-H or U-D stretches. The alkyl compounds did not react with ethylene.

Attempts to reduce the chloride, $ClU(tritox)_3$, with sodium-naphthalene, Na/Hg, or t-BuLi, to form the trivalent $U(tritox)_3$

compound resulted in the isolation of dark-brown oily solids which could not be crystallized or sublimed and were not further characterized.

$(t\text{-Bu})_2CHO^-$ (ditox) Chemistry

The reaction of UCl_4 with three molar equivalents of Li(ditox) in a variety of solvents did not yield any isolable products. Using four molar equivalents in diethyl ether solution allowed isolation of the tetrakis(alkoxide), $U(ditox)_4$. The pinkish-purple compound is extremely soluble in hydrocarbon solvents and may be purified by sublimation (90-95°C, 10^{-3} torr) or crystallization from a minimal amount of pentane (-78°C).

In the crystal structure of the analogous chromium species, $Cr(ditox)_4$, the compound exists as discrete molecules with C_2 symmetry.[3] The O-Cr-O angles are close to tetrahedral [108.8-112.4(2)°]. The strong similarities in the infrared spectra of the chromium and uranium compounds suggest the uranium compound has a similar structure in the solid state. The Cr-O stretch at 718 cm^{-1} is shifted to 660 cm^{-1} in the uranium compound.

The infrared spectrum of the uranium compound has an absorption at 2618 cm^{-1}, which is in the region of "agostic" C-H stretches.[11] A similar peak is not reported for the chromium compound and the crystal structure does not show any unusual close metal-carbon contacts. It is possible that the much larger uranium atom is less coordinatively saturated and attempts to fill in its coordination sphere with close interactions to methyl groups on the ligands. Shannon-Prewitt ionic

radii[14] for the tetravalent ions, coordination number = 6, are U^{4+}= 0.96Å and Cr^{4+}= 0.55Å. These types of agostic interactions have been noted in some manganese-tritox compounds.[4a]

Reaction of metal alkoxides with organolithium or other main-group metal alkyls gives either substitution (Eq. 2-2) or addition (Eq. 2-3).

$$MOR + M'R' \text{ ----> } MR' + M'OR \qquad (2\text{-}2)$$

$$MOR + M'R' \text{ ----> } MM'(OR)(R') \qquad (2\text{-}3)$$

In d-transition metal chemistry, ligand substitution has been observed,[15] whereas with p-block metals, addition reactions are generally the case.[16] In uranium chemistry, both reaction patterns have been observed as deduced by spectroscopic studies (Eq. 2-4 and 2-5).[17]

$$U(OEt)_5 + 8MeLi \text{ ----> } Li_3UMe_8 + 8LiOEt \qquad (2\text{-}4)$$

$$U(OPr^i)_6 + 3MeLi \text{ ----> } Li_3U(OPr^i))_6Me_3 \qquad (2\text{-}5)$$

The addition compounds of the p-block metals are of considerable utility in organic synthesis. They have been called "super-bases" due to their ability to deprotonate hydrocarbons whose pKa's are in the range of 35-50.[16a] Addition compounds derived from metal alkyls and lanthanide amides or alkoxides have found use in the stereospecific alkylation of epoxides.[18] They show promise as useful reagents because their regioselectivity is complementary to that of organocuprates. Even though addition compounds have demonstrated synthetic utility, no crystal structural information is available and their constitution in the solid state is unknown.

The reaction of one molar equivalent of MeLi with $U(ditox)_4$ in hexane gave a pale green solution from which purple crystals were obtained. The compound gave a positive flame-test for lithium,

suggesting that addition of MeLi, rather than substitution, had occurred. Subsequent solution of the crystal structure showed this to be true. An ORTEP drawing of the molecule is shown in Figure 2-3. Tables 2-4 and 2-5 give bond lengths and angles for the compound.

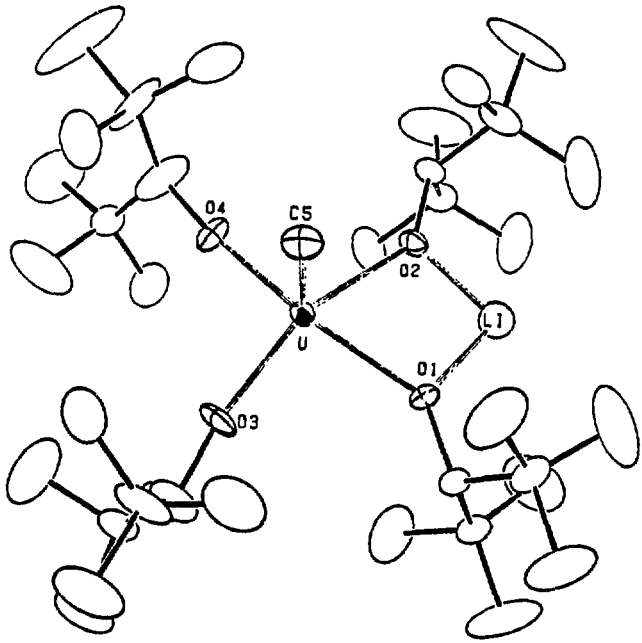

Figure 2-3. ORTEP Diagram of MeLi•U(ditox)$_4$ (ellipsoids shown at 30% probability).

Table 2-4. Bond lengths (Å) for MeLi•U(ditox)$_4$.

U-O1	2.268(4)	Li-O1	1.84(1)
U-O2	2.256(4)	Li-O2	1.82(2)
U-O3	2.101(4)	Li...U	3.07(1)
U-O4	2.104(5)		
U-C5	2.465(7)		

Table 2-5. Intramolecular angles (°) for MeLi•U(ditox)$_4$.

O1-U-O2	72.7(1)	U-O1-C1	143.0(3)
O2-U-O4	92.5(2)	U-O2-C2	141.6(4)
O3-U-O4	97.8(2)	U-O3-C3	169.0(6)
O1-U-O3	92.0(2)	U-O4-C4	175.0(5)
O1-U-O4	159.9(2)		
O2-U-O3	157.9(2)	O1-Li-O2	94.2(6)
Li-O1-C1	120.8(6)	Li-O1-U	96.0(5)
Li-O2-C2	121.3(5)	Li-O2-U	97.1(4)

The geometry about uranium is pseudo-square-pyramidal, with the methyl occupying the apical site and the oxygen atoms in the basal sites. The lithium is two coordinate, bridging two of the alkoxide oxygens. This type of coordination has been observed in the compounds $LiMn[N(SiMe_3)_2](tritox)_2$ and $LiMn(tritox)_2Br_2[Li(thf)_2]$.[4a] The U-O distances are normal for tetravalent uranium compounds. The U-C distance, 2.465(7) Å, of this five-coordinate compound is slightly longer than the U-C distances in the four-coordinate compounds $MeU[N(SiMe_3)_2]_3$, 2.397(13) Å, and $MeU(tritox)_3$, 2.422(8) Å.

The solution properties of the addition compound suggest that the compound dissociates as shown in Eq. 2-6.

$$LiU(Me)(ditox)_4 \text{ ----> } MeLi + U(ditox)_4 \qquad (2\text{-}6)$$

A freshly prepared sample in C_6D_6 or C_7D_8 shows resonances in the ^1H NMR spectrum at 32.2 and 0.12 ppm, each with $\nu_{1/2}$ of ca. 10 Hz, due to the methyne and methyl protons of $U(ditox)_4$ and resonances at 38.2 ($\nu_{1/2}$ = 112 Hz), -2.52 ($\nu_{1/2}$ = 28 Hz), and -204 ($\nu_{1/2}$ = 120 Hz) ppm, in

the area ratio of 2:36:1.5. The latter resonance is in the region of U-C σ-bonds[6] and the other two resonances are presumably due to methyne and methyl protons of the alkoxide in $LiU(Me)(ditox)_4$. The two large resonances due to the t-butyl protons in $U(ditox)_4$ and $LiU(Me)(ditox)_4$ are in an area ratio of 1:1.8. This suggests that in hydrocarbon solvents the reaction shown in Eq. 2-6 exists, assuming that methyllithium is not detected due to its insolubility. The spectrum changes irreversibly on heating, and on cooling the resonances that are identified as being due to $U(ditox)_4$ do not change shape, though their chemical shift is temperature dependent as expected for a paramagnetic compound. Those resonances due to the addition compound broaden into the base-line by -40°C. Clearly the solution constitution is not identical with the solid state constitution, and inferences made on the basis of spectroscopic study in a single phase must be treated conservatively.

Addition versus substi n in these reactions appears to be driven by the solubility properties of the possible products. Under the reaction conditions, Eq. 2-2 leads to substitution, due to the formation of insoluble LiOEt, whereas Eq. 2-3 leads to addition, because $LiOPr^i$ does not precipitate. The lithium salt of the ditox ligand is also soluble, so there is no driving force for substitution. This insolubility of one of the reagents can be quite useful synthetically. For example, the extreme insolubility of some lithium thiolates has been used to make new Ce-alkyl compounds that were not accessible by other routes.[19]

$$[(t\text{-}BuC_5H_4)_2Ce(\mu\text{-}SPr^i)]_2 + 2\ MeLi \longrightarrow [(t\text{-}BuC_5H_4)_2Ce(\mu\text{-}Me)]_2 + 2\ LiSPr^i \qquad (2\text{-}6)$$

$(t\text{-}Bu)_3SiO^-$ (silox) Chemistry

When Wolczanski and co-workers tried to extend their work with the tritox ligand from the Group 4 to the Group 5 metals, they had difficulty isolating stable Group 5-tritox compounds.[20] They believe their difficulties were caused by facile heterolysis of the tritox C-O bond to form the stable tri-t-butyl carbonium ion. Substitution of Si for C, i.e., using ($t\text{-}Bu_3SiO^-$) (silox), should help alleviate this problem. The stability should be enhanced by both the stronger Si-O bond, and the instability of the silicon analogue of the carbonium ion. This was indeed found to be the true, and a variety of Group 5-silox compounds were prepared.[20] There was precedence for this enhanced stability in the work of Weidenbruch and co-workers, who synthesized silox complexes of several different transition metals.[21]

There are a variety of procedures in the literature for preparing siloxH.[22] The synthesis is not as straight-forward as would be expected because of the difficulty in putting three t-butyl groups on silicon. The compound $t\text{-}Bu_2SiCl_2$ is easily prepared from $SiCl_4$ and two molar equivalents of t-BuLi. However, successful routes to substitution of a third chloride by a t-butyl group have not been found. Fortunately, if flouride is substituted for chloride, the substitution can be carried out. The simplest route to produce gram quantities of the ligand involves starting with SiF_4.[22b] The SiF_4 is bubbled through a solution of t-BuLi at 0°C to put on the first two t-butyl groups. Refluxing the $t\text{-}Bu_2SiF_2$ with two more equivalents of t-BuLi in cyclohexane produces $t\text{-}Bu_3SiH$ which may be hydrolyzed to the silanol, $t\text{-}Bu_3SiOH$. The Li or Na salts of the ligand are easily prepared from the reaction of the silanol with n-BuLi or NaH.

respectively.

The preparation of uranium compounds containing the silox ligand was not straight forward, and a variety of conditions were investigated before any product could be made reproducibly. The reaction of UCl_4 with three molar equivalents of Li(silox) in thf, produces a green solution from which a pink powder may be isolated by removal of the thf. Crystallizing the pink powder from Et_2O yields the pink crystalline compound $U(silox)_3Cl_2Li(Et_2O)_n$. The crystals turn opaque when isolated and dried under vacuum. Apparently all of the coordinated Et_2O is removed, as the compound gives a good elemental analysis for the unsolvated species.

As with the tritox compounds, difficulties were encountered in the reaction chemistry. The reaction of the pink compound with a variety of methylating agents, including MeLi, Me_2Mg, and MeMgBr did not yield any isolable products. Attempts at reducing the compound with Na/naphthalene gave the redistribution product $U(silox)_4$. This compound may also be obtained from the reaction of UCl_4 with four molar equivalents of Li(silox) in diethyl ether solution. It is interesting that in this case the tetrakis(silox) compound could be made, whereas only three tritox ligands could be put on uranium. This suggests that the longer Si-O bond (1.66 Å), versus C-O (1.43 Å), moves the bulk of the ligand further away from the metal center, making silox effectively "smaller" than tritox.

The tetrakis(silox) compound is potentially of interest for investigations into the electronic structure of tetravalent uranium, as it should possess close to ideal tetrahedral symmetry. However, crystals of $U(silox)_4$ obtained from saturated pentene solutions occlude

solvent. The occluded solvent is lost upon isolation of the compound, making single-crystal work difficult. The magnetic behavior of $U(silox)_4$ (Fig. 3-11) is different from that of tetrakis(methylborohydride)uranium, reported by Rajnack et al.[24] The magnetic susceptibility of the methylborohydride compound shows temperature independent paramagnetism below ca. 50 K, whereas the silox compound exhibit temperature dependent paramagnetism throughout the examined temperature region (5-200 K). If the uranium ion in each compound is assumed to occupy a site of T_d symmetry, then these species serve as a good example of the role that ligands play in changing the electronic structure of the actinide ion. As was mentioned in Section 1.3, the electronic structure of lanthanide (4f) species remains relatively unperturbed by the ligand environment, whereas ligand field effects may not be ignored in actinide(5f) compounds.

REFERENCES

1. (a) Jones, R.G.; Karmas, G.; Martin, Jr., G.A.; Gilman, H. J. Amer. Chem. Soc. 1956, 78, 4285-4286. (b) Jones, R.G.; Bindschadler, E.; Karmas, G.; Yoeman, F.A.; Gilman, H. J. Amer. Chem Soc. 1956, 78, 4287-4288. (c) Jones, R.G.; Bindschadler, E ; Karmas, G.; Martin, Jr., G.A.; Thirtle, J.R.; Yoeman, F.A.; Gilman, H. J. Amer. Chem. Soc. 1956, 78, 4289-4290. (d) Jones, R.G.; Bindschadler, E.; Blume, D.; Karmas, G.; Martin, Jr., G.A.; Thirtle, J.R.; Gilman, H. J. Amer. Chem. Soc. 1956, 78, 6027-6029. (e) Jones, R.G.; Bindschadler, E.; Blume, D.; Karmas, G.; Martin, Jr., G.A.; Thirtle, J.R.; Yoeman, F.A.; Gilman, H. J. Amer. Chem. Soc. 1956, 78, 6030-6032.

2. Bradley, D.C.; Kapoor, R.N.; Smith, B.C. J. Chem. Soc. 1963, 1023-1027.

3. Bochmann, M.; Wilkinson, G.; Young, G.B.; Hursthouse, M.B.; Malik, K.M.A. J. Chem. Soc., Dalton Trans. 1980, 1863-1871.

4. (a) Murray, B.D.; Power, P.P. J. Amer. Chem. Soc. 1984, 106, 7011-7015. (b) Murray, B.D.; Hope, H.; Power, P.P. J. Amer. Chem. Soc. 1985, 107, 169-173. (c) Olmstead, M.M.; Power, P.P.; Sigel, G. Inorg. Chem. 1986, 25, 1027-1033.

5. Lubben, T.V.; Wolczanski, P.T.; Van Duyne, G.D. Organometallics 1984, 3, 977-983.

6. (a) Chamberlain, L.; Huffman, J.C.; Keddington, J.; Rothwell, I.P. J. Chem. Soc., Chem. Comm. 1982, 805-806. (b) Chamberlain, L.; Keddington, J.; Rothwell, I.P.; Huffman, J.C. Organometallics 1982, 1, 1538-1540. (c) Chamberlain, L.R.; Rothwell, I.P.; Huffman, J.C. Inorg. Chem. 1984, 23, 2575-2578. (d) Latesky, S.L.; Keddington, J.; McMullen, A.K.; Rothwell, I.P.; Huffman, J.C. Inorg. Chem. 1985, 24, 995-1001.

7. Hitchcock, P.B.; Lappert, M.F.; Singh, A.; Taylor, R.G.; Brown, D. J. Chem. Soc., Chem. Comm. 1983, 561-563.

8. Edwards, P.G.; Andersen, R.A.; Zalkin, A. J. Amer. Chem. Soc. 1981, 103, 7792.

9. Cotton, F.A.; Marler, D.O.; Schwotzer, W. Inorg. Chem. 1984, 23, 4211-4215.

10. Brunelli, M.; Perego, G.; Lugli, G.; Mazzei, A. J. Chem. Soc., Dalton Trans. 1979, 861-868.

11. Tolman, C.A. Chem. Rev. 1977, 77, 313.

12. Turner, H.W.; Andersen, R.A.; Zalkin, A.; Templeton, D.H. Inorg. Chem. 1979, 18, 1221-1224.

13. Crabtree, R.H. Chem. Rev. 1985, 85, 245.

14. Shannon, R.D.; Prewitt, C.T., Acta Cryst. 1969, B25, 925-946.

15. Bochmann, M.; Wilkinson, G.; Young, G.B.; Hursthouse, M.B.; Malik, K.M.A. J. Chem. Soc., Dalton Trans. 1980, 901-910.

16. (a) Coates, G.E.; Green, M.L.H.; Wade, K. "Organometallic Compounds" Vol. 1; Methuen: London; 1967. (b) Schlosser, M.; Strunk, S. Tet. Let. 1984, 25, 741-744. (c) Lehmann, R.; Schlosser, M. Tet. Let. 1984, 25, 745-748.

17. Sigurdson, E.; Wilkinson, G. J. Chem. Soc., Dalton Trans. 1977, 812.

18. Mukerji, I.; Wayda, A.; Dabbagh, G.; Bertz, S.H. Ang. Chem. Int. Ed. Engl. 1986, 25, 760-761.

19. Stults, S.; personal communication.

20. LaPointe, R.E.; Wolczanski, P.T.; Van Duyne, G.D. Organometallics 1986, 4, 1810-1818.

21. Weidenbruch, M; Pierrard, C.; Pesel, H. Z. Naturforsch., B: Anorg. Chem., Org. Chem. 1978, 338, 1468-1472.

22. (a) Weidenbruch, M.; Pesel, H.; Peter, W.; Steichen, R. J. Organomet. Chem. 1977, 141, 9. (b) Dexheimer, E.M.; Spialter, L; Smithson, L.D. J. Organomet. Chem. 1975, 102, 21.

23 Edelstein, N. In "Fundamental and Technological Aspects of Organo-f-Element Chemistry"; Marks, T.J.; Fragala, I.L., Eds.; NATO ASI Series C155; Reidel: New York; pp 229-276.

24. Rajnak, K.; Gamp, E.; Shinomoto, R.; Edelstein, N. J. Chem. Phys. 1984, 80, 5942-5950.

CHAPTER THREE

EXPERIMENTAL SECTION

General

All manipulations involving air-sensitive compounds were carried out using standard Schlenk techniques or in a Vacuum Atmospheres inert atmosphere dry box. All reactions requiring elevated pressures were carried out in thick-walled, glass, pressure bottles. All solvents were dried and deoxygenated by distillation under nitrogen from sodium benzophenone ketyl. Deuterated solvents for NMR studies were distilled from potassium under nitrogen and stored over sodium. Other chemicals were of reagent grade, unless otherwise specified.

Infrared spectra were recorded on a Nicolet 5DX FTIR as Nujol mulls between CsI plates. Melting points were measured on a Thomas-Hoover melting point apparatus in capillaries sealed under N_2, and are uncorrected. ^1H NMR spectra were recorded either at 90 MHz on a JEOL FX-90Q spectrometer, or at 200 MHz on a departmental machine at the University of California, Berkelely, and are referenced to tetramethylsilane at $\delta = 0$. Elemental analyses were performed by the analytical laboratories at the University of California, Berkeley. Several compounds did not give satisfactory elemental analyses, and only those that gave satisfactory agreement with theory are recorded in this thesis. Electron impact mass spectra were recorded on either an AEI-MS-12 or KRATOS MS-50 at the University of California, Berkeley.

Magnetic susceptibility measurements were made using an S.H.E.

model 905 superconducting magnetometer (SQUID). Sample preparation involving air-sensitive compounds was carried out in an argon dry box. In a typical experiment, 70-100 mg of the compound was carefully ground with mortar and pestle and weighed in the bottom half of a Kel-F sample container. The two halves of the container were sealed with a small amount of silicone grease and removed from the dry box. The container was tied closed with nylon monofilament thread and suspended in the sample chamber with cotton thread. The chamber was evacuated to 50 microns and refilled with high purity helium three times. Sample measurements were taken automatically at 5 and 40 kG at the following temperatures: from 5-21 K, every 3 K; from 25-50 K, every 5 K; from 50-100 K, every 10 K; and from 100-280 K, every 20 K. All data were corrected for container and sample diamagnetism. Samples exhibiting Curie-Weiss behavior were fit to the Curie-Weiss law $1/\chi = (T - \theta)/C$ using a linear least-squares program written by Dr. E. Gamp. Effective magnetic moments were calculated as $\mu = 2.828\ C^{1/2}$. The plots of $1/\chi_M$ vs. T show the data points with a line that is either drawn through the points or is derived from a least-squares fit of the data to a third-order polynomial, using a fitting program written by W. Polik.

CHAPTER ONE

$U[N(SiMe_3)_2]I_3$

Naphthalene (1.35 g, 10.5 mmol) and excess sodium metal were transferred to a 150 mL round-bottom flask to which approximately 100 mL of tetrahydrofuran was added. The solution turned deep green immediately. This mixture was stirred for two hours, then the green sodium-naphthalene solution was added to a green solution of UCl_4 (4.00 g, 10.5 mmol) in 30 mL tetrahydrofuran. The color turned dark purple and a dark purple precipitate formed. The mixture was stirred 12 h. The "UCl_3" prepared in this manner was not isolated. A solution of $NaN(SiMe_3)_2$ (5.78 g, 31.5 mmol) in 50 mL of tetrahydrofuran was added to the dark purple uranium mixture. The color remained very intense, but appeared more red-purple. After stirring two h, the tetrahydrofuran was removed at reduced pressure and the naphthalene was sublimed (60°C, 10^{-1} torr). The mixture was extracted twice with 200 mL of pentane. The volume was reduced to ca. 30 mL and the solution was cooled slowly to -15°C. Long, dark purple needles were isolated (4.83 g, 63.9% yield). A second crop of needles usually may be obtained. However after the solution has been filtered several times, it begins to show signs of oxidation, and slowly turns brown and oily. The ^1H NMR (C_6D_6, 20°C) was slightly different than the reported value[1]: δ-11.38, $\nu_{1/2}$ = 15 Hz. The infrared spectrum and the melting point were the same as reported.[1] Magnetic susceptibility: A plot of $1/\chi_M$ vs. T is shown in Figure 3-1. A fit of the data, as described in the general experimental section, gave the following values for μ_{eff}(ave.): 5 kG; 35-280K, 3.354(4) B.M. (θ=-12.9(4)K), and 40 kG;

35-280K, 3.385(3) B.M. (θ=-11.1(3)K).

COORDINATION COMPOUNDS

$U[N(SiMe_3)_2]_3(C_5H_5N)$

To a solution of $U[N(SiMe_3)_2]_3$ (0.88 g, 1.2 mmol) in 20 mL of pentane was added 0.10 mL of pyridine (d=0.98 g/mL, 1.2 mmol). The purple-red solution deepened to a darker purple upon addition. The mixture was filtered, the volume of the filtrate was reduced to ca. 5 mL and the solution was cooled slowly to -15°C. Purple blocks were isolated (0.29 g, 30% yield), m.p. 98-100°C. Attempts at recrystallization always yielded a mixture of the pyridine adduct and the base-free starting material. The highest peak in the mass spectrum (e/m = 718 amu) corresponds to the pyridine-free starting material. ^1H NMR (C_6D_6, 32°C): -7.90 (Me_3Si). The pyridine ring protons were not observed, possibly due to an equilibrium in solution between free and coordinated ligand. IR: 1599 w, 1242 s, 1150 w, 1063 w, 1034 w, 985 m, 950 s, 855 s, 838 s, 824 s, 762 m, 698 w, 660 m, 598 m, 373 m cm^{-1}.

$U[N(SiMe_3)_2]_3(NC_5H_4NMe_2)$

A solution of p-dimethylaminopyridine (0.05 g, 0.41 mmol) in 15 mL of pentane was added to a solution of $U[N(SiMe_3)_2]_3$ (0.28 g, 0.39 mmol) in 20 mL pentane. The red-purple solution turned blue-purple. The mixture was filtered, the filtrate was concentrated to ca. 3 mL and cooled to -78°C. Dark purple crystals were isolated (0.19 g, 58% yield), m.p. 125-128°C. ^1H NMR (C_6H_6, 32°C): -5.09(6H), -5.34(54H), -8.77(2H), -20.26(2H). Anal. Calcd. for $C_{25}H_{64}N_5Si_6U$: C, 35.7; H,

7.67; N, 8.32. Found: C, 35.7; H, 7.59; N, 8.35. IR: 1621 s, 1550 m, 1244 s, 1114 w, 1060 w, 1004 m, 952 s, 861 s, 842 s, 832 s, 770 m, 757 w, 666 m, 612 m, 601 m, 532 w, 377 m cm^{-1}.

U[N(SiMe$_3$)$_2$]$_3$(CN-2,6-Me$_2$C$_6$H$_3$)

A solution of 2,6-dimethylphenylisocyanide, sublimed prior to use, (0.06 g, 0.42 mmol) in 10 mL of pentane was added to a solution of U[N(SiMe$_3$)$_2$]$_3$ (0.30 g, 0.42 mmol) in 25 mL of pentane. The color changed immediately to deep blue-green. The solution was filtered, the filtrate was concentrated to 3 mL and cooled to -15°C. Blue-green plates were isolated, (0.17 g, 66.6% yield). ^{1}H NMR (C_7H_8, 32°C): 8.25(1H, t, J=8.5 Hz), 0.71(d, 2H, J=7.3 Hz), -5.39(54H), -9.39(6H). IR: 2200 s (ν_{CN} for free ligand; 2115 cm^{-1}), 1240 s, 1163 w, 957 s, 855 s, 838 s, 825 s, 767 s, 720 w, 660 m, 559 m, 465 w, 379 m cm^{-1}.

U[N(SiMe$_3$)$_2$]$_3$(Ph$_3$PO)

To a suspension of Ph_3PO (0.12 g, 0.42 mmol) in 10 mL of toluene was added a solution of U[N(SiMe$_3$)$_2$]$_3$ (0.30 g, 0.42 mmol) in 25 mL toluene. No color change was observed. The solution was filtered, the volume of the solution was reduced to 3 mL and the solution was cooled to -25°C. Large dark purple crystals were isolated (0.18 g, 43% yield), m.p. 143-150°C. Anal. Calcd. for $C_{36}H_{69}N_3OPSi_6U$: C, 43.3; H, 6.97; N, 4.21. Found: C, 39.1; H, 7.19; N, 3.35. IR: 1439 m, 1246 m 1136 m, 1120 m, 952 s, 887 m, 863 m, 839 s, 772 m, 723 m, 693 m, 665 m, 575 m, 541 s, 378 m cm^{-1}.

$U[N(SiMe_3)_2]_3(t\text{-}BuCN)_2$

To a solution of $U[N(SiMe_3)_2]_3$ (0.90 g, 1.3 mmol) in 20 mL of pentane was added by syringe 0.14 mL t-BuCN (d=0.75, 1.3 mmol). The color changed immediately from dark purple to dark blue. The mixture was filtered, the volume of the filtrate was reduced to ca. 3 mL and the solution was cooled slowly to -15°C. Dark blue plates were isolated (0.32 g, 57% yield, calculated from t-BuCN), m.p. 128-133°C. ^1H NMR (C_7H_8, 25°C): -2.75 (54 H); -10.10 (18 H). Mass Spectrum: M^+= 884. Anal. Calcd. for $C_{28}H_{72}N_5Si_6U$: C, 38.0; H, 8.21; N, 7.91. Found: C, 34.7; H, 8.24; N, 7.28. IR: 2253 m, 1243 s, 1205 w, 960 s, 860 s, 835 s, 825 s, 768 m, 732 w, 720 w, 682 w, 660 m, 600 m cm^{-1}.

$U[N(SiMe_3)_2]_3(t\text{-}BuNC)_2$

To a solution of $U[N(SiMe_3)_2]_3$ (0.46 g, 0.64 mmol) in 20 mL of pentane was added t-BuNC (0.05 g, 0.60 mmol) in 10 mL pentane. The color changed immediately to deep blue. The mixture was filtered, the volume of the filtrate was reduced to ca. 3 mL and the solution was cooled to -15°C. The solid that was isolated was a mixture of mostly blue plates and some blue needles, (0.09 g, 34% yield, calculated from t-BuNC), m.p. 122-128°C. Great care had to be taken to exclude oxygen from the reaction mixture. The product could only be obtained if the glassware was carefully flame-dryed under vacuum before the reaction was carried out, otherwise, decomposition to a brown product could be observed occuring on the walls of the Schlenk tube. ^1H NMR (C_6D_6, 32°C): -4.75 (Me_3Si), -7.88 (Me_3C). The integration of the silylamide to t-BuNC resonances was 3.5:1, as opposed to the expected 3:1 ratio. This suggests the presence of the 1:1 coordination compound, which is

rapidly exchanging with the 2:1 compound, so that the averaged spectrum was observed. This could explain why two different crystal-types were isolated. Anal. Calcd. for $C_{28}H_{72}N_5Si_6U$: C, 38.0; H, 8.21; N, 7.91. Found: C, 36.6; H, 8.33; N, 7.44. IR: 2248 w, 2175 m (this absorption corresponds to ν_{CN} for free t-BuNC), 1255 w, 1242 s, 1205 w, 946 s, 858 s, 836 s, 767 m, 719 w, 680 w, 660 m, 599 m, 520 w, 375 m cm^{-1}.

ONE-ELECTRON OXIDATION/REDISTRIBUTION REACTIONS

$FU[N(SiMe_3)_2]_3$

A solution of $U[N(SiMe_3)_2]_3$ (0.47 g, 0.65 mmol) in 30 mL of pentane was added to a suspension of AgF (0.27 g, 2.1 mmol) in 10 mL of pentane. After stirring for 3 h, the solution turned from deep purple to pale yellow-pink and a silvery-black precipitate formed. The mixture was filtered, the filtrate was concentrated to ca. 5 mL and cooled to -78°C. Pale purple-pink needles were isolated (0.25 g, 52% yield), m.p. 143-145°C. ^1H NMR (C_6D_6, 20°C): -4.63 ($\nu_{1/2}$=150 Hz). Mass spectrum: M^+= 737. Anal. Calcd. for $C_{18}H_{54}N_3FSi_6U$: C, 29.3; H, 7.37; N, 5.69. Found: C, 29.1; H, 7.49; N, 5.84. IR: 1250 s, 931 s, 850 s, 839 s, 817 s, 758 m, 734 m, 681 m, 671 m, 655 m, 610 s, 509 m, 385 m, 376 m cm^{-1}. The U-F stretching frequency in the infrared spectrum is assigned to the absorption at 509 cm^{-1}. Magnetic susceptibility: The plot of $1/\chi_M$ vs. T (Fig. 3-2) was essentially linear over the temperature range measured. The magnetism did not become temperature independent down to 5 K. A fit of the data as

described in the general experimental section gave the following values for μ_{eff}(ave.): 5 kG; 5-280K, 2.91(1) B.M. (θ=-13(1)K), and 40 kG; 7-280K, 2.92(3) B.M. (θ=-7(2)K).

$N_3U[N(SiMe_3)_2]_2I_3$

To a solution of $U[N(SiMe_3)_2]_3$ (1.35 g, 1.88 mmol) in 50 mL of hexane, cooled to -78°C, was added a solution of Ph_3CN_3 (0.54 g, 1.9 mmol) in 20 mL hexane. The color changed from deep purple to brown. After the addition was complete, the mixture was allowed to warm to room temperature, with stirring. As it warmed, the color of the solution acquired a greenish tinge. The mixture was filtered, the volume of the filtrate was reduced to ca. 10 mL and the solution was cooled slowly to -15°C. A mixture of the brown uranium product and off-white bitrityl crystals (identified by ^{1}H NMR) were isolated. The two compounds were physically separated and the uranium compound was recrystallized from toluene (-15°C). Light brown blocks were isolated (0.13 g, 23% yield), m.p. 165-168°C. ^{1}H NMR (C_7H_8, 34°C): -3.65 ($\nu_{1/2}$=15 Hz). Mass spectrum: M^+= 760. Anal. Calcd. for $C_{18}H_{54}N_6Si_6U$: C, 28.4; H, 7.15; N, 11.0. Found: C, 25.9; H, 7.14; N, 11.4. IR: 2120 s, 2106 s, 2082 m, 1395 w, 1299 w, 1249 s, 1185 w, 1170 w, 1154 w, 907 s, 886 s, 847 s, 774 s, 737 w, 724 w, 677 w, 661 s, 615 s, 595 w, 386 m cm^{-1}.

$(NC)U[N(SiMe_3)_2]_3(PhCN)$

To a solution of $U[N(SiMe_3)_2]_3$ (0.51 g, 0.71 mmol) in 30 mL of pentane was added 0.07 mL of benzonitrile (d=1.01 g/mL, 0.69 mmol). The color changed immediately from purple-red to deep blue. After 15 minutes, the color appeared to change to dark green, then after two

hours to red-brown. The pentane was removed, the remaining brown solid was redissolved in warm hexane and the mixture was filtered. The filtrate was concentrated to ca. 5 mL and cooled to -15°C. Very fine, tan needles were isolated, m.p. 148-150°C. Mass spectrum: $[M^+-(HCN)]$ = 820. The next peak in the spectrum corresponded to the metallocycle, e/m = 717 amu. Anal. Calcd. for $C_{26}H_{59}N_5Si_6U$: C, 36.8; H, 7.01; N, 8.26. Found: C, 35.1; H, 6.94; N, 6.59. IR: 2252 w, 2235 w, 2063 s, 1640 w, 1605 w, 1594 w, 1586 w, 1571 w, 1279 w, 1249 m, 1178 w, 969 w, 913 s, 900 s, 844 s, 773 m, 757 w, 734 w, 728 w, 719 w, 695 w, 661 m, 615 m, 590 w, 555 w, 386 m cm^{-1}.

MeU[N(SiMe$_3$)$_2$]$_3$ from U[N(SiMe$_3$)$_2$]$_3$ and MeLi

A solution of U[N(SiMe$_3$)$_2$]$_3$ (0.45 g, 0.63 mmol) in 30 mL of pentane was cooled to -78°C. To this solution was added 3.0 mL of MeLi (0.21 M in diethyl ether, 0.63 mmol). The color changed from deep purple-red to dark blue-black and a fine, very dark blue-black precipitate formed. As the mixture was allowed to warm to room temperature, the color changed slowly to pale tan and a fine brown precipitate formed. The mixture was stirred 30 minutes at room temperature. The pentane was removed and 50 mL of hexane was added. The mixture was filtered, and the volume of the filtrate was reduced until some precipitate began to form. The solution was warmed slightly to redissolve all of the solid, then cooled slowly to -15°C. Large, tan blocks formed (0.21 g, 46% yield) m.p. 132-135°C. The product was identified by comparison of the melting point and infrared spectrum that of the known compound.[2] Magnetic susceptibility: The plot of $1/\chi_M$ vs. T (Fig. 3-3) was separated into two temperature regimes for

determining values for μ_{eff}. As with the flouride, $FU[N(SiMe_3)_2]_3$, the magnetism did not appear to become temperature independent at low temperature, although the plot of $1/\chi_M$ vs. T does start to level off below 20K. A good match was not achieved between the 5 kG and 40 kG data. This may be due to the fact that the compound crystallizes in an acentric space group (R3c), which may cause its magnetism to be highly anisotropic. The microcrystalline material may physically interact with the magnetic field in such a way as to destroy the anisotropy sought by finely grinding the compound. The 40 kG data is collected after the 5 kG data, making it more likely to exhibit problems due to magnetic anisotropy. The values determined for μ_{eff}(ave.) were: 5 kG; 25-100 K, 2.99(1) B.M. (θ=-13.5(3)K); 120-280K, 3.18(1) B.M. (θ=-32(2)K); 40 kG; 25-100K, 3.50(1) B.M. (θ=-12.2(3)K); 120-280K, 2.89(3) B.M. (θ=-60(4)K).

MeU[N(SiMe$_3$)$_2$]$_3$ from U[N(SiMe$_3$)$_2$]$_3$ and Me$_3$Al

To a solution of $U[N(SiMe_3)_2]_3$ (0.27 g, 0.38 mmol) in 20 mL of pentane was added 0.45 mL of $AlMe_3$ (0.84 M in pentane, 0.38 mmol). After stirring 6 h the solution had turned black with a black precipitate. The mixture was filtered and the volume of the filtrate was reduced to ca. 5 mL. Slow cooling of the solution to -15°C yielded long needles that looked black on the outside, but gave a pale tan powder when ground (0.07 g, 25% yield), m.p. 132-135°C. Recrystallization of the needles from pentane yielded tan needles. The identity of the compound was confirmed by comparison of the IR, melting point, and ^1H NMR with the reported values.[2]

{U[N(SiMe$_3$)$_2$]$_2$I$_3$I$_2$(μ-S)

To a solution of U[N(SiMe$_3$)$_2$]$_3$ (0.17 g, 0.24 mmol) in 50 mL of pentane was added a suspension of Ph$_3$PS (0.070 g, 0.24 mmol) in 10 mL of pentane. The solution turned from deep purple to yellow-gold. A small amount of white precipitate formed. After stirring for 30 minutes, the mixture was filtered, the volume of the filtrate was reduced to 5 mL and the solution was cooled to -15°C. The white triphenylphospine formed in the reaction was isolated and the volume of the remaining solution was reduced to 2 mL. Slow cooling of the solution to -78°C produced orange blocks (0.12 g, 69% yield), m.p. 145-147°C. ^{1}H NMR (C$_6$D$_6$, 32°C): . Under the conditions used to obtain the mass spectrum, the compound appears to decompose to HSU[N(SiMe$_3$)$_2$]$_3$, M^+= 750 and [(Me$_3$Si)$_2$N]$_2$UCH$_2$(Me)$_2$SiNSiMe$_3$, M^+= 717. Anal. Calcd. for $C_{36}H_{108}N_6SSi_{12}U_2$: C, 29.4; H, 7.40; N, 5.72. Found: C, 32.0; H, 7.28; N, 5.19. IR: 1249 m, 888 s, 850 s, 775 m, 760 w, 742 w, 722 w, 695 w, 661 m, 616 m, 388 m, 322 m cm^{-1}.

{U[N(SiMe$_3$)$_2$]$_2$I$_3$I$_2$(μ-Se)

A solution of U[N(SiMe$_3$)$_2$]$_3$ (0.43 g, 0.60 mmol) in 30 mL of pentane was added to a suspension of Ph$_3$PSe in 10 mL of pentane. The color changed immediately from dark purple to orange. The mixture was stirred 30 minutes, then the volume was reduced to 10 mL. The reaction mixture was cooled to -15°C to precipitate the triphenylphosphine. After 12 h, the mixture was filtered again and the volume of the orange solution was reduced to 2 mL. Slow cooling to -78°C yielded orange-red crystals (0.31 g, 68% yield), m.p. 145-149°C. ^{1}H NMR (C$_6$D$_6$, 32°C): -6.35 ($\nu_{1/2}$=8.3 Hz). Under the conditions used to obtain the mass

spectrum, the compound appeared to decompose to $HSeU[N(SiMe_3)_2]_3$, M^+= 797 and $[(Me_3Si)_2N]_2\overline{UCH_2(Me)_2SiNSiMe_3}$, M^+= 717. When heated for 5 h at 85°C in toluene, the compound did decompose to the metallocycle, however, no $HSeU[N(SiMe_3)_2]_3$ was observed. Anal. Calcd. for $C_{36}H_{108}N_6SeSi_{12}U_2$: C, 28.5; H, 7.17; N, 5.54. Found: C, 28.2; H, 7.29; N, 5.89. IR: 1301 w, 1250 s, 1174 w, 1096 w, 1028 w, 887 s, 851 s, 775 m, 762 w, 741 w, 723 w, 695 w, 660 m, 616 m, 511 w, 504 w, 388 m cm^{-1}.

[U[N(SiMe$_3$)$_2$]$_3$]$_2$(μ-Te)

A solution of $U[N(SiMe_3)_2]_3$ (1.35 g, 1.88 mmol) in 30 mL of pentane was added to a solution of $n\text{-}Bu_3PTe$ (0.10 g, 0.26 mmol) in 10 mL of pentane at 0°C. The color of the solution changed immediately from deep purple to red. The mixture was filtered and the volume of the filtrate was reduced to ca. 5 mL. Slow cooling to -25°C yielded large red crystals (0.58 g). A second crop of smaller red crystals was obtained (0.35 g, 63% total yield), m.p. 158-159°C. ^1H NMR (C_6D_6, 32°C): -5.94 ($\nu_{1/2}$=9.0 Hz). Under the conditions used to obtain the mass spectrum, the compound appeared to decompose to $HTeU[N(SiMe_3)_2]_3$, M^+= 847 and $[(Me_3Si)_2N]_2\overline{UCH_2(Me)_2SiNSiMe_3}$, M^+= 717. Anal. Calcd. for $C_{36}H_{108}N_6Si_{12}TeU_2$: C, 27.6: H, 6.95; N, 5.37. Found: C, 27.5; H, 7.12; N, 5.62. IR: 1251 s, 1170 w, 1153 w, 886 s, 850 s, 839 sh, 774 m, 738 w, 723 w, 703 w, 659 m, 614 m, 391 m cm^{-1}. Magnetic susceptibility: The plot of $1/\chi_M$ vs. T is shown in Figure 3-4. The magnetism did not become temperature independent down to 5 K, although the plot of $1/\chi_M$ vs. T does start to curve in that direction below 25K. Low and high temperature regions were selected for fitting the data and the values obtained (calculated for the dinuclear compound, with the values per

uranium in brackets) for μ_{eff}(ave.) were: 5 kG; 5-140K, 4.38(1) [3.10] B.M. (θ=-19.4(4)K); 140-280K, 4.64 [3.28] B.M. (θ=-40(3)K).

Reaction of U[N(SiMe$_3$)$_2$]$_3$ and N_2O

Tris[bis(trimethylsilyl)amido]uranium (0.45 g, 0.63 mmol) was dissolved in 20 mL toluene and transferred to a thick-walled glass pressure bottle. The solution was pressurized to 5 atm. with N_2O. The color changed immediately from dark purple to pale gold. The solution was transferred to a small Schlenk flask and the volume was reduced to ca. 10 mL. Slow cooling to -15°C yielded gold needles (0.26 g, 73% yield, calculated for (OU[N(SiMe$_3$)$_2$]$_2$)$_n$), m.p. 171-172°C. The needles appeared to lose solvent slowly and turned opaque after several days under nitrogen. The sample used for elemental analysis was dried under vacuum for 12 h at 60°C. Anal. Calcd. for $C_{12}H_{36}N_2OU$: C, 25.1; H, 6.31; N, 4.87. Found: C, 25.4; H, 6.58; N, 4.98. The highest peaks in the mass spectrum correspond to, (OU[N(SiMe$_3$)$_2$]$_2$)$_3$, M^+= 1722, and [M^+ - HN(SiMe$_3$)$_2$] = 1561. IR: 1264 w, 1248 s, 885 s br, 851 s br, 816 sh, 776 m, 761 w, 732 w, 723 w, 692 w, 680 sh, 669 sh, 660 m, 632 w, 616 m, 469 s br, 386 m cm^{-1}.

TWO-ELECTRON OXIDATION REACTIONS

U[N(SiMe$_3$)$_2$]$_3$[N(p-tolyl)]

To a solution of U[N(SiMe$_3$)$_2$]$_3$ (0.40 g, 0.56 mmol) in pentane (30 mL) was added 0.24 mL p-tolylazide[3] (2.4 M in toluene, 0.58 mmol). The color changed immediately from deep purple-red to dark black-green and

gas was evolved. After stirring five minutes, the pentane was removed under reduced pressure, leaving a black solid. The solid was redissolved in 30 mL hexane, filtered and the filtrate was cooled (-35°C), yielding black, chunky crystals (0.20 g, 43%), m.p. 145-148°C. ^{1}H NMR (C_6D_6, 20°C): 23.89 (3H, $\nu_{1/2}$=9 Hz), 21.32 (2H, $\nu_{1/2}$=13 Hz), 2.75 (2H, $\nu_{1/2}$=33 Hz), -2.12 (54H, $\nu_{1/2}$=35 Hz). Mass spectrum: M^+-823. Anal. Calcd. for $C_{25}H_{26}N_4Si_6U$: C, 36.4; H, 7.46; N, 6.80. Found: C, 31.3; H, 7.63; N, 5.80. IR: 1491 m, 1249 s, 1104 w, 909 s, 842 s, 816 s, 770 s, 760 s, 736 m, 693 w, 676 m, 655 s, 607 s, 519 m, 475 m br, 389 m br cm^{-1}. Magnetic susceptibility: The plot of $1/\chi_M$ vs. T (Fig. 3-5) is slightly curved throughout the whole temperature range. The data was separated into two temperature regimes to determine values for μ_{eff}(ave.), although a straight-line fit to the data may not be appropriate due to the curvature. At 5kG; 5-40K, 1.49(1) B.M. (θ=-1.3(3)K); 140-280K, 2.26(2) B.M. (θ=-98(8)K). At 40kG, 7-40K, 1.56(1) B.M. (θ=0.0(4)K); 140-280K, 2.21(1) B.M. (θ=-86(4)K).

U[N(SiMe$_3$)$_2$]$_3$[N(t-Bu)]

To a solution of U[N(SiMe$_3$)$_2$]$_3$ (0.52 g, 0.72 mmol) in pentane (20 mL) was added 0.80 mL t-butylazide[4] (0.90 M in cyclohexane as determined by ^{1}H NMR, 0.72 mmol). The color changed immediately from deep purple-red to black-green and gas was evolved. The solution volume was reduced to 2 mL and the solution was cooled to -78°C, producing black crystals (0.18 g, 32%), m.p. 113-119°C. A second crop of crystals could not be obtained, as removal of the remaining solvent left a black oil. Difficulties were encountered in the reproducibility of this preparation. Several times no crystalline product could be

obtained, only a black oil remained after the solvent was removed. ^1H NMR (C_6D_6, 20°C): 25.06 (9H, $\nu_{1/2}$=229 Hz); -3.95 (54H, $\nu_{1/2}$=123 Hz). Mass spectrum: M^+= 789. Anal. Calcd. for $C_{22}H_{63}N_4Si_6U$; C, 33.4; H, 8.03; N, 7.09. Found; C, 33.3; H, 8.11; N, 7.14. IR: 1356 m, 1249 s, 1206 m, 1195 m, 1008 m, 993 m, 907 s, 900 s, 848 s, 837 s, 772 s, 698 w, 673 m, 660 s, 607 s, 493 s br, 389 s br cm^{-1}.

U[N(SiMe$_3$)$_2$]$_3$(NSiMe$_3$)

The compound was synthesized by the procedure of Brennan.[5] Magnetic susceptibility: The plot of $1/\chi_M$ vs. T is shown in Figure 3-6. As with U[N(SiMe$_3$)$_2$]$_3$[N(p-tolyl)], the plot is curved throughout the experimental temperature range, and a straight-line fit to the observed curve may not be a good way to treat the data. Fitting low and high temperature regions gave the following values for μ_{eff}(ave.): At 5 kG; 5-40K, 1.61(2) B.M. (θ=-3.6(7)K); 140-240K, 2.04(1) B.M. (θ=-54(4)K). At 40 kG; 5-40K, 1.63(1) B.M. (θ=-4.1(6)K); 140-280K, 2.04 B.M. (θ=-54(3)K).

U[N(SiMe$_3$)$_2$]$_3$[NH(p-tolyl)]

A solution of U[N(SiMe$_3$)$_2$]$_3$ (0.58 g, 0.81 mmol) in pentane (25 mL) was added to a solution of U[N(SiMe$_3$)$_2$]$_3$[N(p-tolyl)] (0.67 g, 0.81 mmol) in pentane (25 mL). The mixture was stirred for 2 h and the color changed from black to dark brown. The volume of the solution was reduced to ca. 5 mL and an orange-brown precipitate formed. The mixture was cooled to -25°C for 24 h to precipitate all of the less soluble product. The mixture was filtered, the precipitate redissolved

in hexane and the solution was concentrated and cooled (-15°C). Brown crystals of $U[N(SiMe_3)_2]_3[NH(p\text{-tolyl})]$ were isolated by filtration (0.20 g, 30%), m.p. 132-135°C. ^1H NMR (C_6D_6, 20°C): -1.83 (54 H), -2.11 (3 H), -2.14 (2H, d, J=12 Hz), -27.89 (2H, d, J=8 Hz), -213.1 (1H). Mass spectrum: $[M^+-1]$ = 823. Anal. Calcd. for $C_{25}H_{25}N_4Si_6U$: . IR: 1609 m, 1507 s, 1268 s, 1261 s, 1247 s, 1180 w, 1109 w, 915 s, 851 s, 836 s, 814 s, 770 s, 735 m, 696 w, 677 m, 657 s, 608 s, 527 m, 463 m br, 381 m br cm^{-1}.

The first filtrate was concentrated to ca. 2 mL and cooled to -15°C, yielding yellow needles of $[(Me_3Si)_2N]_2\overline{UCH_2(Me)_2SiNSiMe_3}$, (0.41 g, 71%). The metallocycle was identified by comparison of the melting point and infrared spectrum with that of the known compound.[6]

DIMERS

$U_2[N(SiMe_3)_2]_4[\mu\text{-}N(p\text{-tolyl})]_2$

To a solution of p-toluidine (0.10 g, 0.93 mmol) in 30 mL of hexane was added 0.24 mL of n-BuLi (3.98 M in hexane, 0.96 mmol). A white precipitate formed immediately. This mixture was added to a suspension of $ClU[N(SiMe_3)_2]_3$ (0.70 g, 0.93 mmol) in 20 mL of hexane. The color changed from pinkish-orange to bright gold and then slowly darkened to red-brown. The mixture was stirred six hours, filtered and the volume of the filtrate was reduced to 4 mL. Slow cooling to -15°C yielded red bricks (0.40 g, 65% yield), m.p. 230-233°C. ^1H NMR (C_6D_6, 20°C): 12.66 (2H), 6.20 (2H), 1.21 (3H), -12.40 (36H). Mass spectrum: The highest peak observed was due to the metallocycle,

$[(Me_3Si)_2N]_2\overline{UCH_2(Me)_2SiNSiMe_3}$, e/m = 717 amu. Anal. Calcd. for $C_{38}H_{86}N_6Si_8U_2$: C, 34.4; H, 6.53; N, 6.33. Found: C, 33.1; H, 6.34; N, 5.96. IR: 1603 w, 1491 m, 1250 s, 1216 s, 1174 m, 955 s, 931 s, 844 s, 816 s, 772 m, 756 m, 727m, 677 w, 657 m, 607 m, 525 m, 480 m, 385 m cm^{-1}. Magnetic susceptibility: The plot of $1/\chi_M$ vs. T is shown in Figure 3-7. Low and high temperature regions were chosen for determining μ_{eff}, however, it should be noted that there is a significant amount of curvature in the $1/\chi_M$ vs. T plot, making a straight line fit to the data of questionable validity. The values obtained for μ_{eff}(ave.) (calculated for the dimer, with monomer values in brackets) were: 5 kG; 5-40K, 6.18(7) [4.37] B.M. (θ=0.4(5)K); 160-280K, 4.72(4) [3.34] B.M. (θ=44(4)K). At 40 kG; 5-40K, 6.94(15) [4.91] B.M. (θ=-3(1)K); 160-280K, 4.80(8) [3.39] B.M. (θ=49(7)K).

$U_2[N(SiMe_3)_2]_4[\mu\text{-}N(H)(2,4,6\text{-}Me_3C_6H_2)]_2$

A solution of 2,4,6-trimethylaniline (0.09 mL, d=1.0 g/mL, 0.67 mmol) in 20 mL of pentane was carefully layered on top of a solution of $U[N(SiMe_3)_2]_3$ (0.50 g, 0.70 mmol) in 30 mL of pentane. The two solutions were allowed to stand undisturbed for 24 h. The mixture was then carefully filtered, and the dark blue-green crystals were isolated (0.12 g, 24.8%), m.p 191-195°C. A small amount of brown solid was always present on the sides of the glassware after the two solutions had mixed. The product was not soluble in hydrocarbon or aromatic solvents and attempts at recrystallization from tetrahydrofuran led to deposition of a brown, oily substance. The ^1H NMR spectrum could not be obtained due to insolubility of the compound. Anal. Calcd. for $C_{42}H_{94}N_6Si_8U_2$: C, 36.5; H, 6.85; N, 6.07. Found: C, 35.6; H, 6.95; N,

5.69. IR: 1300 w, 1292 w, 1250 m, 1242 m, 1215 w, 1207 w, 1154 w, 964 s, 931 w, 872 m, 855 s, 845 s, 817 m, 771 m, 755 w, 737 w, 731 w, 720 w, 654 m, 606 m cm^{-1}. Magnetic susceptibility: A plot of $1/\chi_M$ vs. T is shown in Figure 3-8. A fit of the data to low and high temperature regions gave the following values (calculated for the dimer, with monomer values in brackets) for μ_{eff}(ave.): At 5 kG; 9-60K, 4.06(3) [2.87] B.M. (θ=-22.5(7)K); 80-280K, 4.99(3) [3.53] B.M. (θ=-71(2)K). At 40 kG; 9-60K, 4.01(3) [2.84] B.M. (θ=-21.6(7)K); 80-280K, 4.92(2) [3.48] B.M. (θ=-66(2)K).

CHAPTER TWO

TRITOX COMPOUNDS

Synthesis of t-Bu_3COH (tritoxH)

The alcohol was prepared by a modification of the procedure of Syper.[7] The reaction was carried out in a 1 L, 3-neck, round-bottom flask fitted with a 200 mL pressure-equalized dropping funnel, water-cooled condenser with argon inlet, and large egg-shaped magnetic stirbar. The reaction temperature was kept between -70 and -80°C. A solution of t-BuLi (366 mL, 1.74 M in pentane, 0.640 mmol) was transferred to the flask along with 100 mL Et_2O. Ethyl trimethylacetate (t-BuCOOEt, 48.7 mL, d = 0.856 g/mL, 0.320 mol) was transferred to the dropping funnel along with 100 mL Et_2O. The ethyl trimethylacetate was added to the t-BuLi solution over 45 minutes. During the initial part of the addition, the color of the reaction was bright reddish-orange. This faded to a paler yellow-orange by the time the addition was complete. The mixture was stirred 30 minutes, then allowed to warm to -35°C. The mixture was poured into a 2 L Erlenmeyer flask containing 800 g of crushed ice. The orange color disappeared and a small amount of white solid formed on the sides of the flask. When most of the ice melted, the mixture was transferred to a large separatory funnel, the aqueous layer was separated, and the organic layer was washed with another 200 mL of water. The combined organic layers were dried over $MgSO_4$ and the Et_2O and pentane were removed by rotary evaporation. Lower boiling components were removed by vacuum distillation (maximum temperature 50°C, 10 torr). It was important to use a large round-bottom flask as the stillpot (in this case, a 250 mL

round-bottom flask and a 10 cm Vigreaux column were used), in order to minimize problems due to foaming. The residue in the stillpot solidified on cooling to a sticky, off-white solid which was recrystallized from a MeOH/H_2O (50/50 v/v) mixture, yielding white, slightly sticky crystals which were isolated by filtration and dried under vacuum (47.4 g, 73.9% yield), m.p. 113-115°C. ^{1}H NMR (C_6D_6, 20°C): 1.22(27H), 3.52(1H).

Li(tritox)

The lithium salt of tritoxH was prepared by the procedure of Lubben, Wolczanski, and Van Duyne.[8] White, crystalline tritoxH (3.84 g, 19.2 mmol) was dissolved in 50 mL of pentane and cooled to 0°C. A solution of n-BuLi (9.1 mL, 2.1 M in pentane, 19 mmol) was added to the alcohol over 10 minutes. The white product began to precipitate after the addition was approximately 2/3 complete. The mixture was allowed to warm to room temperature with stirring. The volume of the solution was reduced to 20 mL and the mixture was cooled to -78°C for two days. The white product was isolated by filtration and dried under reduced pressure (3.88 g, 98.0% yield), m.p. 138-140°C. ^{1}H NMR (C_6D_6, 20°C): 1.10. IR: 1378 m, 1362 m, 1352 m, 1201 w, 1180 m, 1115 s, 1032 m, 1019 m, 925 m, 877 s, 710 s, 647 w, 604 w, 578 w, 532 m, 487 m cm^{-1}.

ClU(tritox)$_3$

To UCl_4 (5.30 g, 14.0 mmol) suspended in diethyl ether (50 mL) was added a solution of Li(tritox) (8.64 g, 41.9 mmol) dissolved in ether (100 mL). Within ca. 15 minutes the color changed from green to pink-tan. The mixture was stirred for 3 h, filtered, and the pink filtrate

was cooled to -15°C. Pink crystals were isolated and dried under vacuum (3.21 g). The remaining solid from the initial filtration was extracted with toluene (2x100 mL) and cooled to -15°C yielding 4.62 g of the same product (total yield 64%), m.p. 204-206°C. ^{1}H NMR (C_6D_6, 32°C): 6.39. Mass spectrum: The highest peak corresponded to [M^+ - (t-Bu)] = 814. Anal. Calcd. for $C_{39}H_{81}O_3ClU$: C, 53.8; H, 9.37; Cl, 4.07. Found: C, 52.5; H, 9.31; Cl, 3.77. IR: 1458 s, 1396 s, 1207 w,1189 w, 1044 m, 950 s br, 891 m, 722 m, 697 s, 483 w, 406 w cm^{-1}.

MeU(tritox)$_3$

To ClU(tritox)$_3$ (0.63 g, 0.72 mmol) dissolved in hexane (50 mL) was added 1.6 mL of MeLi (0.52 M in ether, 0.79 mmol). The color changed immediately from pale pink to gold and LiCl precipitated. After stirring one hour, the mixture was filtered and the filtrate was concentrated to 5 mL and cooled (-15°C), yielding large amber crystals (1.51 g, 89.6%), m.p. 199-200°C. ^{1}H NMR (C_6D_6, 20°C): 6.73(81H), -226 (3H). Mass spectrum: [M^+ - 14] = 836. Anal. Calcd for $C_{40}H_{84}O_3U$: C, 56.5; H, 9.95. Found: C, 56.7; H, 10.1. IR: 1394 s, 1370 s, 1206 w, 1189 w, 1047 m, 965 s, 890 m, 693 s, 411 m cm^{-1}. Magnetic susceptibility: The plot of $1/\chi_M$ vs. T (Fig. 3-9) became temperature independent below ca. 40K. A straight line fit of the high temperature region gave the following values for μ_{eff}(ave.): At 5 kG, 80-280K, 3.154(4) B.M. (θ=-54(1)K). At 40 kG, 80-280K, 3.24(1) B.M. (θ=-41(2)K).

EtU(tritox)$_3$

To ClU(tritox)$_3$ (1.65 g, 1.89 mmol) dissolved in toluene (50 mL)

was added a solution of EtLi (0.07 g, 1.94 mmol) in toluene (10 mL). The mixture was stirred for 3 h then the LiCl was allowed to settle. The mixture was filtered, the volume of the filtrate was reduced to 5 mL and the solution was cooled slowly to -15°C. Brown crystals were isolated by filtration (0.95 g, 58%) m.p. 194-196°C. ^{1}H NMR (C_6D_6, 20°C): 6.51(81H), -33.42(3H), -220.0(2H). Anal. Calcd. for $C_{41}H_{86}O_3U$: C, 56.9; H, 10.0. Found: C, 56.8; H, 10.0. IR: 1407 w, 1393 s, 1376 m, 1370 m, 1359 w, 1206 m, 1188 m, 1111 m, 1047 m, 1003 w, 965 s, 931 m, 926 m, 922 m, 890 m, 693 s, 481 w br, 451 w br, 408 m br cm^{-1}.

n-BuU(tritox)$_3$

To a solution of ClU(tritox)$_3$ (1.45 g, 1.66 mmol) in toluene (30 mL) was added 0.8 mL of n-BuLi (2.3 M in pentane, 1.8 mmol). The mixture was stirred for 3 h. The color changed from pink to gold, then to slightly darker brown. The LiCl was allowed to settle out overnight. The mixture was filtered, the volume of the filtrate was reduced to 3 mL and the solution cooled slowly to -15°C. Chunky brown crystals were isolated (0.98 g, 66%), m.p. 171-174°C. ^{1}H NMR (C_6D_6, 20°C): 6.15(81H); -16.94 (3H, t, J=7.14 Hz); -30.19 (2H, d, J=6.84 Hz); -46.77 (2H, d, J=3.63 Hz); -220.4 (2H, br). Anal. Calcd. for $C_{43}H_{90}O_3U$: C, 57.8; H, 10.2. Found: C, 58.0; H, 10.3. IR: 1408 w, 1395 m, 1208 w, 1187 w, 1045 m, 961 s, 929 w, 890 m, 721 m, 691 s, 504 w, 481 w, 404 m cm^{-1}.

(Me$_3$CCH$_2$)U(tritox)$_3$

To a suspension of ClU(tritox)$_3$ (1.13 g, 1.30 mmol) in hexane (50 mL) was added a solution of LiCH$_2$CMe$_3$ in hexane (20 mL). The color

changed from pink to gold and the reaction appeared complete in 1.5 h. Most of the LiCl was allowed to settle (some of it remained suspended in solution, even after 24 h) The mixture was filtered and the hexane was removed. Pentane (20 mL) was added to the residue and the remaining LiCl was allowed to settle. The mixture was filtered and the volume of the filtrate was reduced to 5 mL. The solution was cooled slowly to -15°C yielding yellow-brown crystals (0.34 g, 29%) m.p. 192-197°C. ^{1}H NMR (C_6D_6, 32°C): 5.85 (81H); -27.95 (9H); -191.9 (2H). Anal. Calcd. for $C_{44}H_{92}O_3U$: C, 58.3; H, 10.2. Found: C, 58.8; H, 10.4. IR: 1395 m, 1207 w, 1188 w, 1044 m, 950 s, 891 m, 721 m, 695 m cm^{-1}.

$(Me_3SiCH_2)U(tritox)_3$

To a suspension of $ClU(tritox)_3$ (0.84 g, 0.96 mmol) in hexane (50 mL) was added a solution of $LiCH_2SiMe_3$ (0.09 g, 0.96 mmol) in hexane (30 mL). The mixture was stirred for 2 h and the color changed slowly from pink to yellow. The hexane was removed and 20 mL of pentane was added. The LiCl was allowed to settle, the mixture was filtered and the volume of the filtrate was reduced to 2 mL. The solution was cooled to -78°C for 24 h yielding yellow crystals (0.22 g, 25%) m.p. 184-186°C. No second crop was obtained due to high solubility of the product. ^{1}H NMR (C_6D_6, 20°C): 6.16 (81H); -20.22 (9H); -209.9 (2H). Anal. Calcd. for $C_{43}H_{92}O_3U$: C, 55.9; H, 10.0. Found: C, 57.9; H, 10.6. IR: 1394 s, 1377 m, 1370 m, 1243 m, 1207 w, 1187 w, 1044 m, 955 s, 925 m, 901 m, 849 m, 820 m, 690 s, 510 w, 408 m br cm^{-1}.

$(PhCH_2)U(tritox)_3$

To a suspension of $ClU(tritox)_3$ (1.86 g, 2.13 mmol) in diethyl

ether (50 mL) was added a solution of $LiCH_2Ph(OEt_2)$ (0.37 g, 2.2 mmol) dissolved in diethyl ether (20 mL) The color changed from pink to gold and a white precipitate formed. The mixture was stirred for 3 h, the diethyl ether was removed and hexane (100 mL) was added to the residue. The LiCl was allowed to settle overnight. The mixture was filtered, the volume of the filtrate was reduced to 5 mL and the solution cooled slowly to -15°C yielding small, gold-brown needles (0.95 g, 48%), m.p. 188-190°C. ^1H NMR (C_6D_6, 32°C): 5.93 (81H); -2.20 t J=7.3 Hz (2H); -4.35 t J=7.3 Hz (1H); -32.52 d J=7.3 Hz (2H); -212.2 (2H). Anal. Calcd. for $C_{46}H_{88}O_3U$: C, 59.6; H, 9.57. Found: C, 58.8; H, 9.70. IR: 1595 m, 1490 m, 1394 m, 1377 m, 1369 m, 1212 m, 1186 w, 1044 m, 953 s, 890 m, 800 m, 739 m, 692 s, 594 w, 504 w, 405 m br cm^{-1}.

DITOX COMPOUNDS

Synthesis of $t\text{-Bu}_2CHOH$ (ditoxH)

The alcohol was synthesized by a modification of the procedure of Syper.[7] The reaction was carried out in a 500 mL, 3-neck, round-bottom flask with a 250 mL pressure-equalized dropping funnel, argon inlet, and large egg-shaped magnetic stirbar. The reaction temperature was kept at -45±3°C. A solution of t-BuLi (500 mL, 1.76 M in pentane, 0.850 mol) was transferred to the flask. Ethyl acetate (HCOOEt, 34.3 mL, d = 0.917 g/mL, 0.43 mol) and 75 mL of diethyl ether were placed in the dropping funnel and the contents were added over 1 h. The color changed from clear to bright yellow. Toward the end of the reaction some white precipitate began to form. After the addition was complete, the mixture was stirred for 1 h and the temperature was not allowed to

warm above -30°C. The mixture was poured over 500 g of crushed ice. The yellow color disappeared, but there was still some white solid present in the organic layer. Approximately 300 mL of diethyl ether was added, which dissolved most of the solid. The mixture was separated and the organic layer was washed with 150 mL of water, then dried over $MgSO_4$. The volatile material was removed by rotary evaporation.

The lower boiling components were removed by vacuum distillation (maximum temperature 50°C, 10 torr). The distillation was carried out using a 250 mL round-bottom flask as the stillpot and a 10 cm Vigreaux column. Using a large flask to distill from helped avoid the problem of foaming. The remaining thick, clear liquid in the distillation pot cooled to a sticky, crystalline solid, which was used without further purification.

Li(ditox)

To a solution of ditoxH (6.51 g, 45.1 mmol), dissolved in 50 mL pentane and cooled to 0°C, was added 20.7 mL of *n*-BuLi (2.18 M in pentane, 45.1 mmol). The solution was stirred for 1 h, then allowed to come to room temperature. The volume was reduced to 20 mL, the mixture was warmed to redissolve all of the product that had precipitated, then the clear solution was cooled slowly to -15°C. Large, white crystals were isolated (5.45 g, 80.5%), m.p. 155-160°C. ^{1}H NMR (C_6D_6, 20°C): 3.29 (1H), 1.11 (18H). IR: 2727 w, 2683 w, 2622 m, 2546 w, 2494 w, 1387 m, 1364 m, 1353 m, 1237 w, 1213 w, 1198 w, 1164 m, 1086 s, 1028 m, 1011 s, 948 m, 919 m, 856 w, 770 m, 723 w, 619 s, 554 w, 529 s, 450 s br, 419 sh cm^{-1}.

U(ditox)$_4$

To UCl_4 (5.84 g, 15.4 mmol) suspended in diethyl ether (25 mL) was added a solution of Li(ditox) (9.24 g, 61.5 mmol) in diethyl ether (50 mL). The color of the mixture turned from pale green to a more intense green, then to green-grey and eventually to grey. The mixture was stirred three hours and the ether removed by vacuum. The solid was extracted with pentane (100 mL) and the solution cooled to -78°C. A pink-purple crystalline solid was isolated (4.87 g). A second crop yielded 1.62 g (total yield, 52.0%), m.p. 105-107°C. ^{1}H NMR (C_6D_6, 20°C): 32.12(1H), 0.14(18H). Mass spectrum: M^+= 810. Anal. Calcd. for $C_{36}H_{76}O_4U$: C, 53.3; H, 9.44. Found; C, 53.2; H, 9.49. IR: 2619 w, 1392 s, 1365 s, 1321 w, 1241 w, 1213 w, 1164 m, 1059 s, 1034 m, 1009 s, 980 s, 957 m, 932 m, 919 m, 856 w, 801 w, 762 m, 723 w, 660 s, 618 w, 556 m, 520 w, 450 w, 404 m cm^{-1}. Magnetic susceptibility: The plot of $1/\chi_M$ vs. T is shown in Figure 3-10. At low temperature, the magnetism does not become temperature independent, although it is tapering off slightly. A fit of the data for the low and high temperature regimes gave the following values for μ_{eff}(ave.): At 5 kG; 5-120K, 2.59(1) B.M. (θ=-16.8(4)K); 140-280K, 2.71(1) B.M. (θ=-33(2)K). At 40 kG; 7-120K, 2.52(1) B.M. (θ=-5.1(6)K); 140-280K, 2.76(2) B.M. (θ=-30(3)K).

MeU(ditox)$_4$Li

To a solution of U(ditox)$_4$ (0.65 g, 0.80 mmol) in hexane (50 ml) was added 0.90 mL of MeLi (0.90 M in diethyl ether, 1.0 mmol). The color changed immediately from lavander to pale green. The solution was stirred for five minutes, then the hexane was removed under reduced pressure. As the volume was reduced, a purple solid formed. The solid

was washed with a small amount of pentane (ca. 2 mL) then dissolved in toluene (10 mL). The solution was filtered and the filtrate was cooled (-15°C). Purple crystals (0.21 g, 35.0%) were collected and dried, m.p. 160-165°C. Mass spectrum: $[M^+ - Li]$ = 825. Anal. Calcd. for $C_{37}H_{79}O_4LiU$: C, 53.4; H, 9.56. Found: C, 52.8; H, 9.51. IR data (Nujol, CsI): 1390 s, 1365 s, 1320 w, 1241 w, 1214 w, 1164 w, 1090 w, 1057 s, 1035 w, 1003 s, 956 m, 933 w, 919 w, 959 w, 963 m, 660 m, 646 m, 629 m, 556 w, 518 w, 398 m cm^{-1}.

SILOX COMPOUNDS

Synthesis of $t\text{-Bu}_3SiOH$ (siloxH)

The preparation of siloxH was a modification of the procedure of Dexheimer and Spialter.[9] The reaction sequence was:

1) $SiF_4 + 2\ t\text{-BuLi} \xrightarrow{\text{pentane}} (t\text{-Bu})_2SiF_2 + 2\ LiF$

2) $(t\text{-Bu})_2SiF_2 + 2\ t\text{-BuLi} \xrightarrow{\text{cyclohexane}} t\text{-Bu}_3SiH + 2\ LiF + C_4H_8$

3) $(t\text{-Bu})_3SiH + NaOH/EtOH \xrightarrow{\text{reflux}} (t\text{-Bu})_3SiOH$

The first step of the reaction was carried out in a 2 L, 3-neck, round-bottom flask fitted with water-cooled condenser, N_2 inlet, mechanical stirrer and inlet for the SiF_4. The SiF_4 inlet was an extended 24/40 ground glass joint curved slightly at the end so it could be pointed with the flow of the stirring solution, so as not to become clogged with the LiF formed during the reaction.

A solution of t-BuLi (371 mL, 1.75 M in pentane, 0.650 mol) and an additional 500 mL pentane were transferred into the flask. The solution was cooled to 0°C. The SiF_4 was slowly bubbled into the t-BuLi solution for 1.5 h. The reaction proceeded at a very moderate,

easily controlled rate. The mixture was filtered, the LiF washed with 200 mL pentane and the pentane removed by rotary evaportation. Distillation of the product (50°C, 10 torr) yielded 36.62 g of $(t\text{-Bu})_2SiF_2$, 61.5% yield.

For the second step of the reaction, $(t\text{-Bu})_2SiF_2$ (36.6 g, 0.200 mol) and 150 mL cyclohexane were transferred to a 250 mL round-bottom flask with N_2 inlet, water-cooled condenser, and magnetic stirbar. A pentane solution of t-BuLi (173 mL, 1.75 M, 0.303 mol) was added, then the pentane was removed under reduced pressure. The resulting mixture was heated to reflux for 2 d. After cooling to room temperature, the mixture was filtered, and the product was purified by distillation (50-52°C, 5 torr), yielding 33.2 g of $(t\text{-Bu})_3SiH$, 81.5%.

For the hydrolysis, a mixture of $(t\text{-Bu})_3SiH$ (32.7 g, 0.163 mol), 150 mL of 95% EtOH, and 17.3 g KOH pellets was refluxed for 36 h. The solution was placed in a separatory funnel with 150 mL of water and 150 mL of diethyl ether. The organic layer was separated and another 200 mL of diethyl ether was added to the aqueous layer. The two organic layers were combined and dried over $MgSO_4$. The mixture was filtered and the diethyl ether was removed by rotary evaportation. The remaining solution was transferred to a round-bottom flask with side-arm and the ethanol was removed under reduced pressure (10^{-1} torr). Crude yield was 33.9 g, 95.6%. The solid was recrystallized from pentane before conversion to the lithium salt.

Li(silox)

To a solution of siloxH (8.80 g, 0.0410 mol) in 75 mL pentane was added 19.5 mL of n-BuLi (2.1 M in pentane, 0.041 mol). The mixture was

stirred for 1h, then the volume was reduced to 20 mL and the solution was cooled to -15°C. A white crystalline solid was isolated, that was dried to give a white powder (6.55 g, 71.9%). ^{1}H NMR (C_6D_6, 20°C): 1.16 ppm.

U(silox)$_3$Cl$_2$Li

To solution of UCl_4 (0.45 g, 1.2 mmol) dissolved in 30 mL tetrahydrofuran was added a solution of Li(silox) (0.79 g, 3.6 mmol) dissolved in 20 mL of tetrahydrofuran. The color stayed green, although it became less emerald-green and more grey-green. No precipitate formed. The tetrahydrofuran was removed under vacuum reduced pressure, leaving a pale pink-purple solid. The solid was stirred with 100 mL of diethyl ether for 2 h, which gave a green colored solution and a white precipitate (LiCl). The mixture was filtered and the volume of the filtrate was reduced. Immediately after applying a vacuum to the solution, pink crystals began to form on the sides of the glassware. The filtrate was warmed to redissolve all of the solid, then the solution was cooled slowly to -15°C. Pale pink needles were isolated (0.56 g, 49%), m.p. 320-325°C. The clear pink crystals became opaque when dried under vacuum. The product gave a positive flame test for lithium. Mass spectrum: The highest peak in the spectrum was $[M^+ - (t\text{-}Bu)] = 903$. Anal. Calcd. for $C_{36}H_{81}O_3Si_3LiCl_2U$: C, 44.9; H, 8.48; Cl, 7.37. Found: C, 44.5; H, 8.37; Cl, 6.91. IR: 1305 w, 1196 w, 1170 w, 1153 w, 1122 w, 1093 w, 1049 m, 1014 w, 1006 w, 932 m, 910 m, 860 s, 845 s, 821 s, 801 s, 723 m, 625 s, 573 w, 508 w, 473 s, 414 w, 386 w, 374 w cm^{-1}.

$U(silox)_4$

A solution of Li(silox) (0.82 g, 3.7 mmol) in 20 mL of tetrahydrofuran was added to a solution of UCl_4 (0.35 g, 3.3 mmol) in 10 mL of tetrahydrofuran. The color of the solution changed from green to grey. The solvent was removed, leaving a pink solid. The solid was extracted with 50 mL pentane and crystallized by cooling (-25°C). Pink crystals, that dried to a pink powder, were isolated (0.42 g, 42%). The material did not melt or appear to decompose up to 320°C. ^1H NMR (C_6D_6, 20°C): 0.36 ppm. Mass spectrum: M^+ = 1098. IR: 1386 m, 1364 m, 1012 w, 1005 w, 933 m, 828 s, 722 m, 626 s, 473 s, 290 m cm^{-1}. Magnetic susceptibility: The plot of $1/\chi_M$ vs. T (Fig. 3-11) did not become temperature independent at low temperature. Fitting the low and high temperature regions of the data gave the following values for μ_{eff}(ave.): At 5 kG; 5-90K, 2.690(6) B.M. (θ=-11.1(2)K); 100-200K, 2.82(3) B.M. (θ=-22(3)K). At 40 kG; 7-100K, 2.699(8) B.M. (θ=-10.1(4)K); 100-280K, 2.985(6) B.M. (θ=-34.5(9)K).

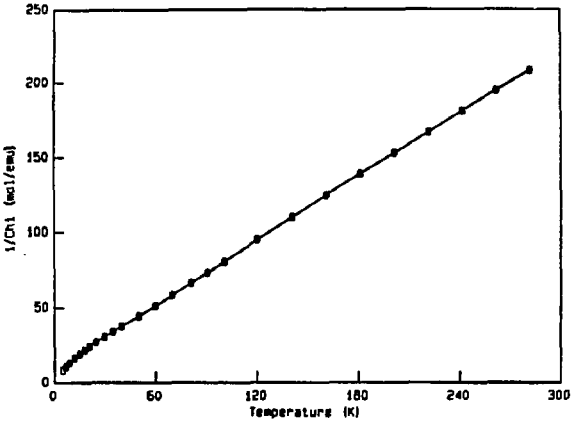

Figure 3-1. Plot of $1/\chi_M$ vs. T for $U[N(SiMe_3)_2]_3$ (5 kG)

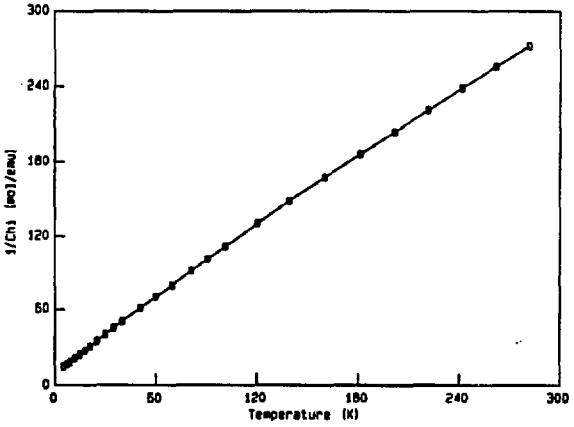

Figure 3-2. Plot of $1/\chi_M$ vs. T for $FU[N(SiMe_3)_2]_3$ (5 kG)

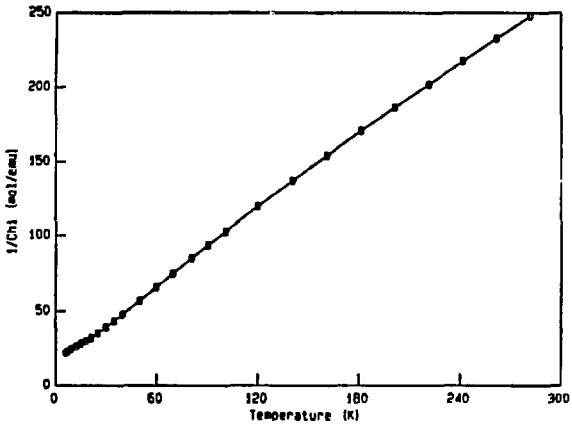

Figure 3-3. Plot of $1/\chi_M$ vs. T for $MeU[N(SiMe_3)_2]_3$ (5 kG)

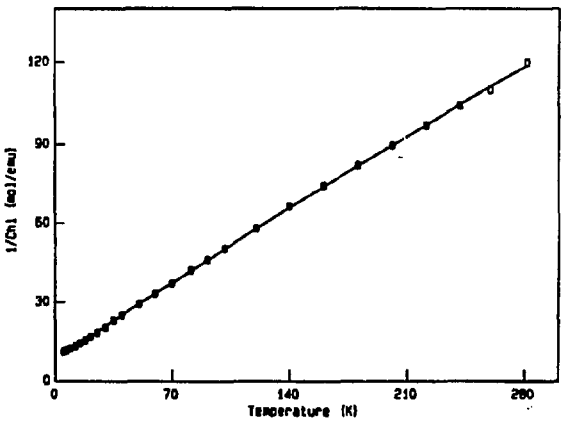

Figure 3-4. Plot of $1/\chi_M$ vs. T for $[U[N(SiMe_3)_2]_3)_2(\mu\text{-Te})$ (5 kG)

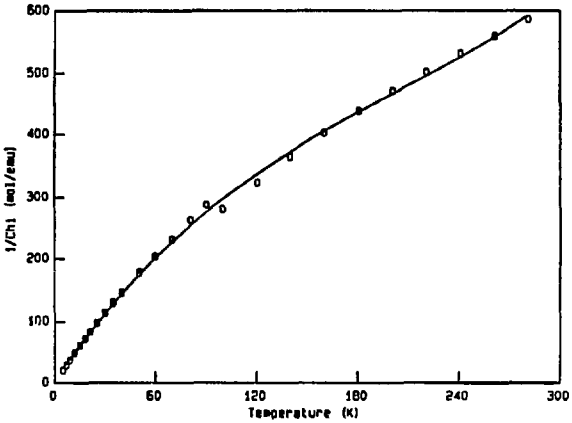

Figure 3-5. Plot of $1/\chi_M$ vs. T for $U[N(SiMe_3)_2]_3[N(p\text{-tolyl})]$ (5 kG)

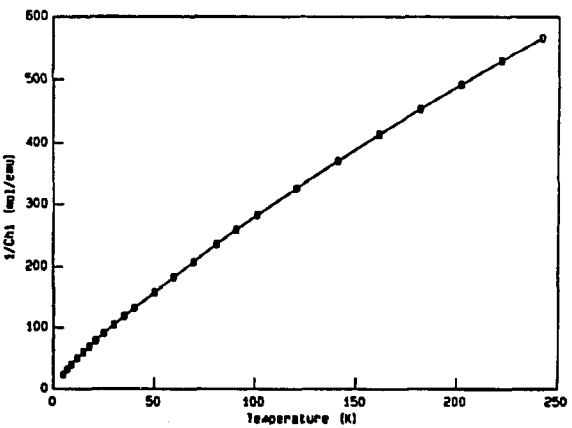

Figure 3-6. Plot of $1/\chi_M$ vs. T for $U[N(SiMe_3)_2]_3(NSiMe_3)$ (5 kG)

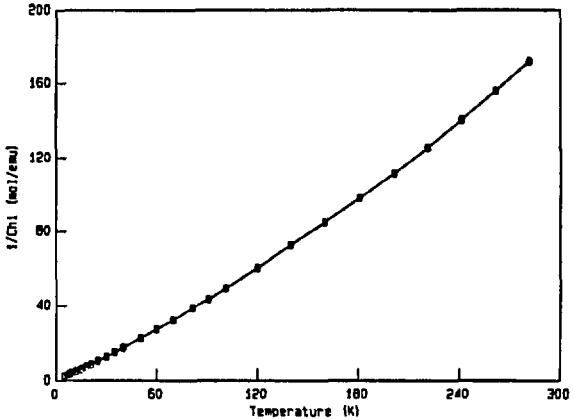

Figure 3-7. Plot of $1/\chi_M$ vs. T for $U_2[N(SiMe_3)_2]_4[\mu\text{-}N(p\text{-tolyl})]_2$

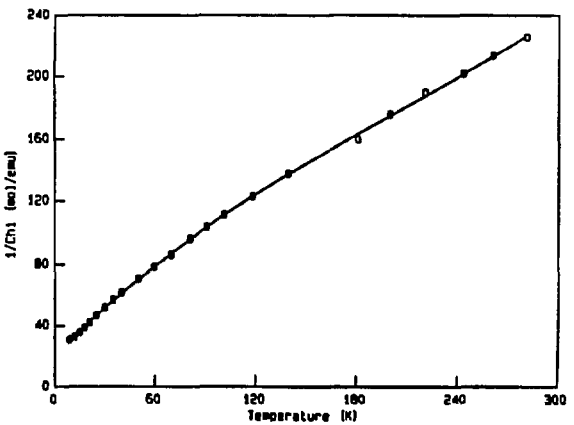

Figure 3-8. $1/\chi_M$ vs. T for $U_2[N(SiMe_3)_2]_4[\mu\text{-}N(H)(2,4,6\text{-}Me_3C_6H_2)]_2$

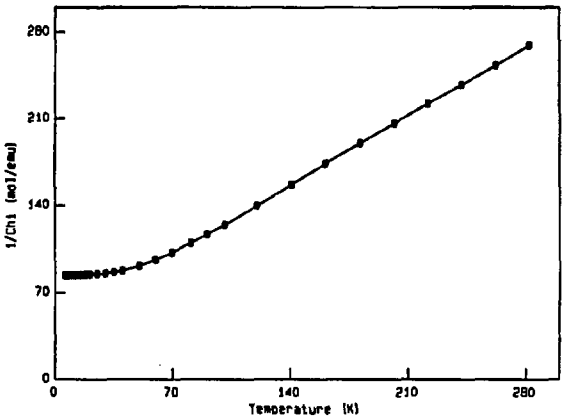

Figure 3-9. Plot of $1/\chi_M$ vs. T for MeU(tritox)$_3$ (5 kG)

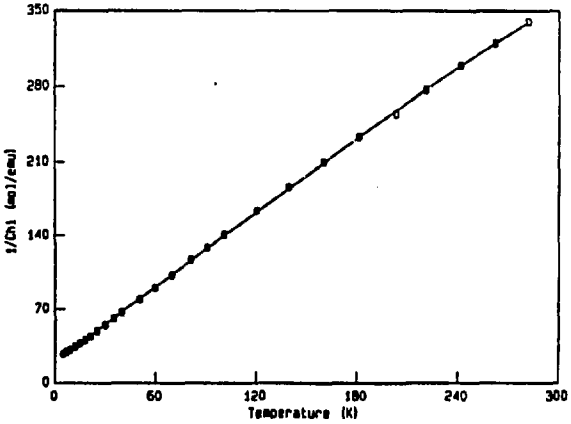

Figure 3-10. Plot of $1/\chi_M$ vs. T for U(ditox)$_4$ (5 kG)

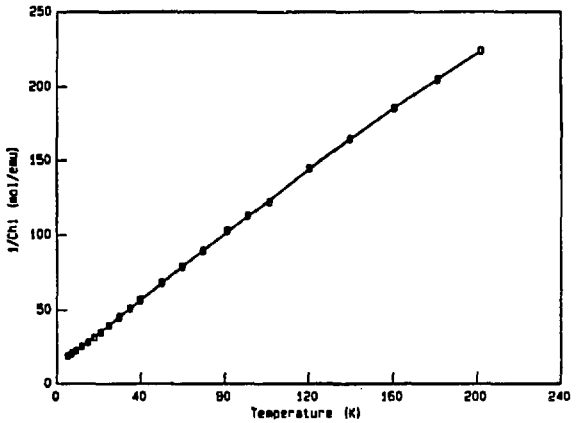

Figure 3-11. Plot of $1/\chi_M$ vs. T for $U(silox)_4$ (5 kG)

X-RAY CRYSTALLOGRAPHY EXPERIMENTAL SECTION

$U[N(SiMe_3)_2]_2I_3 \cdot 1/3(C_6H_{12})$

Deep purple crystals of the compound were obtained by slow cooling of a saturated cyclohexane solution to -15°C. Crystals of appropriate size were mounted in 0.3 mm thin-walled quartz capillaries in an inert-atmosphere glove box. The capillaries were removed from the box and flame sealed. Preliminary precession photographs indicated trigonal Laue symmetry and yielded preliminary cell dimensions.

The crystal used for data collection was of approximate dimensions 0.39 mm x 0.20 mm x 0.20 mm. It was transferred to an Enraf-Nonius CAD-4 diffractometer[10] and cooled to -110°C by a cold flow apparatus previously calibrated by a thermocouple placed at the sample position. The crystal was centered in the beam. Accurate cell dimensions and orientation matrix were determined by a least-squares fit to the setting angles of the unresolved MoKα components of 24 symmetry related reflections with 2θ between 24 and 30°. The search yielded the same Laue symmetry as the precession photographs and systematic absences indicated the space group to be either P31c or $P\bar{3}1c$. The normalized structure factor statistics suggested the choice of the acentric space group, however, a successful solution in the acentric group could not be achieved. A successful solution was found using the space group $P\bar{3}1c$. The final cell parameters and specific data collection parameters are given in Table I.

The 1886 raw intensity data were converted to structure factor amplitudes and their esds by correction for scan speed, background and Lorentz-polarization effects.[11-13] Inspection of the intensity standards showed no appreciable decay in intensity (1.4%) during data

collection. Inspection of the azimuthal scan data[14] showed a variation $I_{min}/I_{max} = 0.90$ for the average curve. An empirical correction for absorption, based on the azimuthal scan data, was applied to the intensities.[14] Removal of systematically absent data and averaging of redundant data left 905 unique data. The redundant data were averaged with an agreement factor, based on F_{obs}, of 1.5% for observed and accepted data and 3.9% for all data.

The structure was solved by Patterson methods and refined *via* standard least-squares and Fourier techniques. In a difference Fourier map calculated following refinement of all non-hydrogen atoms with anisotropic thermal parameters, peaks corresponding to the expected positions of all of the hydrogen atoms were found, as well as a large peak near the origin, *vide infra*. All hydrogens were included in the structure factor calculations in their expected positions based on idealized bonding geometry. All hydrogens were assigned isotropic thermal parameters 1.15 $Å^2$ larger than the equivalent B_{iso} of the atom to which they were bonded. None of the hydrogens were refined in least squares.

After the hydrogen atoms were included in the structure, a model for the electron density near the origin was developed. Hursthouse and Rodesiler found that $Fe[N(SiMe_3)_2]_3$ crystallized with a channel running down the z-axis that is large enough to accomodate a benzene molecule.[19b] Successful refinement of solvent molecules in the channel of any of the tris(bis(trimethylsilyl)amido)metal structures has not been achieved.[19] In this case, the large peak near the origin in the difference Fourier map was able to be refined with anisotropic thermal parameters as a carbon atom with 1/3 occupancy. The symmetry generated

positions gave reasonable bond lengths and angles that showed the atom to be part of a disordered cyclohexane ring. The hydrogen atoms of the cyclohexane molecule were not included. The thermal parameters showed the carbon atom to be severely anisotropic: B(1,1) = 4.7(6), B(2,2) = 3.7(5), B(3,3) = 19(1), with the motion (or disorder) in the z-direction. This model accounted nicely for the electron density found in the channel and the largest peaks in the final difference Fourier map are now associated with the uranium and are not found in the channel.

The final residuals for 55 variables refined against the 651 data for which $F_o^2 > 3\sigma(F_o^2)$ were R = 2.17%, R_w = 2.90% and GOF = 1.267. The R value for all data was 4.95%.

The quantity minimized by the least squares was $\Sigma w(|F_o|-|F_c|)^2$, where w is the weight of a given observation. The p-factor[15], used to reduce the weight of intense reflections, was set to 0.03 throughout the refinement. The analytical forms of the scattering factor tables for the neutral atoms[16] were used and all non-hydrogen scattering factors were corrected for both the real and imaginary components of anomalous dispersion.[17]

Inspection of the residuals ordered in ranges of $\sin(\theta/\lambda)$, $|F_o|$, and parity and value of the individual indices showed no unusual features or trends. A secondary extinction parameter was refined in the final cycles of least squares.[18] Seven reflections were rejected as "bad" data in the final refinement, based on their high values of $w \times \Delta^2$. The highest and lowest peaks in the final difference Fourier map had electron densities of 0.364 and -0.215 $e^{-1}/Å^3$, respectively, and were associated with the uranium atom.

Table I Crystal Data for $U[N(SiMe_3)_2]_3 \cdot 1/3(C_6H_{12})$ (-110±4°C)

Space Group	$P\bar{3}1c$
a, b, Å	16.370(2)
c, Å	8.302(1)
α, deg	90
β, deg	90
γ, deg	120
V, $Å^3$	1926.7(1)
Z	2
fw	719.20
d (calc.) g/cm^3	1.26
μ (calc.) 1/cm	41.88
radiation	MoKα (λ = 0.71073Å)
monochrometer	highly oriented graphite
scan range, type	$3° \leq 2\theta \leq 45°$, θ-2θ
scan speed, deg/min	0.84-6.7, variable
scan width, deg	$\Delta\theta = 0.60 + 0.35 \tan\theta$
reflections collected	1886; +h, +k, ±l
unique reflections	845
reflections, $F_o^2 > 3\sigma(F_o^2)$	654
R, %	2.17
R_w, %	2.90
R_{all}, %	4.95
GOF	1.267
g, e^{-2}	$1.7(3) \times 10^{-7}$
Largest Δ/σ in final least square cycle	0.02

Intensity Standards: 4, 4, -4; 11, -5, -1; -5, 11, 1; measured every hour of X-ray exposure time. Over the period of data collection there was a 1.4% decay in intensity.

Orientation Standards: 3 reflections were checked after every 100 measurements. Crystal orientation was redetermined if any of the reflections were offset from their predicted positions by more than 0.1°. Reorientation was required once throughout the data collection. The cell constants listed were determined at the end of data collection.

$U[N(SiMe_3)_2]I_3(OPPh_3)\cdot 1/2(C_7H_8)$

Deep purple crystals of the compound were obtained by slow cooling of a saturated toluene solution to -25°C. Crystals of appropriate size were mounted in 0.3 mm thin-walled quartz capillaries in an inert-atmosphere glove box. The capillaries were removed from the box and flame sealed. Preliminary precession photographs indicated triclinic Laue symmetry and yielded preliminary cell dimensions.

The crystal used for data collection was of approximate dimensions 0.34 mm x 0.28 mm x 0.25 mm. It was transferred to an Enraf-Nonius CAD-4 diffractometer[10] and cooled to -116°C by a cold flow apparatus previously calibrated by a thermocouple placed at the sample position. The crystal was centered in the beam. Accurate cell dimensions and orientation matrix were determined by a least-squares fit to the setting angles of the unresolved MoKα components of 24 symmetry related reflections with 2θ between 24 and 30°. The search yielded a different triclinic cell than the precession photographs, but did confirm the Laue symmetry. The final cell parameters and specific data collection parameters are given in the Table II.

The 6749 raw intensity data were converted to structure factor amplitudes and their esds by correction for scan speed, background and Lorentz-polarization effects.[11-13] Inspection of the intensity standards showed no appreciable decay in intensity (1.3%) during data collection. Inspection of the azimuthal scan data[14] showed a variation $I_{min}/I_{max} = 0.91$ for the average curve. An empirical correction for absorption, based on the azimuthal scan data, was applied to the intensities.[14] The data collected was a unique set.

The structure was solved by Patterson methods and refined via standard least-squares and Fourier techniques. In a difference Fourier map calculated following refinement of all non-hydrogen atoms with anisotropic thermal parameters, peaks corresponding to the expected positions of all of the hydrogen atoms were found, as well as several large peaks near the origin. All hydrogens were included in the structure factor calculations in their expected positions based on idealized bonding geometry. All hydrogens were assigned isotropic thermal parameters 1.3 $Å^2$ larger than the equivalent B_{iso} of the atom to which they were bonded. None of the hydrogens were refined in least squares. A secondary extinction parameter was refined in the final cycles of least squares.[18]

A Fourier map of the electron density near the origin indicated the presence of a severely disordered toluene molecule. The best model that was found entailed placing three carbon atoms (C19, C20, and C21) where the three largest peaks in the map were located and allowing their position and occupancy to refine. The isotropic thermal parameters of C20 and C21 were constrained to that of C19. The occupancy of each carbon refined to a value greater than one, which was expected due to the fact that the methyl carbon and all of the hydrogen atoms were not able to be included in the model. The largest peaks in the final difference Fourier are still found in the vicinity of the toluene.

The final residuals for 447 variables refined against the 5971 data for which $F_o^2 > 3\sigma(F_o^2)$ were R = 2.28%, R_w = 3.06% and GOF = 1.942. The R value for all data was 4.01%.

The quantity minimized by the least squares was $\Sigma w(|F_o| - |F_c|)^2$,

where w is the weight of a given observation. The p-factor[15], used to reduce the weight of intense reflections, was set to 0.02 in the final stages of refinement. The analytical forms of the scattering factor tables for the neutral atoms[16] were used and all non-hydrogen scattering factors were corrected for both the real and imaginary components of anomalous dispersion.[17]

Inspection of the residuals ordered in ranges of $\sin(\theta/\lambda)$, $|F_o|$, and parity and value of the individual indices showed no unusual features or trends. Several reflections showed anomalously high values of $w \times \Delta^2$, possibly due to multiple reflections. Twenty reflections were rejected prior to the final refinement for this reason. The largest peaks in the final difference Fourier map had electron density of 1.203 and 1.096 $e^{-1}/\text{Å}^3$ and were associated with the disordered toluene molecule.

Table II Crystal Data for $U[N(SiMe_3)_2]_3(OPPh_3)\cdot 1/2(C_7H_8)$ (-116±4°C)

Space Group	$P\bar{1}$
a, Å	12.340(2)
b, Å	12.424(2)
c, Å	19.824(3)
α, deg	100.12(1)
β, deg	93.00(1)
γ, deg	118.91(1)
V, $Å^3$	2580( )
Z	2
fw	997.49
d (calc.) g/cm^3	1.28
μ (calc.) 1/cm	31.69
radiation	MoKα (λ = 0.71073Å)
monochrometer	highly oriented graphite
scan range, type	$3° \leq 2\theta \leq 45°$, θ-2θ
scan speed, deg/min	0.84-6.7, variable
scan width, deg	$\Delta\theta = 0.60 + 0.35 \tan\theta$
reflections collected	6749, +h, ±k, ±l
unique reflections	6749
reflections, $F_o^2 > 3\sigma(F_o^2)$	5991
R, %	2.28
R_w, %	3.06
R_{all}, %	4.01
GOF	1.942
g, e^{-2}	$9.4(9) \times 10^{-8}$
Largest Δ/σ in final least square cycle	0.16

Intensity Standards: 1, -3, -11; 2, -8, 3; -8, 3, 4; measured every hour of X-ray exposure time. Over the period of data collection there was a 1.3% decay in intensity.

Orientation Standards: 3 reflections were checked after every 100 measurements. Crystal orientation was redetermined if any of the reflections were offset from their predicted positions by more than 0.1°. Reorientation was required three times throughout the data collection. The cell constants listed were determined at the end of data collection.

U[N(SiMe$_3$)$_2$]$_3$[N(p-tolyl)]

Black crystals of the compound were obtained by slow cooling of a pentane solution from room temperature to -15°C. Crystals of appropriate size were mounted in 0.3 mm thin-walled quartz capillaries in an inert-atmosphere glove box. The capillaries were removed from the box and flame sealed. Preliminary precession photographs indicated triclinic Laue symmetry, and the space group $P\bar{1}$ was confirmed by subsequent solution and refinement of the structure.

The crystal used for data collection was of approximate dimensions 0.38 mm x 0.30 mm x 0.21 mm. It was transferred to an Enraf-Nonius CAD-4 diffractometer[10] and cooled to -82°C by a cold flow apparatus previously calibrated by a thermocouple placed at the sample position. The crystal was centered in the beam. Accurate cell dimensions and orientation matrix were determined by a least-squares fit to the setting angles of the unresolved MoKα components of 24 symmetry related reflections with 2θ between 24 and 30°. The search yielded the same unit cell as the precession photographs and confirmed the Laue symmetry. The final cell parameters and specific data collection parameters are given in Table III.

The 5210 raw intensity data were converted to structure factor amplitudes and their esds by correction for scan speed, background and Lorentz-polarization effects.[11-13] Inspection of the intensity standards showed no appreciable decay in intensity during data collection. Inspection of the azimuthal scan data[14] showed a variation $I_{min}/I_{max} = 0.58$ for the average curve. An empirical correction for absorption, based on the azimuthal scan data, was applied to the

intensities.[14] Removal of redundant data left 4994 unique data.

The structure was solved by Patterson methods and refined via standard least-squares and Fourier techniques. In a difference Fourier map calculated following refinement of all non-hydrogen atoms with anisotropic thermal parameters, peaks corresponding to the expected positions of all of the hydrogen atoms were found. All hydrogens were included in the structure factor calculations in their expected positions based on idealized bonding geometry. All hydrogens were assigned isotropic thermal parameters 1.3 $Å^2$ larger than the equivalent B_{iso} of the atom to which they were bonded. None of the hydrogens were refined in least squares. A secondary extinction parameter was refined in the final cycles of least squares.[18] Some of the data that was collected just prior to a reorientation appeared to be too low in intensity as evidenced by a large negative Δ. The weights of the worst 91 reflections as determined by a large negative Δ were set to zero.

The final residuals for 326 variables refined against the 4411 data for which $F_o^2 > 3\sigma(F_o^2)$ were R = 3.20%, R_w = 4.52% and GOF = 2.296. The R value for all data was 6.57%.

The quantity minimized by the least squares was $\Sigma w(|F_o|-|F_c|)^2$, where w is the weight of a given observation. The p-factor[15], used to reduce the weight of intense reflections, was set to 0.03 throughout the refinement. The analytical forms of the scattering factor tables for the neutral atoms[16] were used and all non-hydrogen scattering factors were corrected for both the real and imaginary components of anomalous dispersion.[17]

Inspection of the residuals ordered in ranges of $\sin(\theta/\lambda)$, $|F_o|$, and parity and value of the individual indices showed no unusual

features or trends. The highest and lowest peaks in the final difference Fourier map had electron densities of 1.44 and -1.00 $e^{-1}/Å^3$, respectively, and were associated with the uranium atom.

Table III Crystal Data for $U[N(SiMe_3)_2]_3[N(p\text{-tolyl})]$ (-82±4°C)

Space Group	$P\bar{1}$
a, Å	11.425(2)
b, Å	11.978(2)
c, Å	14.081(3)
α, deg	94.69(2)
β, deg	89.98(2)
γ, deg	90.50(2)
V, $Å^3$	1920(1)
Z	2
fw	824.34
d (calc.) g/cm^3	1.425
μ (calc.) 1/cm	42.10
radiation	MoKα (λ = 0.71073Å)
monochrometer	highly oriented graphite
scan range, type	$3° \leq 2\theta \leq 45°$, θ-2θ
scan speed, deg/min	0.84-6.7, variable
scan width, deg	$\Delta\theta = 0.65 + 0.35 \tan\theta$
reflections collected	5210; ±h, +k, ±l
unique reflections	4994
reflections, $F_o^2 > 3\sigma(F_o^2)$	4502
R, %	3.20
R_w, %	4.52
R_{all}, %	6.57
GOF	2.296
g, e^{-2}	$1.5(2) \times 10^{-7}$
Largest Δ/σ in final least square cycle	0.01

Intensity Standards: 7, -2, -3; 4, 6, -5; 0, 5, -8; measured every hour of X-ray exposure time. Over the period of data collection there was a 1.5% decay in intensity.

Orientation Standards: 3 reflections were checked after every 100 measurements. Crystal orientation was redetermined if any of the reflections were offset from their predicted positions by more than 0.1°. Reorientation was required sixteen times during data collection and the cell constants listed were determined at the end of data collection.

U[N(SiMe$_3$)$_2$]$_3$(NSiMe$_3$)

Black crystals of the compound were obtained by slow cooling of a saturated pentane solution. Crystals of appropriate size were mounted in 0.3 mm thin-walled quartz capillaries in an inert-atmosphere glove box. The capillaries were removed from the box and flame sealed. Preliminary precession photographs indicated rhombohedral Laue symmetry and yielded preliminary cell dimensions.

The crystal used for data collection was of approximate dimensions 0.30 mm x 0.20 mm x 0.18 mm. It was transferred to an Enraf-Nonius CAD-4 diffractometer[10] and cooled to -117°C by a cold flow apparatus previously calibrated by a thermocouple placed at the sample position. The crystal was centered in the beam. Accurate cell dimensions and orientation matrix were determined by a least-squares fit to the setting angles of the unresolved MoKα components of 24 symmetry related reflections with 2θ between 24 and 30°. The search yielded the rhombohedral reduced primitive cell. This was converted to the coventional hexagonal for ease of data collection, and all resulrs are reported with respect to the hexagonal cell. The final cell parameters and specific data collection parameters are given in Table IV.

The 1837 raw intensity data were converted to structure factor amplitudes and their esds by correction for scan speed, background and Lorentz-polarization effects.[11-13] Inspection of the intensity standards showed no decay in intensity during data collection. Inspection of the azimuthal scan data[14] showed a variation I_{min}/I_{max} = 0.91 for the average curve. An empirical correction for absorption, based on the azimuthal scan data, was applied to the intensities.[14]

Removal of the systematically absent data left 1639 unique data.

The structure was solved by Patterson methods and refined via standard least-squares and Fourier techniques. The assumption that the space group was acentric was confirmed by the successful solution and refinement of the structure. The test for the correct enantiomer of this crystal resulted in a change in the R-value from 1.9 to 5.8 percent. The original enantiomer was used for the rest of the analysis. In a difference Fourier map calculated following refinement of all non-hydrogen atoms with anisotropic thermal parameters, peaks corresponding to the expected positions of all of the hydrogen atoms were found. All hydrogens were included in the structure factor calculations in their expected positions based on idealized bonding geometry. All hydrogens were assigned isotropic thermal parameters 1.3 $Å^2$ larger than the equivalent B_{iso} of the atom to which they were bonded. None of the hydrogens were refined in least squares. A secondary extinction parameter was refined in the final cycles of least squares.[18]

The final residuals for 100 variables refined against the 1639 data for which $F_o^2 > 3\sigma(F_o^2)$ were R = 1.80%, wR = 2.38% and GOF = 1.284. The R value for all data was 3.46%.

The quantity minimized by the least squares was $\Sigma w(|F_o|-|F_c|)^2$, where w is the weight of a given observation. The p-factor[15], used to reduce the weight of intense reflections, was set to 0.03 throughout the refinement. The analytical forms of the scattering factor tables for the neutral atoms[16] were used and all non-hydrogen scattering factors were corrected for both the real and imaginary components of anomalous dispersion.[17]

Inspection of the residuals ordered in ranges of $\sin(\theta/\lambda)$, $|F_o|$, and parity and value of the individual indexes showed no unusual features or trends. One reflection showed an anomalously high value of $w \times \Delta^2$, and was rejected prior to the final refinement. Two low-angle reflections appeared to be "over-corrected" for extinction, based on an anomalously high ratio of $F_{obs.}$ to $F_{calc.}$, and also were rejected prior to the final refinement. The highest and lowest peaks in the final difference Fourier map had electron densities of 0.581 and -0.218 $e^{-1}/\text{Å}^3$, respectively, and were on the three-fold axis near uranium.

Table IV. Crystal Data for $U[N(SiMe_3)_2]_3(NSiMe_3)$ (117±3°C)

Space Group	R3c
a, b, Å	17.464(2)
c, Å	21.467(2)
α, deg	90
β, deg	90
γ, deg	120
V, $Å^3$	5670(2)
Z	6
fw	806.40
d (calc.) g/cm^3	1.42
μ (calc.) 1/cm	43.06
radiation	MoKα (λ = 0.71073Å)
monochrometer	highly oriented graphite
scan range, type	$3° \leq 2\theta \leq 45°$, θ-2θ
scan speed, deg/min	0.84-6.7, variable
scan width, deg	$\Delta\theta = 0.65 + 0.35 \tan\theta$
reflections collected	1837; +h, +k, ±l
unique reflections	1639
reflections, $F_o^2 > 3\sigma(F_o^2)$	1359
R, %	1.80
R_w, %	2.38
R_{all}, %	3.46
GOF	1.284
g, e^{-2}	$4.5(2) \times 10^{-7}$
Largest Δ/σ in final least square cycle	2.09

Intensity Standards: 5, 2, 12; 11, -9, 2; -2, 11, 2; measured every hour of x-ray exposure time. There was no decay in intensity over the period of data collection.

Orientation Standards: 3 reflections were checked after every 100 measurements. Crystal orientation was redetermined if any of the reflections were offset from their predicted positions by more than 0.1 . Reorientation was required once throughout the data collection. The cell constants listed were determined at the end of data collection.

$U[N(SiMe_3)_2]_2I_3[NH(p\text{-}tolyl)]$

Pale gold crystals of the compound were obtained by slow cooling of a hexane solution from room temperature to -15°C. Crystals of appropriate size were mounted in 0.3 mm thin-walled quartz capillaries in an inert-atmosphere glove box. The capillaries were removed from the box and flame sealed. Preliminary precession photographs indicated triclinic Laue symmetry, and the space group $P\bar{1}$ was confirmed by subsequent solution and refinement of the structure.

The crystal used for data collection was of approximate dimensions 0.34 mm x 0.21 mm x 0.12 mm. It was transferred to an Enraf-Nonius CAD-4 diffractometer[10] and cooled to -75°C by a cold flow apparatus previously calibrated by a thermocouple placed at the sample position. The crystal was centered in the beam. Accurate cell dimensions and orientation matrix were determined by a least-squares fit to the setting angles of the unresolved MoKα components of 24 symmetry related reflectons with 2θ between 24 and 30°. The search yielded the same unit cell as the precession photographs and confirmed the Laue symmetry. The final cell parameters and specific data collection parameters are given in Table V.

The 5150 raw intensity data were converted to structure factor amplitudes and their esds by correction for scan speed, background and Lorentz-polarization effects.[11-13] Inspection of the intensity standards showed no appreciable decay in intensity (<1.0%) during data collection. Inspection of the azimuthal scan data[14] showed a variation $I_{min}/I_{max} = 0.71$ for the average curve. An analytical correction for absorption using the measured size and indexed faces of the crystal and

a 12 x 24 x 6 gaussian grid of internal points was performed after the solution of the structure had confirmed the stoichiometry of the molecule.[14] The maximum and minimum transmission factors were 0.623 and 0.442, respectively. Removal of redundant data left 5020 unique data.

The structure was solved by Patterson methods and refined *via* standard least-squares and Fourier techniques. In a difference Fourier map calculated following refinement of all non-hydrogen atoms with anisotropic thermal parameters, peaks corresponding to the expected positions of all of the hydrogen atoms were found. All hydrogens, except the unique amido-hydrogen, were included in the structure factor calculations in their expected positions based on idealized bonding geometry. All hydrogens were assigned isotropic thermal parameters 1.3 $Å^2$ larger than the equivalent B_{iso} of the atom to which they were bonded. None of the hydrogens were refined in least squares. The amido-hydrogen was placed in its observed position and the N-H bond length was adjusted to 0.85 Å. Attempts to refine the amido-hydrogen with an anisotropic thermal parameter were unsuccsssful.

The final residuals for 326 variables refined against the 4649 data for which $F_o^2 > 3\sigma(F_o^2)$ were R = 1.55%, R_w = 2.13% and GOF = 1.482. The R value for all data was 2.17%.

The quantity minimized by the least squares was $\Sigma w(|F_o|-|F_c|)^2$, where w is the weight of a given observation. The p-factor[15], used to reduce the weight of intense reflections, was set to 0.02 in the final refinement. The analytical forms of the scattering factor tables for the neutral atoms[16] were used and all non-hydrogen scattering factors were corrected for both the real and imaginary components of anomalous

dispersion.[17]

Inspection of the residuals ordered in ranges of $\sin(\theta/\lambda)$, $|F_o|$, and parity and value of the individual indices showed no unusual features or trends. A secondary extinction parameter was refined in the final cycles of least squares.[18] The highest and lowest peaks in the final difference Fourier map had electron densities of 0.632 and -0.375 $e^{-1}/Å^3$, respectively, and were associated with the uranium atom.

Table V Crystal Data for $U[N(SiMe_3)_2]_3[NH(p\text{-tolyl})]$ (-108±4°C)

Space Group	$P\bar{1}$
a, Å	11.506(2)
b, Å	12.035(2)
c, Å	13.987(3)
α, deg	94.77(2)
β, deg	91.13(2)
γ, deg	90.09(1)
V, $Å^3$	1929(1)
Z	2
fw	825.35
d (calc.) g/cm^3	1.4
μ (calc.) 1/cm	41.90
radiation	MoKα (λ = 0.71073Å)
monochrometer	highly oriented graphite
scan range, type	$3° \leq 2\theta \leq 45°$, θ-2θ
scan speed, deg/min	0.84-6.7, variable
scan width, deg	$\Delta\theta = 0.65 + 0.35 \tan\theta$
reflections collected	5150; ±h, +k, ±l
unique reflections	5020
reflections, $F_o^2 > 3\sigma(F_o^2)$	4649
R, %	1.55
R_w, %	2.13
R_{all}, %	2.17
GOF	1.48
g, e^{-2}	$8.8(8) \times 10^{-8}$
Largest Δ/σ in final least square cycle	0.02

Intensity Standards: 2, 3, -9; 0, 8, 0; 8, -1, -2; measured every one hour of X-ray exposure time. Over the period of data collection there was a negligible decay in intensity (<1%).

Orientation Standards: 3 reflections were checked after every 100 measurements. Crystal orientation was redetermined if any of the reflections were offset from their predicted positions by more than 0.1°. Reorientation was required once during data collection and the cell constants listed were those determined at the end of data collection.

$U_2[N(SiMe_3)_2]_4[\mu\text{-}N(H)(2,4,6\text{-}Me_3C_6H_2)]_2$

Deep blue crystals of the compound were obtained by slow diffusion of a pentane solution of 2,4,6-trimethylaniline with a pentane solution of $U[N(SiMe_3)_2]_3$. Crystals of appropriate size were mounted in 0.3 mm thin-walled quartz capillaries in an inert-atmosphere glove box. The capillaries were removed from the box and flame sealed. Preliminary precession photographs indicated monoclinic Laue symmetry and yielded preliminary cell dimensions. Systematic absences were consistent with the space group $P2_1/n$.

The crystal used for data collection was of approximate dimensions 0.39 mm x 0.34 mm x 0.16 mm. It was transferred to an Enraf-Nonius CAD-4 diffractometer[10] and cooled to -75°C by a cold flow apparatus previously calibrated by a thermocouple placed at the sample position. The crystal was centered in the beam. Accurate cell dimensions and orientation matrix were determined by a least-squares fit to the setting angles of the unresolved MoKα components of 24 symmetry related reflections with 2θ between 24 and 30°. The search yielded the same unit cell as the precession photographs and confirmed the Laue symmetry. The final cell parameters and specific data collection parameters are given in Table VI.

The 4351 raw intensity data were converted to structure factor amplitudes and their esds by correction for scan speed, background and Lorentz-polarization effects.[11-13] Inspection of the intensity standards showed no appreciable decay in intensity (1.7%) during data collection. Inspection of the azimuthal scan data[14] showed a variation $I_{min}/I_{max} = 0.48$ for the average curve. An analytical absorption

correction using the measured size and indexed faces of the crystal and a 12 x 14 x 12 gaussian grid of internal points was performed after the solution of the structure had confirmed the stoichiometry of the molecule.[14] The maximum and minimum transmission factors were 0.244 and 0.497 respectively. Removal of redundant and systematically absent data left 3932 unique data.

The structure was solved by Patterson methods and refined via standard least-squares and Fourier techniques. In a difference Fourier map calculated following refinement of all non-hydrogen atoms with anisotropic thermal parameters, peaks corresponding to the expected positions of all of the hydrogen atoms were found. All hydrogens, except the unique amido-hydrogen, were included in the structure factor calculations in their expected positions based on idealized bonding geometry. All hydrogens were assigned isotropic thermal parameters 1.3 $Å^2$ larger than the equivalent B_{iso} of the atom to which they were bonded. None of the hydrogens were refined in least squares. The amido-hydrogen was placed in its observed position and the N-H bond length was adjusted to 0.87 Å. Attempts to refine the amido-hydrogen with an isotropic thermal parameter were unsuccessful.

The final residuals for 263 variables refined against the 3353 data for which $F_o^2 > 3\sigma(F_o^2)$ were R = 1.98%, R_w = 2.55% and GOF = 1.695. The R value for all data was 3.48%.

The quantity minimized by the least squares was $\Sigma w(|F_o|-|F_c|)^2$, where w is the weight of a given observation. The p-factor[15], used to reduce the weight of intense reflections, was set to 0.02 in the final refinement. The analytical forms of the scattering factor tables for the neutral atoms[16] were used and all non-hydrogen scattering factors

were corrected for both the real and imaginary components of anomalous dispersion.[17]

Inspection of the residuals ordered in ranges of $\sin(\theta/\lambda)$, $|F_o|$, and parity and value of the individual indexes showed no unusual features or trends. A secondary extinction parameter was refined in the final cycles of least squares.[18] The weight of one reflection was set to zero for the final refinement based on its anomalously high value of $w \times \Delta^2$. The highest and lowest peaks in the final difference Fourier map had electron densities of 0.630 and -0.922 $e^{-1}/\text{Å}^3$, respectively, and were associated with the uranium atom.

Table VI Crystal Data for $U_2[N(SiMe_3)_2]_4[\mu\text{-}N(H)(2,4,6\text{-}Me_3C_6H_2)]_2$ (-75±4°C)

Space Group	$P2_1/n$
a, Å	16.997(1)
b, Å	11.854(1)
c, Å	15.121(1)
α, deg	90
β, deg	99.10(1)
γ, deg	90
V, Å^3	3008(4)
Z	2
fw	1386.02
d (calc.) g/cm^3	1.53
μ (calc.) 1/cm	52.85
radiation	MoKα (λ = 0.71073Å)
monochrometer	highly oriented graphite
scan range, type	$3° \leq 2\theta \leq 45°$, θ-2θ
scan speed, deg/min	0.84-6.7, variable
scan width, deg	$\Delta\theta = 0.65 + 0.35 \tan\theta$
reflections collected	4351; ±h, +k, +l
unique reflections	3932
reflections, $F_o^2 > 3\sigma(F_o^2)$	3352
R, %	1.98
R_w, %	2.55
R_{all}, %	3.48
GOF	1.695
g, e^{-2}	$1.30(3) \times 10^{-7}$
Largest Δ/σ in final least square cycle	0.01

Intensity Standards: -1, 8, -1; 4, 4, -9; -12, 1, -1; measured hour of X-ray exposure time. Over the period of data collection there was a 1.7% decay in intensity.

Orientation Standards: 3 reflections were checked after every 100 measurements. Crystal orientation was redetermined if any of the reflections were offset from their predicted positions by more than 0.1°. Reorientation was required seven times throughout the data collection. The cell constants listed were determined at the end of data collection.

$U_2[N(SiMe_3)_2]_2I_4[\mu\text{-}N(p\text{-}tolyl)]_2$

Red crystals of the compound were obtained by slow cooling of a saturated hexane solution from room temperature to -25°C. Crystals of appropriate size were mounted in 0.3 mm thin-walled quartz capillaries in an inert-atmosphere glove box. The capillaries were removed from the box and flame sealed. Preliminary precession photographs indicated triclinic Laue symmetry, and the space group $P\bar{1}$ was confirmed by subsequent solution and refinement of the structure.

The crystal used for data collection was of approximate dimensions 0.45 mm x 0.32 mm x 0.21 mm. It was transferred to an Enraf-Nonius CAD-4 diffractometer[10] and cooled to -118°C by a cold flow apparatus previously calibrated by a thermocouple placed at the sample position. The crystal was centered in the beam. Accurate cell dimensions and orientation matrix were determined by a least-squares fit to the setting angles of the unresolved MoKα components of 24 symmetry related reflections with 2θ between 24 and 30°. The search yielded the same unit cell as the precession photographs and confirmed the Laue symmetry. The final cell parameters and specific data collection parameters are given in Table VII.

The 3896 raw intensity data were converted to structure factor amplitudes and their esds by correction for scan speed, background and Lorentz-polarization effects.[11-13] Inspection of the intensity standards showed no appreciable decay in intensity (<1.0%) during data collection. Inspection of the azimuthal scan data[14] showed a variation $I_{min}/I_{max} = 0.62$ for the average curve. An empirical correction for absorption, based on the azimuthal scan data, was applied to the

intensities.[14] Removal of redundant data left 3696 unique data.

The structure was solved by Patterson methods and refined via standard least-squares and Fourier techniques. In a difference Fourier map calculated following refinement of all non-hydrogen atoms with anisotropic thermal parameters, peaks corresponding to the expected positions of all of the hydrogen atoms were found. All hydrogens were included in the structure factor calculations in their expected positions based on idealized bonding geometry. All hydrogens were assigned isotropic thermal parameters 1.3 $Å^2$ larger than the equivalent B_{iso} of the atom to which they were bonded. None of the hydrogens were refined in least squares.

The final residuals for 245 variables refined against the 3451 data for which $F_o^2 > 3\sigma(F_o^2)$ were R = 1.83%, R_w = 2.77% and GOF = 1.580. The R value for all data was 2.24%.

The quantity minimized by the least squares was $\Sigma w(|F_o|-|F_c|)^2$, where w is the weight of a given observation. The p-factor[15], used to reduce the weight of intense reflections, was set to 0.03 throughout the refinement. The analytical forms of the scattering factor tables for the neutral atoms[16] were used and all non-hydrogen scattering factors were corrected for both the real and imaginary components of anomalous dispersion.[17]

Inspaction of the residuals ordered in ranges of $\sin(\theta/\lambda)$, $|F_o|$, and parity and value of the individual indexes showed no unusual features or trends. A secondary extinction parameter was refined in the final cycles of least squares.[18] The highest and lowest peaks in the final difference Fourier map had electron densities of 0.771 and -0.632 $e^{-1}/Å^3$, respectively, and were associated with the uranium atom.

Table VII Crystal Data for $U_2[N(SiMe_3)_2]_4[\mu\text{-}N(p\text{-tolyl})]_2$ (-118±4°C)

Space Group	$P\bar{1}$
a, Å	9.792(1)
b, Å	12.212(1)
c, Å	14.580(3)
α, deg	62.00(1)
β, deg	65.86(1)
γ, deg	80.80(1)
V, $Å^3$	1403.5(2)
Z	2
fw	1327.90
d (calc.) g/cm^3	1.571
μ (calc.) 1/cm	56.61
radiation	MoKα (λ = 0.71073Å)
monochrometer	highly oriented graphite
scan range, type	$3° \leq 2\theta \leq 45°$, θ-2θ
scan speed, deg/min	0.84-6.7, variable
scan width, deg	$\Delta\theta = 0.65 + 0.35 \tan\theta$
reflections collected	3896; ±h, +k, ±l
unique reflections	3696
reflections, $F_o^2 > 3\sigma(F_o^2)$	3451
R, %	1.83
R_w, %	2.77
R_{all}, %	2.24
GOF	1.580
g, e^{-2}	$4.6(1) \times 10^{-7}$
Largest Δ/σ in final least square cycle	0.01

Intensity Standards: -6, -2, -7; -2, -7, -9; -2, -8, -3; measured hour of X-ray exposure time. Over the period of data collection there was a negligible decay in intensity (<1.0%).

Orientation Standards: 3 reflections were checked after every 100 measurements. Crystal orientation was redetermined if any of the reflections were offset from their predicted positions by more than 0.1 . Reorientation was required three times during data collection. The cell constants listed were determined at the end of data collection.

$UMe[OC(t\text{-}Bu)_3]_3$

Pale pinkish-yellow crystals of the compound were obtained by slow crystallization from toluene. Crystals of appropriate size were mounted in 0.3 mm thin-walled quartz capillaries in an inert-atmosphere glove box. The capillaries were removed from the box and flame sealed. Preliminary precession photographs indicated primitive Laue symmetry and yielded preliminary cell dimensions.

The crystal used for data collection was of approximate dimensions 0.35 mm x 0.25 mm x 0.22 mm. It was transferred to an Enraf-Nonius CAD-4 diffractometer[10] and cooled to -85°C by a cold flow apparatus previously calibrated by a thermocouple placed at the sample position. The crystal was centered in the beam. Automatic peak search and indexing procedures yielded the same unit cell as the precession photographs and confirmed the Laue symmetry. The final cell parameters and specific data collection parameters are given in Table VIII.

The 5874 raw intensity data were converted to structure factor amplitudes and their esds by correction for scan speed, background and Lorentz-polarization effects.[11-13] Inspection of the intensity standards showed a slow isotropic decrease of 6.8% of the original intensity. The data were corrected for this decay. Inspection of the azimuthal scan data[14] showed a variation $I_{min}/I_{max} = 0.90$ for the average curve. An empirical correction for absorption, based on the azimuthal scan data, was applied to the intensities.[14] Removal of redundant and systematically absent data left 5339 unique data.

The structure was solved by Patterson methods and refined *via* standard least-squares and Fourier techniques. In a difference Fourier

map calculated following refinement of all non-hydrogen atoms with anisotropic thermal parameters, peaks corresponding to the expected positions of most of the hydrogen atoms were found. All hydrogens were included in the structure factor calculations in their expected positions based on idealized bonding geometry. All hydrogens were assigned isotropic thermal parameters 1.3 $Å^2$ larger than the equivalent B_{iso} of the atom to which they were bonded. None of the hydrogens were refined in least squares. A secondary extinction parameter was refined in the final cycles of least squares.[18] Some reflections were affected by a small amount of twinning and the weights of the worst 300 reflections, as determined by the quantity $w \times \Delta^2$, were set to zero.

The final residuals for 398 variables refined against the 4222 data for which $F_o^2 > 3\sigma(F_o^2)$ were R = 3.19%, R_w = 4.22% and GOF = 2.130. The R value for all data was 5.60%.

The quantity minimized by the least squares was $\Sigma w(|F_o|-|F_c|)^2$, where w is the weight of a given observation. The p-factor[15], used to reduce the weight of intense reflections, was set to 0.03 throughout the refinement. The analytical forms of the scattering factor tables for the neutral atoms[16] were used and all non-hydrogen scattering factors were corrected for both the real and imaginary components of anomalous dispersion.[17]

Inspection of the residuals ordered in ranges of $\sin(\theta/\lambda)$, $|F_o|$, and parity and value of the individual indexes showed no unusual features or trends. The largest peak in the final difference Fourier map had electron density of 2.363 $e^{-1}/Å^3$ and was associated with the uranium atom.

Table VIII Crystal Data for $UMe[OC(t\text{-}Bu)_3]_3$ (-85±4°C)

Space Group	$P2_1/c$
a, Å	21.077(2)
b, Å	12.368(1)
c, Å	16.634(2)
γ, deg	90
β, deg	109.11(1)
γ, deg	90
V, $Å^3$	4097(1)
Z	4
fw	851.14
d (calc.) g/cm^3	1.380
μ (calc.) 1/cm	37.87
radiation	MoKα (λ = 0.71073Å)
monochrometer	highly oriented graphite
scan range, type	$3° \leq 2\theta \leq 45°$, θ-2θ
scan speed, deg/min	0.84-6.7, variable
scan width, deg	$\Delta\theta = 0.65 + 0.35 \tan\theta$
reflections collected	5874; ±h, +k, +l
unique reflections	5339
reflections, $F_o^2 > 3\sigma(F_o^2)$	4706
R, %	3.19
R_w, %	4.22
R_{all}, %	5.60
GOF	1.70
g, e^{-2}	$6.2(6) \times 10^{-8}$
Largest Δ/σ in final least-squares cycle	0.01

Intensity Standards: 14, 1, -5; 4, 8, 2; 7, 2, -11; measured every two hours of X-ray exposure time. Over the period of data collection there was a 6.8% decay in intensity. A linear decay correction was applied to the raw data.

Orientation Standards: 3 reflections were checked after every 250 measurements. Crystal orientation was redetermined if any of the reflections were offset from their predicted positions by more than 0.1°. Reorientation was required once during data collection. The cell constants and errors are given as their final values.

{UMe[OCH(t-Bu)$_2$]$_4$}Li

Purple crystals of the compound were obtained by slow crystallization from toluene. Crystals of appropriate size were mounted in 0.3 mm thin-walled quartz capillaries in an inert-atmosphere glove box. The capillaries were removed from the box and flame sealed. Preliminary precession photographs indicated primitive Laue symmetry and yielded preliminary cell dimensions.

The crystal used for data collection was of approximate dimensions 0.20 mm x 0.20 mm x 0.30 mm. It was transferred to an Enraf-Nonius CAD-4 diffractometer[10] and cooled to -75°C by a cold flow apparatus previously calibrated by a thermocouple placed at the sample position. The crystal was centered in the beam. Automatic peak search and indexing procedures yielded the same unit cell as the precession photographs and confirmed the Laue symmetry. The final cell parameters and specific data collection parameters are given in Table IV.

The 5989 raw intensity data were converted to structure factor amplitudes and their esds by correction for scan speed, background and Lorentz-polarization effects.[11-13] Inspection of the intensity standards showed a slow isotropic decrease of 8.4% of the original intensity. The data were corrected for this decay. Inspection of the azimuthal scan data[14] showed a variation $I_{min}/I_{max} = 0.85$ for the average curve. An empirical correction for absorption, based on the azimuthal scan data, was applied to the intensities.[14] Removal of systematically absent data left 5438 unique data.

The structure was solved by Patterson methods and refined *via* standard least-squares and Fourier techniques. In a difference Fourier map calculated following refinement of all non-hydrogen atoms with

anisotropic thermal parameters, peaks corresponding to the expected positions of most of the hydrogen atoms were found. All hydrogens were included in the structure factor calculations in their expected positions based on idealized bonding geometry. All hydrogens were assigned isotropic thermal parameters 1.3 $Å^2$ larger than the equivalent B_{iso} of the atom to which they were bonded. None of the hydrogens were refined in least squares. The final difference Fourier map suggests possible alternate positions for atoms C3, C4, and the carbon atoms attached to them. The disorder was not able to be modeled.

The final residuals for 383 variables refined against the 4352 data for which $F_o^2 > 3\sigma(F_o^2)$ were R = 3.05%, R_w = 4.08% and GOF = 1.998. The R value for all data was 6.40%.

The quantity minimized by the least squares was $w(|F_o|-|F_c|)^2$, where w is the weight of a given observation. The p-factor[15], used to reduce the weight of intense reflections, was set to 0.03 throughout the refinement. The analytical forms of the scattering factor tables for the neutral atoms[16] were used and all non-hydrogen scattering factors were corrected for both the real and imaginary components of anomalous dispersion.[17]

Inspection of the residuals ordered in ranges of $\sin(\theta/\lambda)$, $|F_o|$, and parity and value of the individual indexes showed no unusual features or trends. There was no evidence of secondary extinction in the low-angle, high-intensity reflections. The weights of two reflections were set to zero for the final refinement, based of their anomalously high values of $w \times \Delta^2$. The largest two peaks in the final difference Fourier map had electron densities of 1.144 and 0.990 $e^{-1}/Å^3$ and were associated with the disordered ligands.

Table IV Crystal Data for $(UMe[OCH(t\text{-}Bu)_2]_4)Li$ (-85±4°C)

Space Group	$P2_1/c$
a, Å	11.654(2)
b, Å	15.874(2)
c, Å	23.406(3)
α, deg	90
β, deg	105.28(1)
γ, deg	90
V, $Å^3$	4177(2)
Z	4
fw	833.01
d (calc.) g/cm^3	1.325
μ (calc.) 1/cm	37.15
radiation	MoKα (λ = 0.71073Å)
monochrometer	highly oriented graphite
scan range, type	$3° \leq 2\theta \leq 45°$, θ-2θ
scan speed, deg/min	0.84-6.7, variable
scan width, deg	$\Delta\theta = 0.65 + 0.35 \tan\theta$
reflections collected	5989; +h, +k, ±l
unique reflections	5438
reflections, $F_o^2 > 3\sigma(F_o^2)$	4354
R, %	3.05
R_w, %	4.08
R_{all}, %	6.40
GOF	2.00
Largest Δ/σ in final least square cycle	1.40

Intensity Standards: 1, 1, -16; 1, 10, 5; 7, 4, -8; measured every hour of X-ray exposure time. Over the period of data collection there was a 8.4% decay in intensity. A linear decay correction was applied to the raw data.

Orientation Standards: 3 reflections were checked after every 250 measurements. Crystal orientation was redetermined if any of the reflections were offset from their predicted positions by more than 0.1°. Reorientation was required twice toward the end of data collection. The cell constants and errors are listed as their final values.

EXPERIMENTAL REFERENCES

1. Andersen, R.A. Inorg. Chem. 1979, 18, 1507-1509.

2. Turner, H.W.; Andersen, R.A.; Zalkin, A.; Templeton, D.H. Inorg. Chem. 1979, 18, 1221-1224.

3. The p-tolylazide was supplied by R. Rosen and synthesized by the procedure used to make o-tolylazide in: Abramovitch, R.A.; Kyba, E.P.; Scriven, E.F.V. J. Org. Chem. 1971, 36, 3797-3803.

4. Pritzkow, W.; Timm, D. J. Prak. Chem. 1966, 32, 178-189.

5. Brennan, J.G.; Ph.D. thesis, University of California, Berkeley, 1986.

6. Simpson, S.J.; Turner, H.W.; Andersen, R.A. Inorg. Chem. 1981, 20, 2991-2995.

7. Syper, L. Rocz. Chem. 1973, 47, 433.

8. Lubben, T.V.; Wolczanski, P.T.; Van Duyne, G.D. Organometallics 1984, 3, 977-983.

9. Dexheimer, E.M.; Spialter, L.; Smithson, L.D J. Organomet. Chem. 1975, 102, 21-27.

10. Instrumentation at the University of California Chemistry Department X-ray Crystallographic Facility (CHEXRAY) consists of two Enraf-Nonius CAD-4 diffractometers, one controlled by a DEC PDP 8/a with an RK05 disk and the other by a DEC PDP 8/e with an RL01 disk. Both use Enraf-Nonius software as described in the CAD-4 Operation Manual, Enraf-Nonius, Delft, Nov. 1977, updated Jan. 1980.

11. Calculations were performed on DEC Microvax II using locally modified Nonius-SDP3 software operating under Micro-VMS operating system.

12. Structure Determination Package User's Guide, 1985, B. A. Frenz and Associates,Inc., College Station, TX 77840.

13. The data reduction formulae are:

$$F_o^2 = \frac{\omega}{Lp}(C-2B) \qquad \sigma_o(F_o^2) = \frac{\omega}{Lp}(C+4B)^{1/2}$$

$$F_o = (F_o^2)^{1/2} \qquad \sigma_o(F) = [F_o^2 + \sigma_o(F_o^2)]^{1/2} - F_o$$

where C is the total count in the scan, B the sum of the two background counts, ω the scan speed used in deg/min, and

$$\frac{1}{Lp} = \frac{\sin 2\theta\,(1 + \cos^2 2\theta_m)}{1 + \cos^2 2\theta_m - \sin^2 2\theta}$$

is the correction for Lorentz and polarization effects for a reflection with scattering angle 2θ and radiation monochromatized with a 50% perfect single-crystal monochrometer with scattering angle $2\theta_m$.

14. Reflections used for azimuthal scans were located near $x = 90°$ and the intensities were measured at 10° increments of rotation of the crystal about the diffraction vector.

15. $$R = \frac{\Sigma||F_o| - |F_c||}{\Sigma|F_o|} \qquad wR = \left[\frac{\Sigma w(|F_o| - |F_c|)^2}{\Sigma w F_o^2}\right]^{1/2}$$

$$GOF = \left[\frac{\Sigma w(|F_o| - |F_c|)^2}{(n_o - n_v)}\right]^{1/2}$$

where n_o is the number of observations, n_v the number of variable parameters, and the weights w were given by

$$w = \frac{1}{\sigma^2(F_o)} \qquad \sigma(F_o^2) = [\sigma_o^2(F_o^2) + (pF^2)^2]^{1/2}$$

where $\sigma^2(F_o)$ is calculated as above from $\sigma(F_o^2)$ and where p is the factor used to lower the weight of intense reflections.

16. D. T. Cromer, J. T. Waber, "International Tables for X-ray Crystallography", Vol. IV, The Kynoch Press, Birmingham, England, 1974, Table 2.2B.

17. D. T. Cromer, ibid., Table 2.3.1.

18. Zachariesen, W. H., Acta Crystallogr., 1983 16, 1139.

19. (a) Eller, P.G.; Bradley, D.C.; Hursthouse, M.B.; Meek, D.W. Coord. Chem. Rev. 1977, 24, 1-95. (b) Hursthouse, M.B.; Rodesiler, P.F. J. Chem. Soc., Dalton Trans. 1972, 2100-2102. (c) Sheldrick, G.M.; Sheldrick. W.S. J. Chem. Soc. (A) 1962, 2279-2282. (d) Allmann, R.; Henke, W.; Krommes, P.; Lorberth, J. J. Organomet. Chem. 1978, 162, 283-287. (e) Ghotra, J.S.; Hursthouse, M.B.; Welch, A.J. J. Chem. Soc., Chem. Comm. 1973, 669-670. (f) Andersen, R.A.; Templeton, D.H.; Zalkin, A. Inorg. Chem. 1978, 17, 2317-2319.19.

Appendix I: Tables of Positional and Thermal Parameters

$U[N(SiMe_3)_2]_3 \cdot 1/3(C_6H_{12})$

Table of Positional Parameters and Their Estimated Standard Deviations

Atom	x	y	z	B(A2)
U	0.333	0.667	0.19511(5)	2.482(8)
Si	0.5489(6)	0.8349(6)	0.3896(1)	2.47(2)
N	0.4938(3)	0.747	0.250	2.20(9)
C1	0.6452(3)	0.8296(3)	0.5025(6)	4.6(1)
C2	0.4581(3)	0.8220(3)	0.5489(4)	3.8(1)
C3	0.5999(3)	0.9551(3)	0.2988(5)	4.0(1)
C4	0.491(1)	0.892(1)	0.238(3)	9.1(5)
H1a	0.6925	0.8359	0.4291	5.3*
H1b	0.6719	0.8794	0.579	5.3*
H1c	0.6198	0.7787	0.5567	5.3*
H2a	0.4387	0.7614	0.5892	4.3*
H2b	0.4871	0.8691	0.6214	4.3*
H2c	0.4103	0.8289	0.4884	4.3*
H3a	0.5523	0.9595	0.2497	4.6*
H3b	0.6237	1.0012	0.3818	4.6*
H3c	0.6497	0.9656	0.2276	4.6*

Starred atoms were included with isotropic thermal parameters.
The thermal parameter given for anisotropically refined atoms is the isotropic equivalent thermal parameter defined as:
(4/3) * [a2*B(1,1) + b2*B(2,2) + c2*B(3,3) + ab(cos gamma)*B(1,2) + ac(cos beta)*B(1,3) + bc(cos alpha)*B(2,3)]
where a,b,c are real cell parameters, and B(i,j) are anisotropic betas.

Table of Anisotropic Thermal Parameters - B's

Name	B(1,1)	B(2,2)	B(3,3)	B(1,2)	B(1,3)	B(2,3)	Beqv
U	1.92(1)	B(1,1)	3.68(2)	B(1,1)	0	0	2.482(8)
Si	2.48(3)	2.25(3)	2.35(4)	0.94(2)	-0.16(3)	-0.23(3)	2.47(2)
N	2.2(2)	2.4(1)	2.0(1)	B(1,1)	0	-0.1(1)	2.20(9)
C1	4.4(1)	4.8(2)	4.8(2)	2.5(1)	-2.0(1)	-1.4(1)	4.6(1)
C2	4.1(2)	3.4(1)	3.0(2)	1.2(1)	0.2(1)	-1.1(1)	3.8(1)
C3	4.1(2)	2.5(1)	4.3(2)	0.8(1)	-0.1(1)	-0.1(1)	4.0(1)
C4	4.7(6)	3.7(5)	19(1)	2.0(4)	2.3(9)	0.9(9)	9.1(5)

The form of the anisotropic temperature factor is:
exp(-0.25(h2a2B(1,1) + k2b2B(2,2) + l2c2B(3,3) + 2hkabB(1,2) + 2hlacB(1,3) + 2klbcB(2,3))) where a,b, and c are reciprocal lattice constants.

$UIN(SiMe_3)_2I_3(OPPh_3)\cdot 1/2(C_7H_8)$

Table of Positional Parameters and Their Estimated Standard Deviations

Atom	x	y	z	B(A2)
U	0.24201(11)	0.09597(1)	0.26156(11)	1.812(3)
P	-0.03758(9)	-0.23120(9)	0.26897(6)	2.22(2)
Si11	0.5417(1)	0.2276(1)	0.37163(7)	2.88(3)
Si12	0.3184(1)	0.1561(1)	0.44177(6)	3.01(3)
Si21	0.3795(1)	0.1589(1)	0.18786(6)	3.13(3)
Si22	0.3631(1)	-0.0617(1)	0.15578(7)	2.82(3)
Si31	0.0298(1)	0.1582(1)	0.17786(8)	3.81(3)
Si32	0.2834(1)	0.3676(1)	0.29591(7)	3.83(3)
O	0.0696(2)	-0.1053(2)	0.2632(1)	2.43(7)
N1	0.3826(3)	0.1696(3)	0.3666(2)	2.36(8)
N2	0.3395(3)	0.0655(3)	0.1675(2)	2.43(8)
N3	0.1522(3)	0.2289(3)	0.2434(2)	2.79(9)
C1	-0.1005(4)	-0.2276(4)	0.2713(2)	2.6(1)
C2	-0.1768(4)	-0.1198(4)	0.3066(3)	4.0(1)
C3	-0.2059(4)	-0.1148(4)	0.3132(3)	4.7(1)
C4	-0.3987(4)	-0.2194(5)	0.2834(3)	4.7(1)
C5	-0.4049(5)	-0.3276(5)	0.2478(4)	5.4(2)
C6	-0.2968(4)	-0.3314(4)	0.2414(3)	4.1(1)
C7	-0.0079(4)	-0.2758(3)	0.3461(2)	2.5(1)
C8	-0.0918(5)	-0.3093(5)	0.3927(3)	4.4(1)
C9	-0.0637(5)	-0.3394(5)	0.4627(3)	5.2(2)
C10	0.0484(5)	-0.3362(4)	0.4668(3)	4.5(1)
C11	0.1316(5)	-0.3027(5)	0.4213(3)	4.7(1)
C12	0.1047(4)	-0.2734(4)	0.3609(3)	4.1(1)
C13	-0.0648(4)	-0.3551(4)	0.1972(2)	2.7(1)
C14	-0.1056(4)	-0.4769(4)	0.2039(3)	3.9(1)
C15	-0.1389(5)	-0.5719(4)	0.1459(3)	5.2(2)
C16	-0.1108(5)	-0.5436(5)	0.0826(3)	5.6(2)
C17	-0.0608(5)	-0.4238(5)	0.0752(3)	5.2(2)
C18	-0.0446(5)	-0.3287(4)	0.1328(3)	3.9(1)
C19	0.3895(8)	0.4205(8)	0.9745(5)	16.8(2)*
C20	0.389(1)	0.546(1)	1.0279(6)	16.8*
C21	0.534(1)	0.629(1)	1.0628(7)	16.8*
C111	0.6858(5)	0.1816(4)	0.3675(3)	4.7(1)
C112	0.6866(5)	0.3075(5)	0.3882(3)	4.7(1)
C113	0.6382(5)	0.3489(5)	0.4536(3)	4.7(1)
C121	0.1438(4)	0.0772(5)	0.4213(3)	4.0(1)

Table of Positional Parameters and Their Estimated Standard Deviations (cont.)

Atom	x	y	z	B(A2)
C122	0.3538(6)	0.0585(5)	0.4919(3)	6.1(2)
C123	0.3648(5)	0.3888(5)	0.5043(3)	4.7(1)
C211	0.4886(4)	0.3197(4)	0.1461(3)	3.7(1)
C212	0.2556(6)	0.0989(5)	0.0298(3)	5.3(2)
C213	0.5288(5)	0.1852(6)	0.0736(3)	5.9(2)
C221	0.3828(4)	-0.1687(4)	0.2252(3)	3.5(1)
C222	0.2758(5)	-0.1786(5)	0.0718(3)	4.5(1)
C223	0.5385(4)	-0.0219(5)	0.1594(3)	4.7(1)
C311	-0.0163(5)	-0.0893(5)	0.1369(3)	5.3(2)
C312	-0.1139(5)	0.1545(6)	0.2876(4)	7.6(2)
C313	0.0614(5)	0.2438(5)	0.1847(3)	4.9(1)
C321	0.1856(7)	0.3639(6)	0.3658(3)	8.3(2)
C322	0.2885(5)	0.4892(4)	0.2492(3)	4.4(1)
C323	0.3693(6)	0.4362(5)	0.3488(3)	6.2(2)
H111A	0.5639	0.0505	0.4833	6.1*
H111B	0.6493	0.0435	0.3237	6.1*
H111C	0.6736	0.1393	0.3735	6.1*
H112A	0.5606	0.2511	0.2568	6.1*
H112B	0.5968	0.3803	0.3849	6.1*
H112C	0.6917	0.3328	0.3827	6.1*
H113A	0.6286	0.4168	0.4589	6.1*
H113B	0.6179	0.3180	0.4921	6.1*
H113C	0.7246	0.3887	0.4518	6.1*
H121A	0.1214	0.1232	0.3967	5.2*
H121B	0.1113	-0.0066	0.3946	5.2*
H121C	0.1897	0.0742	0.4633	5.2*
H122A	0.3312	-0.0288	0.4621	7.8*
H122B	0.4399	0.1023	0.5183	7.8*
H122C	0.3856	0.0441	0.5298	7.8*
H123A	0.4526	0.3556	0.5176	6.1*
H123B	0.3374	0.3564	0.4827	6.1*
H123C	0.3261	0.2916	0.5442	6.1*
H211A	0.4718	0.3565	0.1081	4.8*
H211B	0.4363	0.3716	0.1156	4.8*

Table of Positional Parameters and Their Estimated Standard Deviations (cont.)

Atom	x	y	z	B(A2)
H211C	0.3331	0.3138	0.1689	4.8*
H212A	0.1779	0.0755	0.0428	6.9*
H212B	0.2791	0.1452	-0.0081	6.9*
H212C	0.2475	0.0139	0.0043	6.9*
H213A	0.5191	0.1859	0.0521	7.7*
H213B	0.5434	0.2354	0.0483	7.7*
H213C	0.5964	0.2271	0.1187	7.7*
H221A	0.3435	-0.0559	0.2634	4.6*
H221B	0.2144	-0.1017	0.2219	4.6*
H221C	0.3172	-0.2195	0.2198	4.6*
H222A	0.1892	-0.2012	0.0678	5.9*
H222B	0.3055	-0.1415	0.0336	5.9*
H222C	0.2018	-0.2519	0.0691	5.9*
H223A	0.5663	0.0236	0.1252	6.1*
H223B	0.5761	0.0284	0.2041	6.1*
H223C	0.5344	-0.0975	0.1511	6.1*
H311A	0.0536	-0.0115	0.1286	6.9*
H311B	-0.0431	-0.0586	0.1786	6.9*
H311C	-0.0029	-0.0428	0.0991	6.9*
H312A	-0.1339	0.1127	0.2448	9.9*
H312B	-0.0978	0.2398	0.2238	9.9*
H312C	-0.1021	0.1116	0.1787	9.9*
H313A	0.0049	0.3288	0.1224	6.4*
H313B	0.1276	0.2394	0.0839	6.4*
H313C	-0.0118	0.2648	0.0787	6.4*
H321A	0.1885	0.3834	0.3912	10.8*
H321B	0.1433	0.4448	0.3965	10.8*
H321C	0.0239	0.3488	0.3456	10.8*
H322A	0.1268	0.4602	0.2254	5.7*

Table of Positional Parameters and Their Estimated Standard Deviations (cont.)

Atom	x	y	z	B(A2)
H322B	0.2360	0.6665	0.2816	6.7*
H322C	0.2646	0.6814	0.2164	6.7*
H323A	0.4217	0.4398	0.3858	8.8*
H323B	0.3985	0.5193	0.3667	8.8*
H323C	0.3722	0.3849	0.3694	8.8*
H2	-0.0988	-0.0459	0.3263	5.3*
H3	-0.2824	-0.0483	0.3382	6.2*
H4	-0.4741	-0.2174	0.2878	6.1*
H5	-0.4835	-0.3992	0.2257	7.8*
H6	-0.2986	-0.4862	0.2166	5.3*
H8	-0.1695	-0.3118	0.3834	5.8*
H9	-0.1212	-0.3628	0.4848	6.7*
H10	0.0674	-0.3581	0.5866	5.8*
H11	0.2895	-0.2989	0.4317	6.1*
H12	0.1633	-0.2518	0.3293	5.3*
H14	-0.1178	-0.4962	0.2483	5.8*
H15	-0.1628	-0.6563	0.1583	6.7*
H16	-0.1268	-0.6888	0.0432	7.3*
H17	-0.0562	-0.4842	0.0389	6.8*
H18	-0.0141	-0.2447	0.1266	5.1*

Starred atoms were included with isotropic thermal parameters.
The thermal parameter given for anisotropically refined atoms is the isotropic equivalent thermal parameter defined as:
(4/3) * [a2*B(1,1) + b2*B(2,2) + c2*B(3,3) + ab(cos gamma)*B(1,2) + ac(cos beta)*B(1,3) + bc(cos alpha)*B(2,3)]
where a,b,c are real cell parameters, and B(i,j) are anisotropic betas.

Table of Anisotropic Thermal Parameters - B's

Name	B(1,1)	B(2,2)	B(3,3)	B(1,2)	B(1,3)	B(2,3)	Beqv
U	1.888(4)	1.762(4)	1.728(5)	0.819(3)	0.169(4)	0.315(4)	1.812(3)
P	2.16(3)	1.94(3)	2.64(4)	1.07(2)	0.56(3)	0.47(3)	2.22(2)
S11	2.75(4)	3.03(4)	2.79(5)	1.64(3)	-0.48(4)	0.17(4)	2.88(3)
S12	3.96(5)	2.92(4)	2.14(5)	1.79(3)	0.27(4)	0.48(4)	3.01(3)
S21	3.17(4)	3.55(4)	2.39(5)	1.38(3)	0.73(4)	0.92(4)	3.13(3)
S22	2.39(4)	2.82(4)	3.14(5)	1.32(3)	0.98(4)	0.23(4)	2.82(3)
S31	2.55(4)	3.98(4)	5.16(6)	1.42(3)	-0.87(4)	2.26(4)	3.81(3)
S32	6.18(5)	3.41(4)	3.28(5)	3.32(3)	1.17(5)	1.89(4)	3.83(3)

Table of Anisotropic Thermal Parameters - B's (Continued)

Name	B(1,1)	B(2,2)	B(3,3)	B(1,2)	B(1,3)	B(2,3)	Beqv
O	2.52(9)	2.15(8)	2.6(1)	1.16(6)	.54(9)	.61(8)	2.43(7)
N1	2.5(1)	2.0(1)	2.4(1)	1.1(8)	-.1(1)	.1(1)	2.36(8)
N2	2.1(1)	2.6(1)	2.1(1)	.98(8)	.4(1)	.3(1)	2.43(8)
N3	3.0(1)	2.9(1)	3.0(1)	1.67(8)	.5(1)	1.3(1)	2.79(9)
C1	2.7(1)	2.6(1)	3.1(2)	1.71(9)	.8(1)	.8(1)	2.6(1)
C2	3.2(2)	3.9(2)	5.0(2)	2.1(1)	.6(2)	-.2(2)	4.0(1)
C3	4.8(2)	5.1(2)	5.9(3)	3.0(1)	1.1(2)	.9(2)	4.7(1)
C4	3.4(2)	6.0(2)	6.4(3)	3.2(1)	1.4(2)	2.3(2)	4.7(1)
C5	3.0(2)	4.0(2)	8.2(4)	1.9(1)	.6(2)	.9(2)	5.4(2)
C6	2.3(2)	3.2(2)	6.5(3)	1.3(1)	.7(2)	.7(2)	4.1(1)
C7	2.0(1)	1.9(1)	2.0(2)	1.1(1)	.0(1)	.0(1)	2.5(1)
C8	4.0(2)	6.1(2)	3.0(2)	2.0(1)	1.4(2)	1.7(2)	4.4(1)
C9	5.4(2)	7.5(2)	3.0(2)	3.5(2)	1.6(2)	3.2(2)	5.2(2)
C10	5.9(2)	4.7(2)	3.9(2)	3.1(1)	.9(2)	2.1(2)	4.5(1)
C11	5.0(2)	6.2(2)	5.2(2)	3.9(1)	1.2(2)	3.0(2)	4.7(1)
C12	3.9(2)	5.7(2)	4.7(2)	3.4(1)	1.9(2)	2.9(2)	4.1(1)
C13	1.7(1)	2.2(1)	3.7(2)	.9(1)	.3(1)	-.1(1)	2.7(1)
C14	3.9(2)	2.7(1)	4.7(2)	1.8(1)	-.5(2)	.1(2)	3.9(1)
C15	5.2(2)	2.7(2)	6.5(3)	2.2(1)	-1.6(2)	-1.3(2)	5.2(2)
C16	4.5(2)	5.5(2)	5.6(3)	2.9(1)	-.7(2)	-2.3(2)	5.6(2)
C17	4.5(2)	4.9(2)	4.1(2)	1.5(2)	.9(2)	-1.0(2)	5.2(2)
C18	3.7(2)	3.2(2)	3.3(2)	.8(1)	.8(2)	.0(2)	3.9(1)

Table of Anisotropic Thermal Parameters - B's (Continued)

Name	B(1,1)	B(2,2)	B(3,3)	B(1,2)	B(1,3)	B(2,3)	Beqv
C111	5.0(2)	4.9(2)	5.2(3)	3.6(1)	0.2(2)	0.5(2)	4.7(1)
C112	2.8(2)	5.2(2)	4.9(2)	1.1(2)	0.4(2)	1.6(2)	4.7(1)
C113	3.4(2)	4.7(2)	4.7(3)	1.9(1)	-1.4(2)	-1.0(2)	4.7(1)
C121	3.9(2)	3.9(2)	3.3(2)	1.5(1)	1.2(2)	0.2(2)	4.0(1)
C122	9.0(3)	7.2(2)	4.5(2)	5.2(2)	1.6(2)	3.6(2)	6.1(2)
C123	4.6(2)	4.7(2)	3.7(2)	2.1(1)	0.0(2)	-1.0(2)	4.7(1)
C211	4.0(2)	3.3(2)	3.6(2)	1.4(1)	0.5(2)	1.4(1)	3.7(1)
C212	6.6(3)	5.5(2)	2.8(2)	2.2(2)	-0.4(2)	1.1(2)	5.3(2)
C213	5.7(2)	7.5(2)	6.1(2)	3.5(2)	4.0(2)	3.6(2)	5.9(2)
C221	3.4(2)	3.0(1)	4.9(2)	1.9(1)	1.7(2)	1.4(1)	3.5(1)
C222	4.2(2)	4.3(2)	4.2(2)	1.8(1)	0.9(2)	-0.5(2)	4.5(1)
C223	3.3(2)	5.9(2)	5.5(3)	2.7(1)	1.7(2)	1.8(2)	4.7(1)
C311	4.8(2)	3.4(2)	5.1(2)	0.3(2)	-2.5(2)	1.1(2)	5.3(2)
C312	3.8(2)	9.6(2)	12.3(4)	3.9(2)	2.7(2)	7.2(2)	7.6(2)
C313	4.4(2)	4.6(2)	4.9(2)	1.4(2)	-0.9(2)	2.1(2)	4.9(1)
C321	14.8(3)	7.5(2)	7.2(3)	8.0(2)	7.0(2)	3.6(2)	8.3(2)
C322	5.3(2)	3.3(2)	5.4(3)	2.6(1)	0.9(2)	1.5(2)	4.4(1)
C323	9.1(3)	3.3(2)	4.6(3)	2.6(2)	-3.1(2)	-0.6(2)	6.2(2)

The form of the anisotropic temperature factor is:
exp[-0.25(h2a2B(1,1) + k2b2B(2,2) + l2c2B(3,3) + 2hkabB(1,2) + 2hlacB(1,3) + 2klbcB(2,3))) where a,b, and c are reciprocal lattice constants.

$U[N(SiMe_3)_2]_2I_3[N(p\text{-}tolyl)]$

Table of Positional Parameters and Their Estimated Standard Deviations

Atom	x	y	z	B(A2)
U	0.17698(2)	0.24493(2)	0.21481(2)	1.714(5)
Si11	0.3569(2)	0.0666(2)	0.3486(2)	2.59(4)
Si12	0.2501(2)	-0.0192(2)	0.1615(2)	2.41(4)
Si21	0.2193(2)	0.4665(2)	0.3816(1)	2.27(4)
Si22	0.3975(2)	0.4392(2)	0.2182(2)	2.48(4)
Si31	-0.0796(2)	0.3689(2)	0.1608(2)	2.28(4)
Si32	-0.1095(2)	0.1618(2)	0.2752(2)	2.47(4)
N1	0.2604(5)	0.0889(5)	0.2511(4)	2.0(1)
N2	0.2746(5)	0.3549(5)	0.2781(4)	2.0(1)
N3	-0.0195(5)	0.2574(5)	0.2225(4)	2.1(1)
N4	0.2142(5)	0.2447(5)	0.0884(4)	2.4(1)
C1	0.2238(7)	0.2438(6)	-0.0186(5)	2.4(1)
C2	0.3322(7)	0.2459(7)	-0.0639(6)	3.1(2)
C3	0.3395(8)	0.2418(7)	-0.1619(6)	3.5(2)
C4	0.2403(8)	0.2352(6)	-0.2193(6)	3.4(2)
C5	0.1321(8)	0.2341(6)	-0.1742(6)	3.2(2)
C6	0.1234(7)	0.2382(6)	-0.0761(5)	2.8(2)
C7	0.249(1)	0.2318(7)	-0.3265(6)	4.5(2)
C111	0.3958(8)	0.1993(7)	0.4288(6)	3.9(2)
C112	0.2848(9)	-0.0232(8)	0.4333(7)	5.0(2)
C113	0.5001(8)	0.0029(8)	0.3115(7)	4.5(2)
C121	0.2351(9)	-0.1603(7)	0.2892(7)	4.6(2)
C122	0.3715(8)	-0.0243(7)	0.0732(6)	3.8(2)
C123	0.1884(7)	0.0824(7)	0.0974(6)	3.4(2)
C211	0.3264(7)	0.4960(7)	0.4816(6)	3.4(2)
C212	0.1837(7)	0.3745(7)	0.4388(6)	3.0(2)
C213	0.1505(8)	0.6020(7)	0.3564(6)	3.5(2)
C221	0.4889(7)	0.3155(8)	0.1792(7)	3.9(2)
C222	0.3588(7)	0.5144(6)	0.1122(5)	2.6(2)
C223	0.4933(7)	0.5376(8)	0.2938(6)	4.0(2)

Table of Positional Parameters and Their Estimated Standard Deviations (cont.)

Atom	x	y	z	B(A2)
C311	0.0486(7)	0.4561(6)	0.1218(5)	2.7(2)
C312	-0.1768(7)	0.3211(8)	0.0658(7)	4.4(2)
C313	-0.1663(8)	0.4644(7)	0.2526(6)	3.9(2)
C321	-0.0162(7)	0.0695(7)	0.3443(6)	3.4(2)
C322	-0.2132(7)	0.2287(6)	0.3661(6)	3.4(2)
C323	-0.2885(8)	0.0747(7)	0.1868(7)	3.8(2)
H111A	0.4433	0.1824	0.4715	5.0*
H111B	0.4366	0.2463	0.3882	5.0*
H111C	0.3259	0.2342	0.4424	5.0*
H112A	0.3351	-0.0329	0.4049	6.2*
H112B	0.2148	0.0113	0.4661	6.2*
H112C	0.2659	-0.0942	0.4818	6.2*
H113A	0.5455	-0.0085	0.3659	5.7*
H113B	0.4868	-0.0688	0.2764	5.7*
H113C	0.5486	0.0504	0.2719	5.7*
H121A	0.2258	-0.2153	0.1586	6.0*
H121B	0.3031	-0.1744	0.2448	6.0*
H121C	0.1685	-0.1595	0.2586	6.0*
H122A	0.3574	-0.0048	0.0259	4.9*
H122B	0.3751	0.0436	0.0438	4.9*
H122C	0.4432	-0.0365	0.1845	4.9*
H123A	0.0966	-0.0561	0.0491	4.5*
H123B	0.0448	0.0013	0.1423	4.5*
H123C	0.1098	0.0723	0.0711	4.5*
H211A	0.2894	0.5344	0.5338	4.4*
H211B	0.3569	0.4267	0.4995	4.4*
H211C	0.3897	0.5399	0.4688	4.4*
H212A	0.0719	0.4101	0.4865	4.0*
H212B	0.0448	0.3595	0.3848	4.0*
H212C	0.1383	0.3851	0.4442	4.0*

Table of Positional Parameters and Their Estimated Standard Deviations (cont.)

Atom	x	y	z	B(A2)
H213A	0.1217	0.6391	0.4129	4.5*
H213B	0.2879	0.6486	0.3288	4.5*
H213C	0.0882	0.5888	0.3117	4.5*
H221A	0.5559	0.3383	0.1463	4.9*
H221B	0.5121	0.2778	0.2331	4.9*
H221C	0.4439	0.2648	0.1375	4.9*
H222A	0.4279	0.5372	0.0814	3.5*
H222B	0.3145	0.4655	0.0682	3.5*
H222C	0.3129	0.5782	0.1389	3.5*
H223A	0.5586	0.5588	0.2557	5.2*
H223B	0.4586	0.6826	0.3137	5.2*
H223C	0.5287	0.5828	0.3461	5.2*
H311A	0.0875	0.5177	0.0927	3.5*
H311B	0.0898	0.4841	0.1738	3.5*
H311C	0.0851	0.4123	0.0763	3.5*
H312A	-0.2888	0.3843	0.0389	5.7*
H312B	-0.1138	0.2775	0.0192	5.7*
H312C	-0.2398	0.2766	0.0881	5.7*
H313A	-0.1971	0.5233	0.2191	5.8*
H313B	-0.2291	0.4234	0.2779	5.8*

Table of Positional Parameters and Their Estimated Standard Deviations (cont.)

Atom	x	y	z	B(A2)
H313C	-0.1175	0.4945	0.3827	5.0*
H321A	-0.0643	0.0164	0.3731	4.5*
H321B	0.0373	0.0295	0.3818	4.5*
H321C	0.0262	0.1129	0.3915	4.5*
H322A	-0.2586	0.1714	0.3912	4.5*
H322B	-0.1691	0.2678	0.4149	4.5*
H322C	-0.2628	0.2781	0.3357	4.5*
H323A	-0.2479	0.0248	0.2195	4.0*
H323B	-0.2493	0.1215	0.1634	4.0*
H323C	-0.1518	0.0328	0.1432	4.0*
H7A	0.1714	0.2277	-0.3525	5.0*
H7B	0.2869	0.2968	-0.3438	5.0*
H7C	0.2985	0.1678	-0.3493	5.0*
H2	0.4815	0.2495	-0.0266	3.9*
H3	0.4145	0.2413	-0.1988	4.6*
H5	0.0619	0.2386	-0.2186	4.2*
H6	0.0486	0.2354	-0.0475	3.7*

Starred atoms were included with isotropic thermal parameters.
The thermal parameter given for anisotropically refined atoms is the isotropic equivalent thermal parameter defined as:
(4/3) * [a2*B(1,1) + b2*B(2,2) + c2*B(3,3) + ab(cos gamma)*B(1,2) + ac(cos beta)*B(1,3) + bc(cos alpha)*B(2,3)]
where a,b,c are real cell parameters, and B(i,j) are anisotropic betas.

Table of Anisotropic Thermal Parameters -- B's

Name	B(1,1)	B(2,2)	B(3,3)	B(1,2)	B(1,3)	B(2,3)	Beqv
U	1.584(5)	1.885(9)	1.816(9)	0.168(8)	0.005(8)	0.032(8)	1.714(5)
S(11	2.68(8)	2.85(9)	2.34(8)	0.51(7)	-0.22(7)	0.41(7)	2.59(4)
S(12	2.45(8)	2.38(8)	2.38(8)	0.51(7)	0.08(7)	0.18(7)	2.41(4)
S(21	2.25(8)	2.43(8)	2.08(9)	-0.04(7)	0.02(7)	-0.08(7)	2.27(4)
S(22	1.98(8)	2.92(8)	2.35(8)	-0.12(7)	0.07(7)	0.55(7)	2.48(4)
S(31	1.86(7)	2.49(8)	2.55(8)	0.41(7)	0.04(7)	0.45(7)	2.28(4)
S(32	2.88(8)	2.32(8)	2.98(9)	0.05(7)	0.56(7)	-0.03(7)	2.47(4)
N1	1.9(2)	2.6(2)	1.7(2)	0.3(2)	-0.2(2)	0.6(2)	2.0(1)
N2	1.7(2)	1.6(2)	2.7(2)	-0.1(2)	-0.3(2)	0.2(2)	2.0(1)
N3	2.3(2)	2.0(2)	2.0(2)	-0.3(2)	-0.2(2)	-0.1(2)	2.1(1)
N4	2.3(2)	2.1(2)	2.7(3)	0.3(2)	0.2(2)	-0.2(2)	2.4(1)
C1	3.2(3)	1.5(3)	2.5(3)	-0.2(2)	0.6(3)	-0.3(2)	2.4(1)
C2	3.4(3)	3.1(3)	2.8(3)	0.5(3)	0.6(3)	-0.0(3)	3.1(2)
C3	4.6(4)	3.0(3)	2.9(3)	0.0(3)	1.6(3)	-0.1(3)	3.5(2)
C4	5.6(4)	2.0(3)	2.6(3)	0.3(3)	0.9(3)	-0.1(3)	3.4(2)
C5	5.1(4)	1.5(3)	3.1(3)	-0.2(3)	-0.6(3)	0.2(3)	3.2(2)
C6	3.3(3)	2.5(3)	2.5(3)	0.4(3)	-0.2(3)	0.2(3)	2.8(2)
C7	7.5(5)	3.3(4)	2.5(4)	-0.2(4)	0.9(4)	-0.3(3)	4.5(2)
C111	5.9(4)	3.2(4)	2.7(3)	0.0(3)	-1.6(3)	0.4(3)	3.9(2)
C112	6.2(5)	5.3(4)	4.0(4)	-0.8(4)	-1.0(4)	3.0(3)	5.0(2)

Table of Anisotropic Thermal Parameters - B's (Continued)

Name	B(1,1)	B(2,2)	B(3,3)	B(1,2)	B(1,3)	B(2,3)	Beqv
C113	3.9(4)	5.2(4)	4.3(4)	2.1(3)	-1.1(3)	-0.3(4)	4.5(2)
C121	5.4(5)	2.8(4)	5.4(5)	-0.3(4)	-0.8(4)	-0.6(4)	4.6(2)
C122	4.1(4)	3.7(4)	3.3(4)	1.7(3)	1.1(3)	-0.6(3)	3.8(2)
C123	3.1(3)	3.2(3)	3.0(4)	-0.2(3)	0.0(3)	-0.9(3)	3.4(2)
C211	3.2(3)	4.1(4)	2.7(3)	-0.3(3)	-0.4(3)	-1.0(3)	3.4(2)
C212	2.9(3)	3.6(4)	2.5(3)	-0.4(3)	0.1(3)	-0.2(3)	3.0(2)
C213	4.5(4)	2.9(3)	2.9(3)	0.3(3)	0.2(3)	-0.2(3)	3.5(2)
C221	2.3(3)	5.1(4)	4.3(4)	0.9(3)	0.8(3)	0.3(4)	3.9(2)
C222	3.0(3)	2.6(3)	2.3(3)	0.0(3)	0.3(3)	0.9(3)	2.6(2)
C223	3.2(4)	5.4(4)	3.5(4)	-1.2(3)	-0.6(3)	0.5(3)	4.0(2)
C311	2.0(3)	3.2(3)	2.3(3)	0.5(3)	-0.1(3)	1.0(3)	2.7(2)
C312	2.4(3)	5.7(5)	5.2(4)	0.0(3)	-1.2(3)	1.5(4)	4.4(2)
C313	4.6(4)	3.4(4)	4.0(4)	1.6(3)	1.5(3)	1.1(3)	3.9(2)
C321	3.4(3)	3.6(4)	3.1(3)	0.4(3)	0.8(3)	1.0(3)	3.4(2)
C322	3.9(4)	2.0(3)	4.5(4)	0.0(3)	1.0(3)	1.3(3)	3.4(2)
C323	3.7(4)	3.0(3)	4.6(4)	-0.7(3)	0.4(3)	0.3(3)	3.8(2)

The form of the anisotropic temperature factor is:
exp[-0.25(h2a2B(1,1) + k2b2B(2,2) + l2c2B(3,3) + 2hkabB(1,2) + 2hlacB(1,3) + 2klbcB(2,3))] where a,b, and c are reciprocal lattice constants.

$U[N(SiMe_3)_2]_3(NSiMe_3)$

Table of Positional Parameters and Their Estimated Standard Deviations

Atom	x	y	z	B(A2)
U	0.000	0.000	0.000	1.728(3)
Si1	0.000	0.000	0.1785(1)	4.10(5)
Si21	0.1065(6)	0.2324(8)	-0.7988(7)	2.42(3)
Si22	-0.1447(7)	0.1845(8)	0.2454(8)	2.78(3)
N1	0.000	0.000	0.0000(4)	3.1(1)
N2	0.0322(2)	0.1385(2)	-0.0229(2)	2.01(8)
C1	0.1114(5)	0.0794(4)	0.2816(3)	5.8(2)
C211	0.1497(3)	0.1354(3)	-0.1285(2)	3.2(1)
C212	0.0616(3)	0.2410(3)	-0.1433(3)	3.5(1)
C213	0.2034(3)	0.3043(3)	-0.0462(2)	3.3(1)
C221	-0.1283(4)	0.0935(4)	0.0494(3)	4.0(1)
C222	0.0559(3)	0.2396(3)	0.0944(3)	3.9(1)
C223	-0.0329(3)	0.2600(3)	-0.0141(3)	4.1(1)
H1A	0.1096	0.0781	0.2458	7.5*
H1B	0.1528	0.0632	0.1874	7.5*
H1C	0.1284	0.1372	0.1874	7.5*
H211A	0.1748	0.1139	-0.0987	4.1*
H211B	0.1889	0.0871	-0.1489	4.1*
H211C	0.1926	0.1711	-0.1582	4.1*
H212A	0.0395	0.2761	-0.1268	4.6*
H212B	0.1066	0.2748	-0.1728	4.6*
H212C	0.0149	0.1988	-0.1635	4.6*
H213A	0.1828	0.3384	-0.0257	4.3*
H213B	0.2339	0.2876	-0.0172	4.3*
H213C	0.2431	0.3383	-0.0787	4.3*

Table of Positional Parameters and Their Estimated Standard Deviations (cont.)

Atom	x	y	z	B(A2)
H221A	-0.1629	0.0664	0.0132	5.2*
H221B	-0.1228	0.0506	0.0730	5.2*
H221C	-0.1568	0.1181	0.0738	5.2*
H222A	0.1123	0.2847	0.0812	5.1*
H222B	0.0286	0.2645	0.1151	5.1*
H222C	0.0617	0.1978	0.1183	5.1*
H223A	0.0223	0.3156	-0.0276	5.3*
H223B	-0.0782	0.2418	-0.0491	5.3*
H223C	-0.0597	0.2891	0.0148	5.3*

Starred atoms were included with isotropic thermal parameters.
The thermal parameter given for anisotropically refined atoms is the isotropic equivalent thermal parameter defined as:
(4/3) * [a2*B(1,1) + b2*B(2,2) + c2*B(3,3) + ab(cos gamma)*B(1,2) + ac(cos beta)*B(1,3) + bc(cos alpha)*B(2,3)]
where a,b,c are real cell parameters, and B(i,j) are anisotropic betas.

Table of Anisotropic Thermal Parameters - B's

Name	B(1,1)	B(2,2)	B(3,3)	B(1,2)	B(1,3)	B(2,3)	Beqv
U	1.671(6)	B(1,1)	1.843(8)	B(1,1)	0	0	1.728(3)
S(1	5.1(1)	B(1,1)	2.1(1)	B(1,1)	0	0	4.1(0(5)
S(21	2.22(4)	1.84(4)	3.14(6)	0.97(3)	-0.13(5)	0.31(5)	2.42(3)
S(22	2.30(4)	2.40(4)	3.82(5)	1.30(3)	-0.59(5)	-0.90(5)	2.78(3)
N1	2.9(2)	B(1,1)	3.3(4)	B(1,1)	0	0	3.1(1)
N2	1.5(1)	1.7(1)	2.9(2)	0.03(8)	-0.5(1)	-0.3(1)	2.0(1(8)
C1	7.2(3)	6.1(2)	3.2(3)	2.5(2)	-1.4(3)	-0.3(2)	5.8(2)
C211	3.4(2)	2.6(2)	3.4(2)	1.5(1)	0.0(2)	0.5(2)	3.2(1)
C212	3.2(2)	3.1(2)	4.2(2)	1.5(1)	-0.5(2)	1.2(2)	3.5(1)
C213	2.1(2)	2.5(2)	4.9(3)	0.0(1)	0.0(2)	-0.2(2)	3.3(1)
C221	3.3(2)	3.4(2)	4.4(3)	1.0(2)	0.7(2)	-1.4(2)	4.0(1)
C222	4.1(2)	4.2(2)	3.9(2)	2.4(1)	-1.0(2)	-2.1(2)	3.9(1)
C223	3.4(2)	3.2(2)	6.3(3)	2.2(1)	-1.3(2)	-1.2(2)	4.1(1)

The form of the anisotropic temperature factor is:
exp[-0.25(h2a2B(1,1) + k2b2B(2,2) + l2c2B(3,3) + 2hkabB(1,2) + 2hlacB(1,3) + 2klbcB(2,3))] where a,b, and c are reciprocal lattice constants.

$U[N(SiMe_3)_2]_2[_3[NH(p\text{-}tolyl)]$

Table of Positional Parameters and Their Estimated Standard Deviations

Atom	x	y	z	B(A2)
U	0.17926(1)	0.25618(1)	0.28347(1)	1.864(2)
Si1	0.3564(1)	0.4357(1)	0.1492(1)	2.68(2)
Si2	0.2553(1)	0.5288(1)	0.3366(1)	2.66(2)
Si3	-0.0732(1)	0.1299(1)	0.3357(1)	2.14(2)
Si4	-0.1836(1)	0.3358(1)	0.2278(1)	2.29(2)
Si5	0.4038(1)	0.0593(1)	0.2812(1)	2.64(2)
Si6	0.2222(1)	0.0369(1)	0.1187(1)	2.35(2)
N1	0.272(2)	0.411(2)	0.247(2)	2.31(5)
N2	-0.016(2)	0.243(2)	0.283(2)	1.98(5)
N3	0.288(2)	0.186(2)	0.222(2)	2.12(5)
N4	0.251(2)	0.268(2)	0.431(2)	2.58(5)
C1	0.232(3)	0.263(2)	0.530(2)	2.44(5)
C2	0.121(3)	0.268(3)	0.566(2)	2.64(6)
C3	0.182(3)	0.271(3)	0.663(2)	3.49(8)
C4	0.193(4)	0.269(3)	0.729(2)	3.93(8)
C5	0.344(3)	0.264(3)	0.694(3)	4.14(8)
C6	0.325(3)	0.268(3)	0.596(3)	3.31(7)
C7	0.172(5)	0.272(4)	0.536(3)	6.2(1)
C11	0.277(4)	0.528(3)	0.462(3)	4.85(9)
C12	0.497(3)	0.506(4)	0.185(3)	5.3(1)
C13	0.396(3)	0.393(3)	0.079(3)	4.31(8)
C21	0.239(3)	0.659(3)	0.288(3)	4.29(9)
C22	0.378(3)	0.532(3)	0.426(3)	4.23(8)
C23	0.117(3)	0.598(3)	0.483(2)	2.93(7)
C31	-0.171(3)	0.171(3)	0.437(2)	3.37(7)
C32	0.061(3)	0.048(3)	0.332(2)	2.53(6)
C33	-0.156(3)	0.031(3)	0.258(3)	3.36(7)
C41	-0.211(3)	0.264(3)	0.136(3)	3.30(7)
C42	-0.016(3)	0.427(3)	0.166(3)	3.41(7)

Table of Positional Parameters and Their Estimated Standard Deviations (cont.)

Atom	x	y	z	B(A2)
C43	-0.1959(3)	0.4242(3)	0.3139(3)	3.52(8)
C51	0.5848(3)	0.1798(3)	0.3171(3)	4.23(9)
C52	0.4984(3)	-0.0436(4)	0.2857(3)	4.66(9)
C53	0.3661(3)	-0.0112(3)	0.3982(2)	3.43(7)
C61	0.1554(3)	-0.0998(3)	0.1413(3)	3.58(8)
C62	0.3252(3)	0.0183(3)	0.0173(2)	3.38(7)
C63	0.1839(3)	0.1277(3)	0.0727(2)	3.28(7)
HN4	0.3228	0.2755	0.4174	3.8*
H2	0.0553	0.2729	0.5248	3.4*
H3	0.0237	0.2734	0.6866	4.4*
H5	0.3724	0.2644	0.7378	5.2*
H6	0.4848	0.2563	0.5744	4.4*
H7B	0.1928	0.3448	0.0667	8.2*
H7C	0.0921	0.2579	0.0473	8.2*
H7A	0.2183	0.2174	0.0648	8.2*
H11C	0.3244	0.5299	0.0098	6.2*
H11A	0.2864	0.4877	0.0439	6.2*
H11B	0.2633	0.5944	0.0945	6.2*
H12C	0.4823	0.5795	0.2167	6.6*
H12A	0.5391	0.4648	0.2298	6.6*
H12B	0.6434	0.5158	0.1313	6.6*
H13C	0.4434	0.2693	0.1198	6.5*
H13A	0.3293	0.2629	0.0532	6.5*
H13B	0.4412	0.3192	0.0268	6.5*
H21C	0.3893	0.6799	0.2585	6.5*
H21A	0.1773	0.6681	0.2417	6.5*
H21B	0.2226	0.7163	0.3389	6.5*
H22C	0.3683	0.6876	0.4767	6.6*
H22A	0.3892	0.4625	0.4529	6.6*
H22B	0.4477	0.5523	0.3964	6.6*
H23C	0.1853	0.5625	0.4498	3.7*

Table of Positional Parameters and Their Estimated Standard Deviations (cont.)

Atom	x	y	z	B(A2)
H23A	0.0526	0.4945	0.3594	3.7*
H23B	0.1221	0.4343	0.4369	3.7*
H31C	-0.1387	0.2156	0.4865	4.4*
H31A	-0.2368	0.2123	0.4153	4.4*
H31B	-0.2885	0.1859	0.4648	4.4*
H32C	0.0234	-0.0163	0.4889	3.2*
H32A	0.1832	0.0272	0.3328	3.2*
H32B	0.0932	0.0934	0.4314	3.2*
H33C	-0.1034	-0.0386	0.2828	4.2*
H33A	-0.2289	0.0676	0.2233	4.2*
H33B	-0.1872	0.0032	0.1988	4.2*
H41C	-0.1788	0.2285	0.0886	4.4*
H41A	-0.2621	0.2157	0.1677	4.4*
H41B	-0.2574	0.3176	0.1069	4.4*
H42C	-0.0627	0.4784	0.1259	4.5*
H42A	0.0485	0.4657	0.1971	4.5*
H42B	0.0247	0.3814	0.1077	4.5*
H43C	-0.2454	0.4722	0.2888	4.5*
H43A	-0.2428	0.3785	0.3585	4.5*
H43B	-0.1463	0.4598	0.3573	4.5*

Table of Positional Parameters and Their Estimated Standard Deviations (cont.)

Atom	x	y	z	B(A2)
H51C	0.5317	0.2113	0.2611	5.3*
H51A	0.4654	0.2358	0.3559	5.3*
H51B	0.5788	0.1545	0.3522	5.3*
H52C	0.5553	-0.0675	0.2418	6.0*
H52A	0.4433	-0.1071	0.1853	6.0*
H52B	0.5178	-0.0187	0.1587	6.0*
H53C	0.4368	-0.0296	0.4232	4.5*
H53A	0.3224	0.0388	0.4325	4.5*
H53B	0.3235	-0.0767	0.3732	4.5*
H61C	0.2134	-0.1513	0.1588	4.6*
H61A	0.1818	-0.0984	0.1928	4.6*
H61B	0.1144	-0.1318	0.0846	4.6*
H62C	0.2868	-0.0288	-0.0386	4.4*
H62A	0.3626	0.0788	0.0848	4.4*
H62B	0.3868	-0.0483	0.0346	4.4*
H63C	0.0664	0.0918	0.0175	4.0*
H63A	0.0482	0.1451	0.1218	4.0*
H63B	0.1371	0.1968	0.0553	4.0*

Starred atoms were included with isotropic thermal parameters.
The thermal parameter given for anisotropically refined atoms is the isotropic equivalent thermal parameter defined as:
(4/3) * [a2*B(1,1) + b2*B(2,2) + c2*B(3,3) + ab(cos gamma)*B(1,2) + ac(cos beta)*B(1,3) + bc(cos alpha)*B(2,3)]
where a,b,c are real cell parameters, and B(i,j) are anisotropic betas.

Table of Anisotropic Thermal Parameters - B's

Name	B(1,1)	B(2,2)	B(3,3)	B(1,2)	B(1,3)	B(2,3)	Beqv
U	1.554(4)	1.987(4)	2.091(4)	-0.186(4)	0.128(4)	0.394(4)	1.864(2)
S11	2.68(4)	3.28(4)	2.92(4)	-0.61(3)	0.34(3)	1.04(3)	2.88(2)
S12	2.68(3)	2.48(3)	2.92(4)	-0.48(3)	-0.22(3)	0.36(3)	2.66(2)
S13	1.83(3)	2.29(3)	2.35(3)	-0.22(3)	0.06(3)	0.58(3)	2.14(2)
S14	1.96(3)	2.28(3)	2.77(3)	-0.05(3)	-0.26(3)	0.55(3)	2.29(2)
S15	1.93(3)	3.46(4)	2.62(3)	0.49(3)	0.21(3)	0.64(3)	2.64(2)
S16	2.38(3)	2.77(3)	2.88(3)	0.15(3)	0.19(3)	0.21(3)	2.35(2)
N1	2.01(9)	2.5(1)	2.5(1)	-0.22(8)	0.05(8)	0.78(9)	2.31(5)
N2	1.88(9)	2.01(9)	2.1(1)	-0.11(9)	-0.01(8)	0.12(8)	1.98(5)
N3	2.00(9)	2.5(1)	1.93(9)	0.13(8)	0.58(8)	0.42(8)	2.12(5)
N4	2.5(1)	2.8(1)	2.5(1)	-0.09(9)	0.23(9)	0.37(9)	2.58(5)
C1	2.9(1)	1.5(1)	2.8(1)	-0.1(1)	-0.5(1)	0.2(1)	2.44(6)
C2	2.9(1)	2.5(1)	2.5(1)	-.	-0.1(1)	0.1(1)	2.64(6)
C3	5.2(2)	2.4(1)	2.9(1)	-	0.5(1)	0.2(1)	3.49(8)
C4	7.3(2)	1.9(1)	2.5(1)	-0.2(1)	-0.5(1)	0.3(1)	3.93(8)
C5	6.4(2)	2.3(1)	3.7(1)	-0.5(1)	-3.5(1)	0.6(1)	4.14(8)
C6	3.5(1)	2.4(1)	4.1(2)	-0.2(1)	-1.2(1)	0.5(1)	3.31(7)
C7	12.3(3)	3.9(2)	2.5(2)	-0.2(2)	-0.3(2)	0.4(1)	6.2(1)
C11	5.3(2)	5.8(2)	3.9(2)	0.7(2)	0.7(1)	2.5(1)	4.85(9)
C12	3.5(2)	6.9(2)	5.6(2)	-1.9(2)	1.3(1)	0.8(2)	5.3(1)

Table of Anisotropic Thermal Parameters - B's (Continued)

Name	B(1,1)	B(2,2)	B(3,3)	B(1,2)	B(1,3)	B(2,3)	Beqv
C13	5.8(2)	4.5(2)	3.6(2)	-0.3(1)	1.0(1)	0.5(1)	4.31(8)
C21	5.5(2)	2.8(1)	4.8(2)	-0.5(1)	0.8(2)	0.8(1)	4.29(9)
C22	7.6(2)	4.8(2)	4.2(2)	-1.1(1)	-1.0(1)	-0.2(2)	4.23(8)
C23	3.1(1)	2.9(1)	2.8(1)	0.1(1)	0.2(1)	0.0(1)	2.93(7)
C31	2.6(1)	4.3(2)	3.4(1)	0.1(1)	0.8(1)	1.2(1)	3.37(7)
C32	2.8(1)	2.7(1)	2.5(1)	0.1(1)	0.2(1)	0.7(1)	2.53(6)
C33	3.5(1)	2.6(1)	4.0(2)	-0.9(1)	-1.1(1)	0.7(1)	3.36(7)
C41	2.9(1)	3.3(1)	3.9(2)	-0.2(1)	-1.1(1)	0.7(1)	3.38(7)
C42	2.9(1)	3.3(1)	4.2(2)	-0.3(1)	-0.6(1)	1.6(1)	3.41(7)
C43	3.1(1)	2.7(1)	4.8(2)	0.7(1)	0.1(1)	0.3(1)	3.52(8)
C51	2.4(1)	5.8(2)	4.5(2)	-0.6(1)	-0.4(1)	1.0(2)	4.23(9)
C52	3.5(2)	6.3(2)	4.1(2)	2.5(1)	0.5(1)	0.3(2)	4.66(9)
C53	3.3(1)	3.8(1)	3.3(1)	0.5(1)	-0.4(1)	1.2(1)	3.43(7)
C61	3.8(2)	3.3(1)	3.5(2)	-0.5(1)	0.2(1)	-0.1(1)	3.58(8)
C62	3.5(1)	4.1(2)	2.5(1)	0.4(1)	0.6(1)	-0.2(1)	3.38(7)
C63	3.3(1)	4.2(2)	2.1(1)	0.6(1)	-0.2(1)	0.4(1)	3.28(7)

The form of the anisotropic temperature factor is:
exp(-0.25(h2a2B(1,1) + k2b2B(2,2) + l2c2B(3,3) + 2hkabB(1,2) + 2hlacB(1,3) + 2klbcB(2,3))) where a,b, and c are reciprocal lattice constants.

$U_2[N(SiMe_3)_2]_2I_4[\mu\text{-}N(H)(2,4,6\text{-}Me_3C_6H_2)]_2$

Table of Positional Parameters and Their Estimated Standard Deviations

Atom	x	y	z	B(A2)
U	0.48487(1)	0.04242(1)	0.12356(1)	1.885(3)
SI11	0.44996(8)	0.3585(1)	0.1499(0)	2.82(3)
SI12	0.36915(7)	0.1781(1)	0.24657(8)	2.66(3)
SI21	0.53378(8)	-0.1661(1)	0.20583(8)	2.99(3)
SI22	0.64536(7)	0.0318(1)	0.3854(8)	2.48(3)
N1	0.4317(2)	0.2117(3)	0.1713(2)	2.18(7)
N2	0.5614(2)	-0.0378(3)	0.2482(2)	2.15(7)
N3	0.5793(2)	0.0732(3)	0.0198(2)	2.15(7)
C1	0.6589(2)	0.0384(3)	0.0149(3)	2.11(9)
C2A	0.7844(3)	0.2482(4)	-0.0083(3)	3.0(1)
C2	0.7181(2)	0.1146(4)	-0.0039(3)	2.48(9)
C3	0.7927(3)	0.0728(4)	-0.0131(3)	3.3(1)
C4	0.8122(3)	-0.0395(4)	-0.0056(4)	3.7(1)
C4A	0.8938(3)	-0.0823(6)	-0.0178(5)	6.3(2)
C5	0.7548(3)	-0.1127(4)	0.0158(3)	3.2(1)
C6	0.6787(2)	-0.0772(4)	0.0266(3)	2.38(9)
C6A	0.6241(3)	-0.1688(4)	0.0589(3)	2.7(1)
C111	0.3613(3)	0.4274(5)	0.0881(4)	4.8(1)
C112	0.4855(4)	0.4335(4)	0.2549(4)	5.4(2)
C113	0.5291(3)	0.3645(4)	0.0777(3)	3.6(1)
C121	0.2746(3)	0.2689(5)	0.2344(4)	5.2(1)
C122	0.3381(3)	0.0278(4)	0.2388(3)	3.8(1)
C123	0.4198(3)	0.1883(5)	0.3668(3)	4.2(1)
C211	0.4853(4)	-0.1552(5)	0.3884(4)	5.6(1)
C212	0.6167(3)	-0.2694(4)	0.3893(4)	5.3(1)
C213	0.4595(3)	-0.2312(4)	0.1952(3)	3.1(1)
C221	0.6589(3)	0.0488(5)	0.4243(3)	4.4(1)
C222	0.6445(3)	0.1779(4)	0.2569(4)	4.0(1)
C223	0.7484(3)	-0.0323(4)	0.2788(4)	4.1(1)

Table of Positional Parameters and Their Estimated Standard Deviations (cont.)

Atom	x	y	z	B(A2)
H3	0.8322	0.1245	-0.0252	4.3*
H5	0.7675	-0.1986	0.0215	4.2*
H21	0.7588	0.2768	-0.0216	3.9*
H22	0.6666	0.2566	-0.0538	3.9*
H23	0.6929	0.2662	0.0477	3.9*
H41	0.8957	-0.1618	-0.0188	8.2*
H42	0.9833	-0.0648	-0.0763	8.2*
H43	0.9332	-0.0479	0.0252	8.2*
H61	0.5747	-0.1252	0.0654	3.5*
H62	0.6158	-0.2226	0.0286	3.5*
H63	0.6479	-0.1078	0.1182	3.5*
H111C	0.3767	0.5813	0.0736	6.2*
H111A	0.3414	0.3878	0.0346	6.2*
H111B	0.3218	0.4319	0.1249	6.2*
H112B	0.4998	0.5874	0.2361	7.0*
H112C	0.4448	0.4388	0.2893	7.0*
H112A	0.5384	0.3972	0.2073	7.0*
H113B	0.5358	0.4418	0.0542	4.7*
H113C	0.5778	0.3352	0.1085	4.7*
H113A	0.5138	0.3238	0.0237	4.7*
H121B	0.2451	0.2488	0.1763	6.8*
H121C	0.2448	0.2378	0.2783	6.8*
H121A	0.2867	0.3388	0.2422	6.8*
H122B	0.3866	0.0869	0.2739	4.9*
H122C	0.3877	0.0107	0.1728	4.9*
H122A	0.3841	-0.0188	0.2364	4.9*
H123B	0.4382	0.2651	0.3089	5.6*
H123C	0.3847	0.1583	0.4041	5.6*
H123A	0.4673	0.1466	0.3736	5.6*
H211B	0.4653	-0.2278	0.4017	7.9*
H211C	0.5232	-0.1383	0.4374	7.9*

Table of Positional Parameters and Their Estimated Standard Deviations (cont.)

Atom	x	y	z	B(A2)
H211A	0.4425	-0.1027	0.3708	7.3*
H212B	0.6541	-0.2439	0.3586	6.8*
H212C	0.5961	-0.3486	0.3238	6.8*
H212A	0.6423	-0.2763	0.2588	6.8*
H213B	0.4838	-0.2438	0.3437	4.1*
H213C	0.4415	-0.3889	0.2157	4.1*
H213A	0.4154	-0.1816	0.1883	4.1*
H221B	0.6981	0.0784	0.4494	5.7*
H221C	0.6858	0.0798	0.4388	5.7*
H221A	0.6513	-0.0348	0.4483	5.7*
H222B	0.5995	0.2171	0.2784	5.2*
H222C	0.6918	0.2157	0.2818	5.2*
H222A	0.6417	0.1754	0.1926	5.2*
H223B	0.7839	0.0137	0.3244	5.4*
H223C	0.7468	-0.1053	0.3847	5.4*
H223A	0.7398	-0.0379	0.2168	5.4*
HN3	0.5728	0.1439	0.0858	3.8*

Starred atoms were included with isotropic thermal parameters.
The thermal parameter given for anisotropically refined atoms is the isotropic equivalent thermal parameter defined as:
(4/3) * [a2*B(1,1) + b2*B(2,2) + c2*B(3,3) + ab(cos gamma)*B(1,2) + ac(cos beta)*B(1,3) + bc(cos alpha)*B(2,3)]
where a,b,c are real cell parameters, and B(i,j) are anisotropic betas.

Table of Anisotropic Thermal Parameters - B's

Name	B(1,1)	B(2,2)	B(3,3)	B(1,2)	B(1,3)	B(2,3)	Beqv
U	2.#38(6)	1.#82(6)	1.563(6)	#.29#(6)	#.248(5)	#.#61(6)	1.##5(3)
S111	3.27(5)	1.93(5)	3.21(5)	#.44(5)	#.31(5)	#.#4(5)	2.82(3)
S112	2.64(5)	2.89(5)	2.61(5)	#.44(5)	#.07(4)	-#.16(5)	2.66(3)
S121	3.78(6)	2.57(5)	2.27(5)	-#.79(5)	-#.56(5)	#.63(5)	2.99(3)
S122	2.38(5)	2.36(5)	2.47(5)	-#.17(4)	-#.32(4)	#.16(4)	2.48(3)
N1	2.3(1)	1.9(1)	2.1(1)	#.4(1)	#.1(1)	-#.#(1)	2.1#(7)
N2	2.5(1)	2.#(1)	1.8(1)	-#.2(1)	-#.#(1)	#.5(1)	2.15(7)
N3	1.5(1)	2.#(1)	2.9(2)	#.#(1)	#.2(1)	#.3(1)	2.15(7)
C1	1.#(2)	2.6(2)	1.9(2)	-#.4(1)	#.1(1)	-#.1(2)	2.11(9)
C2A	2.6(2)	3.#(2)	3.3(2)	-#.#(2)	#.3(2)	#.1(2)	3.#(1)
C2	2.3(2)	2.9(2)	1.#(2)	-#.4(2)	-#.#(1)	-#.4(2)	2.4#(9)
C3	2.4(2)	4.1(2)	3.4(2)	-#.#(2)	#.9(2)	-#.5(2)	3.3(1)
C4	2.3(2)	4.9(3)	4.#(2)	#.4(2)	#.9(2)	-#.5(2)	3.7(1)
C4A	3.#(2)	7.3(4)	9.2(4)	#.9(2)	2.6(2)	-#.3(3)	6.3(2)
C5	3.1(2)	3.3(2)	3.2(2)	#.7(2)	#.5(2)	-#.6(2)	3.2(1)
C6	2.2(2)	2.5(2)	2.2(2)	#.2(2)	#.4(1)	-#.3(2)	2.3#(9)
C6A	2.7(2)	2.6(2)	2.7(2)	#.2(2)	#.4(2)	#.4(2)	2.7(1)
C111	4.7(2)	3.9(2)	5.#(3)	1.#(2)	1.2(2)	1.5(2)	4.#(1)
C112	#.#(4)	2.#(2)	5.1(3)	-#.4(2)	#.2(3)	-1.2(2)	5.4(2)
C113	3.5(2)	2.6(2)	4.#(2)	-#.#(2)	#.6(2)	1.1(2)	3.6(1)
C121	3.7(2)	6.#(3)	6.5(3)	1.7(2)	2.2(2)	#.9(3)	5.2(1)
C122	3.7(2)	4.2(3)	3.#(2)	-#.#(2)	1.6(2)	#.2(2)	3.#(1)
C123	4.9(2)	4.9(3)	2.#(2)	-#.#(2)	1.#(2)	-#.6(2)	4.2(1)
C211	7.#(3)	6.6(3)	3.#(2)	-3.3(2)	#.5(2)	#.9(2)	5.6(1)
C212	5.7(3)	3.#(2)	6.#(3)	-#.3(2)	-2.2(2)	1.5(2)	5.3(1)
C213	3.5(2)	2.4(2)	3.3(2)	-#.7(2)	-#.#(2)	-#.#(2)	3.1(1)
C221	4.3(2)	5.7(3)	2.6(2)	-#.#(2)	-#.#(2)	-#.4(2)	4.4(1)
C222	3.5(2)	3.1(2)	5.#(3)	-#.6(2)	-#.5(2)	#.#(2)	4.#(1)
C223	2.9(2)	4.6(3)	4.6(3)	-#.#(2)	-#.2(2)	#.#(2)	4.1(1)

The form of the anisotropic temperature factor is:
exp(-#.25(h2a2B(1,1) + k2b2B(2,2) + l2c2B(3,3) + 2hkabB(1,2) + 2hlacB(1,3) + 2klbcB(2,3))) where a,b, and c are reciprocal lattice constants.

$U_2[N(SiMe_3)_2]_2I_4[\mu\text{-}N(p\text{-tolyl})]_2$

Table of Positional Parameters and Their Estimated Standard Deviations

Atom	x	y	z	B(A2)
U	0.0231(1)	0.1138(1)	0.3613(1)	1.748(3)
Si11	0.0396(1)	0.4194(9)	0.2389(8)	2.68(3)
Si12	0.2824(1)	0.3352(9)	0.3189(8)	2.41(2)
Si21	-0.1813(1)	0.0288(9)	0.2186(7)	2.38(2)
Si22	0.2326(1)	0.0973(1)	0.1851(8)	3.67(3)
N1	0.1354(3)	0.2995(2)	0.2986(2)	2.00(7)
N2	0.0586(3)	0.0823(3)	0.2118(2)	2.15(7)
N3	0.1268(3)	-0.0491(3)	0.4536(2)	2.07(7)
C1	0.2311(4)	-0.1368(3)	0.4322(3)	1.86(8)
C2	0.3725(4)	-0.1413(3)	0.4342(3)	2.47(9)
C3	0.4746(4)	-0.2269(3)	0.4189(3)	2.54(9)
C4	0.4421(4)	-0.3181(3)	0.3836(3)	2.5(1)
C5	0.3012(5)	-0.3274(4)	0.3838(4)	4.4(1)
C6	0.1972(4)	-0.2236(3)	0.4008(3)	3.5(1)
C7	0.5578(5)	-0.3991(3)	0.3541(3)	3.6(1)
C111	-0.1415(4)	0.3638(4)	0.2562(3)	3.3(1)
C112	0.1415(6)	0.4976(5)	0.0764(4)	5.6(2)
C113	-0.0163(5)	0.5394(4)	0.2838(4)	4.7(1)
C121	0.2188(5)	0.3568(4)	0.4492(3)	3.5(1)
C122	0.3358(5)	0.4782(4)	0.1976(4)	4.3(1)
C123	0.4288(4)	0.2893(4)	0.3353(3)	3.2(1)
C211	-0.0891(5)	-0.1199(4)	0.2158(3)	4.2(1)
C212	-0.2472(4)	0.0122(3)	0.3591(3)	2.68(9)
C213	-0.1724(5)	0.1455(4)	0.1893(3)	3.8(1)
C221	0.3742(5)	0.1417(4)	0.1377(3)	4.3(1)
C222	0.2892(6)	-0.0527(5)	0.0948(5)	8.5(2)
C223	0.2484(7)	0.2174(7)	-0.0348(4)	8.2(2)

Table of Positional Parameters and Their Estimated Standard Deviations (cont.)

Atom	x	y	z	B(A2)
H111A	-0.1956	0.4190	0.2191	4.3*
H111B	-0.1200	0.2947	0.2273	4.3*
H111C	-0.1957	0.3145	0.3346	4.3*
H112A	0.0836	0.5627	0.0435	7.3*
H112B	0.2349	0.5311	0.0551	7.3*
H112C	0.1580	0.4393	0.0474	7.3*
H113A	-0.0604	0.6021	0.2426	6.1*
H113B	-0.0795	0.5015	0.3613	6.1*
H113C	0.0786	0.5751	0.2743	6.1*
H121A	0.2923	0.3760	0.4591	4.6*
H121B	0.1432	0.4225	0.4425	4.6*
H121C	0.1601	0.2823	0.5122	4.6*
H122A	0.4736	0.4933	0.2130	5.7*
H122B	0.4365	0.4667	0.1314	5.7*
H122C	0.3322	0.5472	0.1865	5.7*
H123A	0.4982	0.2321	0.3463	4.1*
H123B	0.3786	0.1344	0.3986	4.1*
H123C	0.4601	0.1978	0.2696	4.1*
H211A	-0.1828	-0.1403	0.2195	5.5*
H211B	-0.0120	-0.1139	0.1466	5.5*
H211C	-0.0671	-0.1823	0.2767	5.5*
H212A	-0.3396	-0.0156	0.3689	3.5*
H212B	-0.2168	-0.0460	0.4172	3.5*
H212C	-0.2597	0.0096	0.3618	3.5*
H213A	-0.2687	0.1114	0.1186	4.9*
H213B	-0.1946	0.2200	0.1160	4.9*
H213C	-0.0903	0.1624	0.0368	4.9*

Table of Positional Parameters and Their Estimated Standard Deviations (cont.)

Atom	x	y	z	B(A2)
H221A	0.4782	0.1582	0.0883	5.6*
H221B	0.3492	0.2182	0.1415	5.6*
H221C	0.3758	0.0758	0.2079	5.6*
H222A	0.3848	-0.0411	0.0363	11.1*
H222B	0.2935	-0.1158	0.1643	11.1*
H222C	0.2176	-0.0782	0.0795	11.1*
H223A	0.3373	0.2223	-0.0597	10.7*
H223B	0.1683	0.1967	-0.0538	10.7*
H223C	0.2184	0.2957	-0.0335	10.7*
H2	0.4888	-0.0846	0.4518	3.2*
H3	0.5697	-0.2278	0.4139	3.3*
H5	0.2744	-0.3641	0.3658	5.7*
H6	0.1884	-0.2268	0.4084	4.6*
H7A	0.5164	-0.4495	0.3374	4.7*
H7B	0.6434	-0.3533	0.2983	4.7*
H7C	0.5863	-0.4582	0.4159	4.7*

Starred atoms were included with isotropic thermal parameters.
The thermal parameter given for anisotropically refined atoms is the isotropic equivalent thermal parameter defined as:
(4/3) * [a2*B(1,1) + b2*B(2,2) + c2*B(3,3) + ab(cos gamma)*B(1,2) + ac(cos beta)*B(1,3) + bc(cos alpha)*B(2,3)]
where a,b,c are real cell parameters, and B(i,j) are anisotropic betas.

Table of Anisotropic Thermal Parameters - B's

Name	B(1,1)	B(2,2)	B(3,3)	B(1,2)	B(1,3)	B(2,3)	Beqv
U	2.168(5)	1.566(5)	1.712(4)	-0.008(4)	-0.574(3)	-0.664(3)	1.748(3)
S111	2.72(4)	1.74(3)	3.21(3)	0.15(3)	-1.62(3)	-0.61(2)	2.68(3)
S112	2.38(3)	2.25(3)	2.89(3)	-0.18(3)	-1.19(2)	-1.16(2)	2.41(2)
S121	2.59(4)	2.69(3)	2.35(3)	-0.05(3)	-1.03(2)	-1.39(2)	2.38(2)
S122	2.45(4)	6.39(5)	2.92(3)	-0.56(3)	-0.32(3)	-3.03(2)	3.67(3)
N1	2.1(1)	1.58(9)	2.15(9)	0.03(8)	-0.84(7)	-0.65(6)	2.00(7)
N2	2.4(1)	2.4(1)	2.02(8)	0.17(8)	-1.05(7)	-1.15(6)	2.15(7)
N3	1.6(1)	2.3(1)	2.58(8)	0.38(8)	-0.84(7)	-1.23(6)	2.07(7)
C1	1.8(1)	1.9(1)	1.6(1)	0.0(1)	-0.33(8)	-0.87(7)	1.86(8)
C2	1.8(1)	2.6(1)	3.6(1)	0.3(1)	-1.02(9)	-1.91(8)	2.47(9)
C3	2.0(1)	2.7(1)	3.5(1)	0.4(1)	-1.15(9)	-1.89(8)	2.54(9)
C4	2.4(1)	2.2(1)	2.5(1)	0.6(1)	-0.7(1)	-1.04(9)	2.5(1)
C5	3.4(2)	4.4(1)	7.8(2)	1.2(1)	-2.6(1)	-4.6(1)	4.4(1)
C6	2.5(1)	3.7(1)	6.3(1)	1.2(1)	-2.5(1)	-3.33(9)	3.5(1)
C7	3.3(2)	3.1(1)	4.6(1)	1.3(1)	-1.1(1)	-2.63(9)	3.6(1)
C111	3.0(1)	2.8(1)	4.1(1)	0.4(1)	-2.2(1)	-1.0(1)	3.3(1)
C112	4.9(2)	5.0(3)	4.1(2)	-0.5(2)	-2.1(1)	0.7(2)	5.6(2)
C113	5.0(2)	2.8(1)	7.9(2)	1.6(1)	-3.8(1)	-3.0(1)	4.7(1)
C121	3.6(2)	3.7(1)	4.7(1)	0.5(1)	-2.4(1)	-2.66(9)	3.5(1)
C122	3.8(2)	3.7(2)	4.9(2)	-1.4(1)	-1.6(1)	-1.0(1)	4.3(1)
C123	2.6(1)	4.1(2)	3.5(1)	0.5(1)	-1.66(9)	-1.95(9)	3.2(1)
C211	4.8(2)	3.7(1)	4.6(1)	-0.9(1)	-0.6(1)	-3.00(9)	4.2(1)
C212	2.4(1)	2.7(1)	3.4(1)	-0.2(1)	-0.96(9)	-1.65(8)	2.68(9)
C213	3.7(2)	5.2(2)	3.2(1)	0.1(1)	-2.0(1)	-1.8(1)	3.8(1)
C221	2.4(2)	7.0(2)	4.3(1)	0.2(1)	-0.8(1)	-3.7(1)	4.3(1)
C222	3.3(2)	12.6(2)	12.2(2)	-0.0(2)	0.7(2)	****(1)	8.5(2)
C223	5.5(3)	14.2(5)	2.7(2)	-3.0(3)	-0.9(2)	-1.7(2)	8.2(2)

The form of the anisotropic temperature factor is:
exp[-0.25(h2a2B(1,1) + k2b2B(2,2) + l2c2B(3,3) + 2hkabB(1,2) + 2hlacB(1,3) + 2klbcB(2,3))] where a,b, and c are reciprocal lattice constants.

$UMe[OC(t\text{-}Bu)_3]_3$

Table of Positional Parameters and Their Estimated Standard Deviations

Atom	x	y	z	B(A²)
U	0.23494(1)	0.05417(2)	0.04199(1)	1.481(5)
O1	0.1538(2)	0.1447(4)	-0.0315(3)	2.2(1)
O2	0.3175(2)	0.1412(3)	0.1194(2)	1.97(9)
O3	0.2593(2)	-0.0935(4)	-0.0618(3)	2.2(1)
C1	0.1045(3)	0.2285(5)	-0.0719(4)	2.2(1)
C2	0.3827(3)	0.1767(6)	0.1721(4)	2.3(1)
C3	0.2568(3)	-0.1926(5)	-0.0582(4)	2.4(2)
C4	0.1986(3)	-0.0877(7)	0.1512(4)	2.9(2)
C11	0.0368(3)	0.1663(6)	-0.1262(4)	2.9(2)
C12	0.0959(3)	0.2992(6)	0.0055(4)	2.9(2)
C13	0.1357(3)	0.2945(5)	-0.1298(4)	2.3(1)
C21	0.3718(3)	0.2895(5)	0.2123(4)	1.9(1)
C22	0.4259(3)	0.1867(5)	0.1878(4)	2.5(2)
C23	0.4097(4)	0.0828(5)	0.2435(4)	2.6(2)
C31	0.2673(3)	-0.1524(6)	-0.1388(4)	2.7(2)
C32	0.3184(3)	-0.2668(5)	0.0079(4)	2.4(1)
C33	0.1847(4)	-0.2433(6)	-0.0599(5)	3.3(2)
C111	0.0428(4)	0.1112(7)	-0.2076(5)	4.3(2)
C112	0.0215(4)	0.0699(6)	-0.0757(6)	4.1(2)
C113	-0.0263(4)	0.2381(7)	-0.1556(5)	4.6(2)
C121	0.0587(4)	0.2443(9)	0.0514(5)	5.7(2)
C122	0.0672(4)	0.4139(7)	-0.0195(5)	4.3(2)
C123	0.1618(4)	0.3895(7)	0.0793(5)	4.0(2)
C131	0.0928(4)	0.3668(6)	-0.1986(5)	3.5(2)
C132	0.1989(4)	0.3669(6)	-0.0788(5)	3.0(2)
C133	0.1749(3)	0.2173(6)	-0.1752(4)	3.3(2)
C211	0.3188(3)	0.2868(6)	0.2446(4)	2.5(2)
C212	0.3545(4)	0.3845(6)	0.1478(5)	3.1(2)
C213	0.4316(3)	0.3298(6)	0.2887(4)	2.8(2)

Table of Positional Parameters and Their Estimated Standard Deviations (cont.)

Atom	x	y	z	B(A2)
C221	0.3843(4)	0.2357(7)	0.0209(4)	3.3(2)
C222	0.4912(3)	0.2529(7)	0.1418(4)	3.6(2)
C223	0.4472(4)	0.0771(6)	0.0799(5)	3.5(2)
C231	0.4864(4)	0.0826(6)	0.2898(5)	3.3(2)
C232	0.3787(4)	0.0847(7)	0.3147(5)	3.7(2)
C233	0.3891(4)	-0.0386(6)	0.2857(5)	3.3(2)
C311	0.3107(4)	-0.0598(6)	-0.1241(5)	3.8(2)
C312	0.2862(5)	-0.2423(7)	-0.1056(5)	4.6(2)
C321	0.3073(4)	-0.2257(7)	0.0112(5)	3.5(2)
C322	0.3163(4)	-0.3057(6)	-0.0204(5)	3.4(2)
C323	0.3219(4)	-0.2689(6)	0.1028(4)	3.1(2)
C331	0.1296(4)	-0.1545(7)	-0.0768(5)	4.7(2)
C332	0.1799(4)	-0.3088(7)	0.0214(5)	4.0(2)
C333	0.1682(4)	-0.3208(7)	-0.1315(5)	4.3(2)
C313	0.2020(5)	-0.0978(7)	-0.2005(5)	4.3(2)
H111A	0.0081	0.0761	-0.2362	5.2*
H111B	0.0502	0.1641	-0.2438	5.2*
H111C	0.0766	0.0593	-0.1925	5.2*
H112A	-0.0186	0.0362	-0.1098	5.0*
H112B	0.0575	0.0195	-0.0622	5.0*
H112C	0.0161	0.0955	-0.0242	5.0*
H113A	-0.0630	0.1947	-0.1862	4.9*
H113B	-0.0345	0.2677	-0.1068	4.9*
H113C	-0.0282	0.2941	-0.1984	4.9*
H121A	0.0478	0.2893	0.0956	6.2*
H121B	0.0076	0.2317	0.0115	6.2*
H121C	0.0787	0.1769	0.0741	6.2*
H122A	0.0644	0.4491	0.0298	5.3*

Table of Positional Parameters and Their Estimated Standard Deviations (cont.)

Atom	x	y	z	B(A2)
H122B	0.0972	0.4526	-0.0418	5.3*
H122C	0.0247	0.4088	-0.0611	5.3*
H123A	0.1549	0.3524	0.1233	5.4*
H123B	0.1776	0.2485	0.1886	5.4*
H123C	0.1945	0.3446	0.0596	5.4*
H131A	0.1166	0.4023	-0.2287	4.2*
H131B	0.0580	0.3229	-0.2359	4.2*
H131C	0.0719	0.4182	-0.1718	4.2*
H132A	0.2178	0.4025	-0.1167	4.5*
H132B	0.1848	0.4188	-0.0466	4.5*
H132C	0.2329	0.3224	-0.0489	4.5*
H133A	0.1949	0.2597	-0.2803	4.0*
H133B	0.2083	0.1777	-0.1348	4.0*
H133C	0.1427	0.1782	-0.2111	4.0*
H211A	0.3858	0.3551	0.2676	3.0*
H211B	0.2705	0.2711	0.1977	3.0*
H211C	0.3162	0.2325	0.2865	3.0*
H212A	0.3496	0.4488	0.1762	3.6*
H212B	0.3986	0.3939	0.1253	3.6*

Table of Positional Parameters and Their Estimated Standard Deviations (cont.)

Atom	x	y	z	B(A2)
H212C	0.3147	0.3689	0.1033	3.6*
H213A	0.4283	0.3571	0.3888	3.6*
H213B	0.4456	0.2783	0.3339	3.6*
H213C	0.4782	0.3379	0.2722	3.6*
H221A	0.4114	0.2413	-0.0146	4.0*
H221B	0.3465	0.1915	-0.0053	4.0*
H221C	0.3695	0.3062	0.0388	4.0*
H222A	0.5127	0.2542	0.1888	4.3*
H222B	0.4881	0.3237	0.1537	4.3*
H222C	0.5195	0.2197	0.1921	4.3*
H223A	0.4722	0.0897	0.0424	4.2*
H223B	0.4738	0.0385	0.1282	4.2*
H223C	0.4881	0.0364	0.0589	4.2*
H231A	0.4988	0.0263	0.3294	3.9*
H231B	0.5882	0.0716	0.2675	3.9*
H231C	0.4996	0.1583	0.3159	3.9*
H232A	0.3966	0.0285	0.3637	4.6*
H232B	0.3873	0.1527	0.3429	4.6*
H232C	0.3318	0.0754	0.2983	4.6*

Table of Positional Parameters and Their Estimated Standard Deviations (cont.)

Atom	x	y	z	B(A2)
H233A	0.4849	-0.0037	0.2487	3.9*
H233B	0.3418	-0.0346	0.1834	3.9*
H233C	0.4868	-0.0432	0.1612	3.9*
H311A	0.3229	-0.0398	-0.1767	4.5*
H311B	0.3034	0.0086	-0.0995	4.5*
H311C	0.3686	-0.0033	-0.0863	4.6*
H312A	0.2911	-0.2135	-0.2396	5.5*
H312B	0.3267	-0.2755	-0.1559	5.5*
H312C	0.2512	-0.2959	-0.2047	5.5*
H313A	0.2185	-0.0754	-0.2587	5.3*
H313B	0.1668	-0.1477	-0.2146	5.3*
H313C	0.1987	-0.0362	-0.1735	5.3*
H321A	0.4218	-0.2716	0.0459	4.1*
H321B	0.3981	-0.2232	-0.0444	4.1*
H321C	0.3537	-0.1542	0.0347	4.1*
H322A	0.3537	-0.4248	0.0171	4.1*
H322B	0.2769	-0.4197	-0.0175	4.1*
H322C	0.3171	-0.3987	-0.0765	4.1*
H323A	0.3584	-0.3138	0.1342	3.7*
H323B	0.3282	-0.1975	0.1249	3.7*
H323C	0.2812	-0.2976	0.1278	3.7*
H331A	0.0088	-0.1859	-0.0799	5.4*
H331B	0.1424	-0.1855	-0.0276	5.4*
H331C	0.1278	-0.1154	-0.1251	5.4*
H332A	0.1882	-0.3561	0.0684	4.6*
H332B	0.1639	-0.2341	0.0385	4.6*
H332C	0.1484	-0.3195	-0.0337	4.6*
H333A	0.1177	-0.3547	-0.1333	5.1*
H333B	0.1566	-0.2941	-0.1043	5.1*
H333C	0.1916	-0.3852	-0.1214	5.1*
H41	0.2223	-0.0618	0.1985	3.6*
H42	0.1798	0.0536	0.1792	3.6*
H43	0.1683	-0.0478	0.1251	3.6*

Starred atoms were included with isotropic thermal parameters.
The thermal parameter given for anisotropically refined atoms is the isotropic equivalent thermal parameter defined as:
(4/3) * [a2*B(1,1) + b2*B(2,2) + c2*B(3,3) + ab(cos gamma)*B(1,2) + ac(cos beta)*B(1,3) + bc(cos alpha)*B(2,3)]
where a,b,c are real cell parameters, and B(i,j) are anisotropic betas.

Table of Anisotropic Thermal Parameters - B's

Name	B(1,1)	B(2,2)	B(3,3)	B(1,2)	B(1,3)	B(2,3)	Beqv
U	1.228(8)	1.649(9)	1.434(8)	-0.045(9)	0.243(6)	-0.048(9)	1.481(5)
O1	1.4(2)	2.7(2)	2.2(2)	0.5(2)	0.4(1)	0.9(2)	2.2(1)
O2	1.2(2)	2.5(2)	1.9(2)	-0.0(1)	0.0(1)	-0.5(2)	1.97(9)
O3	2.0(2)	2.0(2)	1.8(2)	-0.1(2)	0.6(1)	-0.5(2)	2.2(1)
C1	1.9(2)	2.6(3)	1.6(2)	0.3(2)	0.1(2)	1.0(2)	2.2(1)
C2	2.0(2)	2.4(3)	2.2(2)	0.1(2)	0.4(2)	-0.3(2)	2.3(1)
C3	3.5(3)	1.9(3)	1.7(2)	-0.3(2)	0.0(2)	-0.3(2)	2.4(2)
C4	3.0(3)	3.4(3)	2.4(3)	-0.3(3)	1.0(2)	0.4(3)	2.9(2)
C11	1.9(3)	3.4(3)	2.8(3)	-0.6(3)	0.0(2)	0.3(3)	2.9(2)
C12	2.3(3)	4.0(4)	2.3(3)	1.1(3)	0.7(2)	0.3(3)	2.9(2)
C13	2.0(2)	2.3(3)	2.6(2)	-0.1(2)	1.0(2)	0.9(2)	2.3(1)
C21	0.9(2)	2.1(3)	2.4(3)	-0.1(2)	0.0(2)	-0.1(2)	1.9(1)
C22	2.3(3)	2.8(3)	2.4(2)	-0.0(2)	0.9(2)	-0.5(2)	2.5(2)
C23	3.1(3)	2.2(3)	1.8(3)	0.6(3)	-0.1(2)	-0.0(2)	2.6(2)
C31	3.6(3)	2.4(3)	2.5(2)	-0.9(3)	1.6(2)	-0.2(2)	2.7(2)
C32	3.0(3)	2.1(3)	1.8(2)	0.2(2)	0.6(2)	-0.1(2)	2.4(1)
C33	3.0(3)	2.5(3)	4.0(3)	-0.6(3)	0.7(3)	0.5(3)	3.3(2)
C111	3.5(4)	4.5(4)	3.8(4)	-0.3(3)	-0.3(3)	-0.2(3)	4.3(2)
C112	2.6(3)	4.2(4)	5.2(4)	-0.8(3)	0.8(3)	1.5(3)	4.1(2)

Table of Anisotropic Thermal Parameters - B's (Continued)

Name	B(1,1)	B(2,2)	B(3,3)	B(1,2)	B(1,3)	B(2,3)	Beqv
C113	1.6(3)	5.3(4)	4.5(4)	0.4(3)	0.1(3)	1.3(3)	4.0(2)
C121	3.4(3)	8.8(5)	3.9(3)	1.6(4)	1.9(2)	0.6(4)	5.2(2)
C122	3.7(3)	4.6(4)	4.6(4)	2.1(3)	1.4(3)	-0.2(3)	4.3(2)
C123	4.2(4)	5.0(5)	3.3(3)	0.8(3)	0.6(3)	-1.7(3)	4.6(2)
C131	3.4(3)	3.6(4)	4.0(3)	0.6(3)	1.6(2)	1.4(3)	3.5(2)
C132	2.4(3)	3.2(4)	5.7(4)	-0.4(3)	1.2(3)	-0.0(3)	3.8(2)
C133	3.1(3)	3.5(3)	3.6(3)	0.3(3)	1.7(2)	0.3(3)	3.3(2)
C211	1.8(2)	3.0(3)	2.7(3)	-0.1(2)	0.7(2)	-0.6(2)	2.5(2)
C212	3.0(3)	2.1(3)	4.1(3)	-0.0(3)	1.2(2)	0.0(3)	3.1(2)
C213	2.1(3)	2.8(3)	3.4(3)	-0.7(3)	0.8(2)	-1.1(3)	2.8(2)
C221	3.5(3)	4.2(4)	2.3(3)	0.1(3)	1.0(2)	-0.0(2)	3.3(2)
C222	2.3(3)	4.9(4)	4.0(3)	-0.3(3)	1.0(2)	-0.5(3)	3.6(2)
C223	3.3(3)	4.1(4)	3.4(3)	0.4(3)	1.3(2)	-1.1(3)	3.5(2)
C231	3.1(3)	3.0(3)	3.0(3)	0.1(3)	-0.1(3)	-0.5(3)	3.3(2)
C232	3.8(3)	4.0(4)	3.0(3)	-0.4(3)	0.8(3)	0.7(3)	3.7(2)
C233	3.8(4)	2.5(3)	3.0(3)	-0.2(3)	0.1(3)	0.0(3)	3.3(2)
C311	4.6(4)	3.4(4)	3.0(3)	-0.3(3)	2.1(2)	0.4(3)	3.8(2)
C312	7.9(4)	3.5(4)	2.9(3)	0.2(4)	2.6(3)	-0.9(3)	4.6(2)
C321	2.7(3)	3.9(4)	3.7(3)	0.7(3)	0.0(2)	0.4(3)	3.5(2)
C322	4.0(4)	1.9(3)	3.3(3)	0.5(3)	1.0(3)	0.0(3)	3.4(2)
C323	3.4(3)	3.3(3)	1.9(3)	0.0(3)	-0.2(2)	0.1(3)	3.1(2)
C331	3.2(3)	4.2(4)	6.1(4)	0.7(3)	0.0(3)	0.0(4)	4.7(2)
C332	4.0(4)	3.9(4)	3.7(3)	-0.6(3)	1.9(3)	0.3(3)	4.0(2)
C333	4.3(4)	3.0(3)	4.4(4)	-1.7(3)	-0.4(3)	-0.9(3)	4.3(2)
C313	5.4(4)	3.0(3)	3.5(3)	-0.5(3)	-0.1(3)	0.7(3)	4.3(2)

The form of the anisotropic temperature factor is:
exp[-0.25(h2a2B(1,1) + k2b2B(2,2) + l2c2B(3,3) + 2hkabB(1,2) + 2hlacB(1,3) + 2klbcB(2,3))] where a,b, and c are reciprocal lattice constants.

UMe[OCH(t-Bu)$_2$]$_4$Li

Table of Positional Parameters and Their Estimated Standard Deviations

Atom	x	y	z	B(A2)
U	0.24867(2)	0.27857(1)	0.28126(1)	1.828(4)
O1	0.1377(4)	0.3682(3)	0.3258(2)	2.84(9)
O2	0.1319(4)	0.3682(3)	0.2184(2)	2.76(9)
O3	0.3681(5)	0.2483(3)	0.3628(2)	3.9(1)
O4	0.3571(4)	0.2437(3)	0.2262(2)	3.7(1)
C1	0.1282(6)	0.3818(4)	0.3818(3)	2.8(1)
C2	0.1886(6)	0.3797(4)	0.1488(3)	2.9(1)
C3	0.4316(9)	0.2319(6)	0.4236(4)	6.3(2)
C4	0.4219(8)	0.2231(6)	0.1851(5)	9.1(2)
C5	0.1241(6)	0.1588(5)	0.2678(3)	4.8(2)
C11	-0.0889(6)	0.3688(5)	0.3817(3)	4.5(2)
C12	0.1789(6)	0.4721(4)	0.3985(3)	3.5(2)
C21	-0.0256(7)	0.3626(5)	0.1194(3)	4.5(2)
C22	0.1641(6)	0.4668(4)	0.1421(3)	3.4(2)
C31	0.3885(9)	0.1463(5)	0.4423(4)	6.6(2)
C32	0.5588(7)	0.2614(6)	0.4349(3)	5.3(2)
C41	0.3724(7)	0.1393(5)	0.1837(4)	7.2(2)
C42	0.5467(6)	0.2407(6)	0.2849(3)	4.4(2)
C111	-0.0378(9)	0.2696(6)	0.3629(5)	8.7(3)
C112	-0.1838(9)	0.4144(9)	0.3381(7)	11.8(5)
C113	-0.0296(8)	0.3783(9)	0.4433(4)	10.5(3)
C121	0.163(1)	0.5887(7)	0.4581(4)	10.5(3)
C122	0.3813(8)	0.4607(6)	0.4832(5)	8.4(3)
C123	0.118(1)	0.5389(7)	0.3539(6)	11.0(4)
C211	-0.0487(8)	0.2672(5)	0.1248(4)	5.7(2)
C212	-0.1898(8)	0.4873(7)	0.1512(7)	10.4(4)
C213	-0.062(1)	0.3868(8)	0.0546(4)	12.0(3)
C221	0.2943(7)	0.4668(6)	0.1795(4)	5.8(2)
C222	0.1894(9)	0.5418(6)	0.1624(6)	9.0(3)
C223	0.173(1)	0.4792(7)	0.0782(4)	10.5(3)
C311	0.2578(9)	0.1568(7)	0.4481(5)	8.1(3)
C312	0.456(1)	0.1284(7)	0.5864(4)	10.3(4)

Table of Positional Parameters and Their Estimated Standard Deviations (cont.)

Atom	x	y	z	B(A2)
C313	0.4882(9)	0.0743(5)	0.3975(4)	7.0(3)
C321	0.629(1)	0.2670(8)	0.4989(5)	9.4(4)
C322	0.625(1)	0.1917(9)	0.4865(6)	12.7(4)
C323	0.5716(7)	0.3422(6)	0.4819(4)	5.9(2)
C411	0.387(1)	0.0689(6)	0.1985(6)	10.5(4)
C412	0.2463(9)	0.1503(6)	0.1253(4)	7.3(3)
C413	0.438(1)	0.1124(9)	0.1063(6)	21.1(4)
C421	0.5646(7)	0.3324(6)	0.2361(4)	6.7(3)
C422	0.681(1)	0.189(1)	0.2503(6)	13.4(5)
C423	0.629(1)	0.2374(9)	0.1665(6)	11.8(4)
L1	0.057(1)	0.4161(8)	0.2501(6)	4.4(3)*
H1	0.1658	0.3491	0.4151	3.7*
H2	0.1486	0.3438	0.1261	3.0*
H3	0.4114	0.2605	0.4535	8.1*
H4	0.4842	0.2684	0.1477	11.1*
H5B	0.0546	0.1679	0.2636	5.0*
H5C	0.1306	0.1054	0.2343	5.0*
H5A	0.1386	0.1258	0.3046	5.0*
H111C	0.0152	0.2336	0.3988	10.9*
H111A	-0.1171	0.2576	0.3632	10.9*
H111B	-0.0279	0.2617	0.3244	10.9*
H112C	-0.0956	0.4059	0.2989	15.5*
H112A	-0.1798	0.3908	0.3402	15.5*
H112B	-0.0995	0.4724	0.3402	15.5*
H113C	-0.0137	0.4264	0.4569	13.6*
H113A	-0.1102	0.3567	0.4416	13.6*
H113B	0.0214	0.3328	0.4702	13.6*
H121C	0.2845	0.4637	0.4881	12.9*
H121A	0.1937	0.5563	0.4668	12.9*
H121B	0.0002	0.5010	0.4598	12.9*
H122C	0.3121	0.4523	0.3663	10.7*

Table of Positional Parameters and Their Estimated Standard Deviations (cont.)

Atom	x	y	z	B(A2)
H122A	0.3353	0.5228	0.4128	18.7*
H122B	0.3387	0.4298	0.4319	18.7*
H123C	0.0343	0.5418	0.3468	14.1*
H123A	0.1528	0.5918	0.3644	14.1*
H123B	0.1353	0.5236	0.3154	14.1*
H211C	-0.0298	0.2532	0.1646	7.5*
H211A	-0.1384	0.2576	0.1861	7.5*
H211B	-0.0818	0.2379	0.1844	7.5*
H212C	-0.0978	0.4657	0.1536	13.0*
H212A	-0.1099	0.3943	0.1336	13.0*
H212B	-0.0914	0.3861	0.1927	13.0*
H213C	-0.0172	0.3558	0.0332	15.1*
H213A	-0.1446	0.3753	0.0382	15.1*
H213B	-0.0486	0.4456	0.0584	15.1*
H221C	0.3376	0.4223	0.1668	7.2*
H221A	0.3317	0.5185	0.1765	7.2*
H221B	0.2981	0.4557	0.2282	7.2*
H222C	0.1898	0.5349	0.2835	11.0*
H222A	0.1451	0.5914	0.1867	11.0*
H222B	0.0244	0.5448	0.1486	11.0*
H223C	0.0934	0.4779	0.0518	13.2*
H223A	0.2851	0.5339	0.0746	13.2*
H223B	0.2191	0.4376	0.0677	13.2*
H311C	0.2146	0.1721	0.4813	18.4*
H311A	0.2282	0.1858	0.4514	18.4*
H311B	0.2588	0.2884	0.4671	18.4*
H312C	0.4394	0.1622	0.5328	12.6*
H312A	0.4238	0.0679	0.5151	12.6*
H312B	0.5363	0.1163	0.5188	12.6*
H313C	0.4084	0.0693	0.3958	8.0*

Table of Positional Parameters and Their Estimated Standard Deviations (cont.)

Atom	x	y	z	B(A2)
H313A	0.3732	0.0226	0.4009	8.0*
H313B	0.3522	0.0097	0.3503	8.0*
H321C	0.6364	0.2131	0.5149	11.5*
H321A	0.7092	0.2064	0.4981	11.5*
H321B	0.5951	0.3055	0.5181	11.5*
H322C	0.5918	0.1873	0.3678	15.2*
H322A	0.7578	0.2089	0.4144	15.2*
H322B	0.6238	0.1454	0.4273	15.2*
H323C	0.5291	0.3052	0.4148	7.4*
H323A	0.6535	0.3578	0.4113	7.4*
H323B	0.5423	0.3329	0.3611	7.4*
H411A	0.3529	0.0156	0.1784	5.2*
H411B	0.4641	0.0588	0.2196	5.2*
H411C	0.3383	0.0793	0.2262	5.2*
H412C	0.2333	0.1952	0.0962	8.9*
H412A	0.2117	0.1883	0.1055	8.9*
H412B	0.2843	0.1653	0.1539	8.9*
H413C	0.5167	0.1871	0.1225	23.9*
H413A	0.4819	0.0621	0.0969	23.9*
H413B	0.4226	0.1563	0.0758	23.9*
H421C	0.5335	0.3388	0.2689	8.4*
H421A	0.6481	0.3438	0.2482	8.4*
H421B	0.5264	0.3746	0.2898	8.4*
H422C	0.5954	0.1325	0.2435	16.9*
H422A	0.6851	0.2824	0.2721	16.9*
H422B	0.5637	0.1968	0.2873	16.9*
H423A	0.7879	0.2561	0.1879	14.2*
H423B	0.6341	0.1796	0.1872	14.2*
H423C	0.6848	0.2695	0.1316	14.2*

Starred atoms were included with isotropic thermal parameters.
The thermal parameter given for anisotropically refined atoms is the isotropic equivalent thermal parameter defined as:
(4/3) * [a2*B(1,1) + b2*B(2,2) + c2*B(3,3) + ab(cos gamma)*B(1,2) + ac(cos beta)*B(1,3) + bc(cos alpha)*B(2,3)]
where a,b,c are real cell parameters, and B(i,j) are anisotropic betas.

Table of Anisotropic Thermal Parameters - B's

Name	B(1,1)	B(2,2)	B(3,3)	B(1,2)	B(1,3)	B(2,3)	Beqv
U	1.0017(8)	2.0014(9)	1.6005(8)	0.148(9)	0.363(7)	0.127(5)	1.020(4)
O1	3.0(2)	3.5(2)	2.1(2)	0.4(2)	1.0(1)	-0.5(2)	2.84(9)
O2	3.0(2)	3.0(2)	2.1(2)	0.4(2)	0.4(1)	0.7(2)	2.76(9)
O3	4.4(2)	3.2(2)	2.0(2)	0.1(2)	-1.4(2)	0.9(2)	3.9(1)
O4	4.1(2)	3.2(2)	4.6(2)	0.2(2)	2.5(1)	-0.9(2)	3.7(1)
C1	3.2(3)	3.0(3)	2.5(2)	0.0(2)	0.9(2)	-0.5(2)	2.8(1)
C2	3.5(3)	2.7(3)	2.0(2)	0.2(2)	0.2(2)	0.5(2)	2.9(1)
C3	6.2(5)	5.8(4)	5.3(4)	-0.5(4)	-1.5(4)	1.8(4)	6.3(2)
C4	7.5(4)	9.0(5)	13.6(5)	-3.6(4)	7.7(3)	-7.4(4)	9.1(2)
C5	5.0(3)	3.3(3)	3.6(3)	-0.7(3)	1.2(3)	-0.0(3)	4.0(2)
C11	4.3(3)	5.0(4)	5.0(3)	-0.7(3)	2.5(2)	-1.7(3)	4.5(2)
C12	4.3(3)	3.3(3)	3.0(3)	-0.2(3)	1.4(2)	-0.6(3)	3.5(2)
C21	5.0(4)	3.9(4)	3.5(3)	-0.5(3)	-1.0(3)	1.0(3)	4.5(2)
C22	4.5(3)	2.7(3)	3.0(3)	-0.2(3)	0.7(2)	0.4(3)	3.4(2)
C31	10.2(6)	3.4(3)	3.7(4)	-0.8(4)	-2.5(4)	1.9(3)	6.6(2)
C32	3.4(3)	9.3(6)	2.9(3)	0.4(4)	0.3(3)	0.5(4)	5.3(2)
C41	7.9(4)	3.0(4)	12.7(5)	-1.4(3)	7.3(3)	-4.0(3)	7.2(2)
C42	3.5(3)	6.6(4)	3.0(3)	0.4(3)	1.0(2)	-0.0(3)	4.4(2)
C111	8.2(4)	7.6(5)	12.6(6)	-4.3(4)	6.7(4)	-4.2(5)	8.7(3)
C112	3.7(5)	11.7(9)	10(1)	0.2(6)	-0.1(6)	3.2(9)	11.0(5)
C113	7.3(4)	10(1)	8.2(4)	-5.7(5)	5.0(3)	-6.5(5)	10.5(3)

Table of Anisotropic Thermal Parameters - B's (Continued)

Name	B(1,1)	B(2,2)	B(3,3)	B(1,2)	B(1,3)	B(2,3)	Beqv
C121	16.0(7)	9.9(6)	7.8(4)	-6.9(5)	7.1(4)	-6.0(4)	10.5(3)
C122	5.2(4)	6.1(5)	14.8(7)	-2.3(4)	4.2(4)	-4.2(5)	8.4(3)
C123	15(1)	4.3(5)	10.5(8)	0.4(6)	-1.7(8)	1.8(5)	11.0(4)
C211	5.4(4)	4.9(4)	5.7(4)	-1.4(4)	-0.5(4)	0.5(4)	5.7(2)
C212	3.7(4)	6.3(6)	21(1)	0.0(4)	1.9(6)	-1.0(7)	10.4(4)
C213	10.5(6)	15.6(8)	5.7(5)	-7.5(6)	-5.1(5)	5.7(5)	12.0(3)
C221	3.6(3)	4.9(4)	8.7(5)	-0.7(3)	1.1(3)	0.5(4)	5.8(2)
C222	6.7(5)	4.5(5)	16.7(8)	-0.1(4)	4.8(5)	-1.7(6)	9.0(3)
C223	14.9(7)	12.3(7)	4.3(4)	-7.4(5)	2.4(4)	1.8(4)	10.5(3)
C311	8.4(6)	7.7(5)	7.6(5)	-1.7(5)	0.9(5)	2.8(5)	8.1(3)
C312	14.3(9)	8.9(6)	5.2(5)	-2.0(7)	-1.8(6)	3.4(5)	10.3(4)
C313	7.7(5)	4.0(4)	7.9(6)	0.8(4)	-0.4(5)	0.9(4)	7.0(3)
C321	9.3(7)	11.0(8)	5.2(5)	-1.7(6)	-2.8(5)	0.3(5)	9.4(4)
C322	13.1(7)	11.0(8)	17.1(8)	2.7(6)	9.5(5)	-2.5(7)	12.7(4)
C323	3.8(3)	7.3(5)	6.3(4)	-0.6(4)	0.5(3)	1.0(4)	5.9(2)
C411	7.7(6)	4.8(5)	15.8(9)	2.1(5)	-2.5(6)	-3.0(6)	10.5(4)
C412	10.9(6)	5.5(4)	6.8(4)	-2.6(4)	4.3(4)	-2.7(4)	7.3(3)
C413	18.6(6)	18.7(8)	34.1(7)	****(6)	21.3(4)	****(5)	21.1(4)
C421	4.1(4)	6.3(5)	10.0(6)	-1.0(4)	2.2(4)	-2.3(5)	6.7(3)
C422	14(1)	14(1)	8.5(7)	2.0(9)	-3.5(8)	3.7(7)	13.4(5)
C423	8.1(5)	14(1)	16.4(8)	-3.4(6)	8.5(4)	-4.6(7)	11.8(4)

The form of the anisotropic temperature factor is:
exp[-0.25(h2a2B(1,1) + k2b2B(2,2) + l2c2B(3,3) + 2hkabB(1,2) + 2hlacB(1,3) + 2klbcB(2,3))] where a,b, and c are reciprocal lattice constants.